Fundamentals of Particle Detectors and Developments in Detector Technologies for Future Experiments

Werner Riegler, CERN

Lecture 3&4/5

Abstract:

This lecture series will first review the elementary processes and techniques on which particle detectors are based. These must always be kept in mind when discussing the limits of existing technologies and motivations for novel developments. Using the examples of LHC detectors, the limits of state of the art detectors will be outlined and the current detector R&D trends for the LHC upgrade and other future experiments will be discussed. This discussion will include micro-pattern gas detectors, novel solid state detector technologies and trends in microelectronics.

Outline

1) History of Instrumentation

Cloud Chambers/Bubble Chambers/Geiger Counters/Scintillators/Electronics/Wire Chambers

2) Electro-Magnetic Interaction of Charged Particles with Matter

Excitation/ Ionization/ Bethe Bloch Formula/ Range of Particles/ PAI model/ Ionization Fluctuation/ Bremsstrahlung/ Pair Production/ Showers/ Multiple Scattering

3) Signals/Gas Detectors

Detector Signals/ Signal Theorems/

Gaseous Detectors/ Wire Chambers/ Drift Chamber/ TPCs/ RPCs/ Limits of Gaseous Detectors/ Current Trends in Gaseous Detector Development

4) Solid State Detectors

Principles of Solid State Detectors/ Diamond Detectors/ Silicon Detectors/ Limits of Solid State Detectors/ Current Trends in Solid State Detectors

5) Calorimetry & Selected Topics

EM showers/ Hadronic Showers/ Crystal Calorimeters/ Noble Liquid Caloirimeters/ Current Trends in Calorimetry

Creation of the Signal

The charged particles traversing matter leave excited atoms, ionization electrons/holes and ions behind.

Excitation:
The photons emitted by the excited atoms can be detected with photon detectors like photomultipliers or semiconductor photon detectors.

Ionization:
By applying an electric field in the detector volume, the ionization electrons and ions are moving, which induces signals on metal electrodes. These signals are then read out by appropriate readout electronics.

Creation of the Signal

From a modern detector text book:

… It is important to realize that the signals from wire chambers operating in proportional mode are primarily generated by *induction* due to the moving charges rather than by the *collection* of these charges on the electrodes …

… When a charged […] particle traverses the gap, it ionizes the atoms […]. Because of the presence of an electric field, the electrons and ions created in this process drift to their respective electrodes. The charge collected at these electrodes forms the […] signal, in contrast to gaseous detectors described above, where the signal corresponds to the current *induced* on the electrodes by the drifting charges (ions). …

These statements are completely wrong !

***All* signals in particle detectors are due to *induction* by moving charges. Once the charges have arrived at the electrodes the signals are 'over'.**

Principle of Signal Induction by Moving Charges

A point charge q at a distance z_0

Above a grounded metal plate 'induces' a surface charge.

The total induced charge on the surface is –q.

Different positions of the charge result in different charge distributions.

The total induced charge stays –q.

The electric field of the charge must be calculated with the boundary condition that the potential φ=0 at z=0.

For this specific geometry the method of images can be used. A point charge –q at distance $-z_0$ satisfies the boundary condition → electric field.

The resulting charge density is

$\sigma(x,y) = \varepsilon_0 E_z(x,y)$

$\int\sigma(x,y)dxdy = -q$

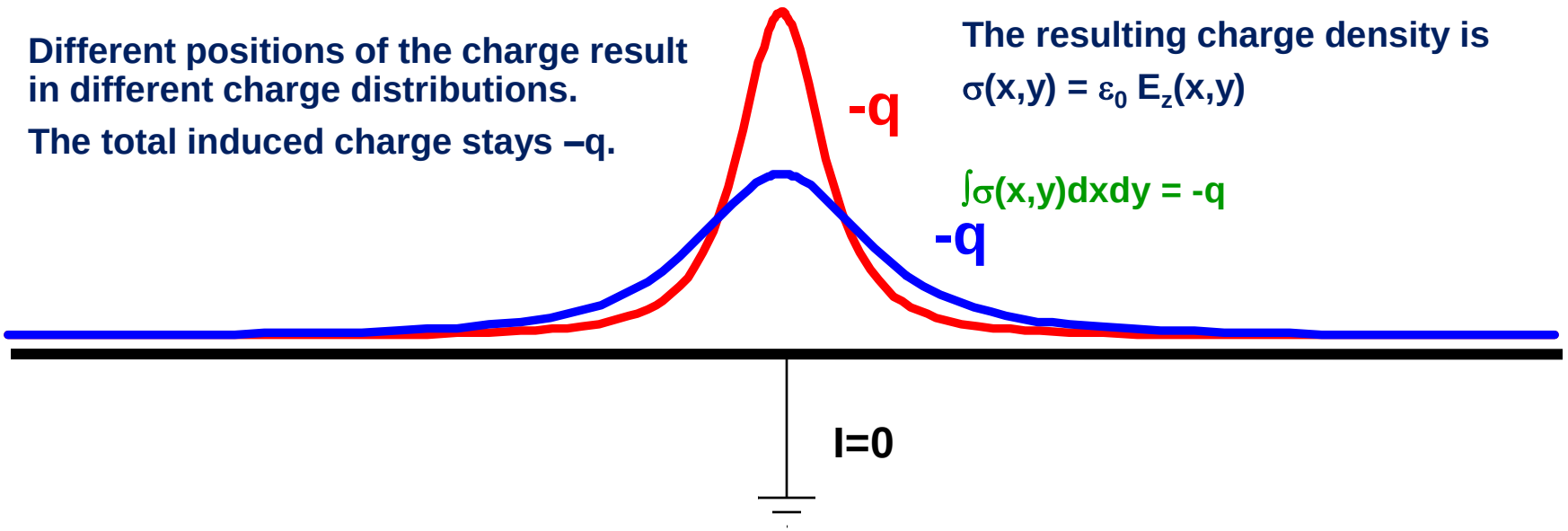

$$E_z(x,y) = -\frac{qz_0}{2\pi\varepsilon_0(x^2+y^2+z_0^2)^{\frac{3}{2}}} \qquad E_x = E_y = 0 \qquad \sigma(x,y) = \varepsilon_0 E_z(x,y) \qquad Q = \int_{-\infty}^{\infty}\int_{-\infty}^{\infty}\sigma(x,y)dxdy = -q$$

Principle of Signal Induction by Moving Charges

If we segment the grounded metal plate and if we ground the individual strips the surface charge density doesn't change with respect to the continuous metal plate.

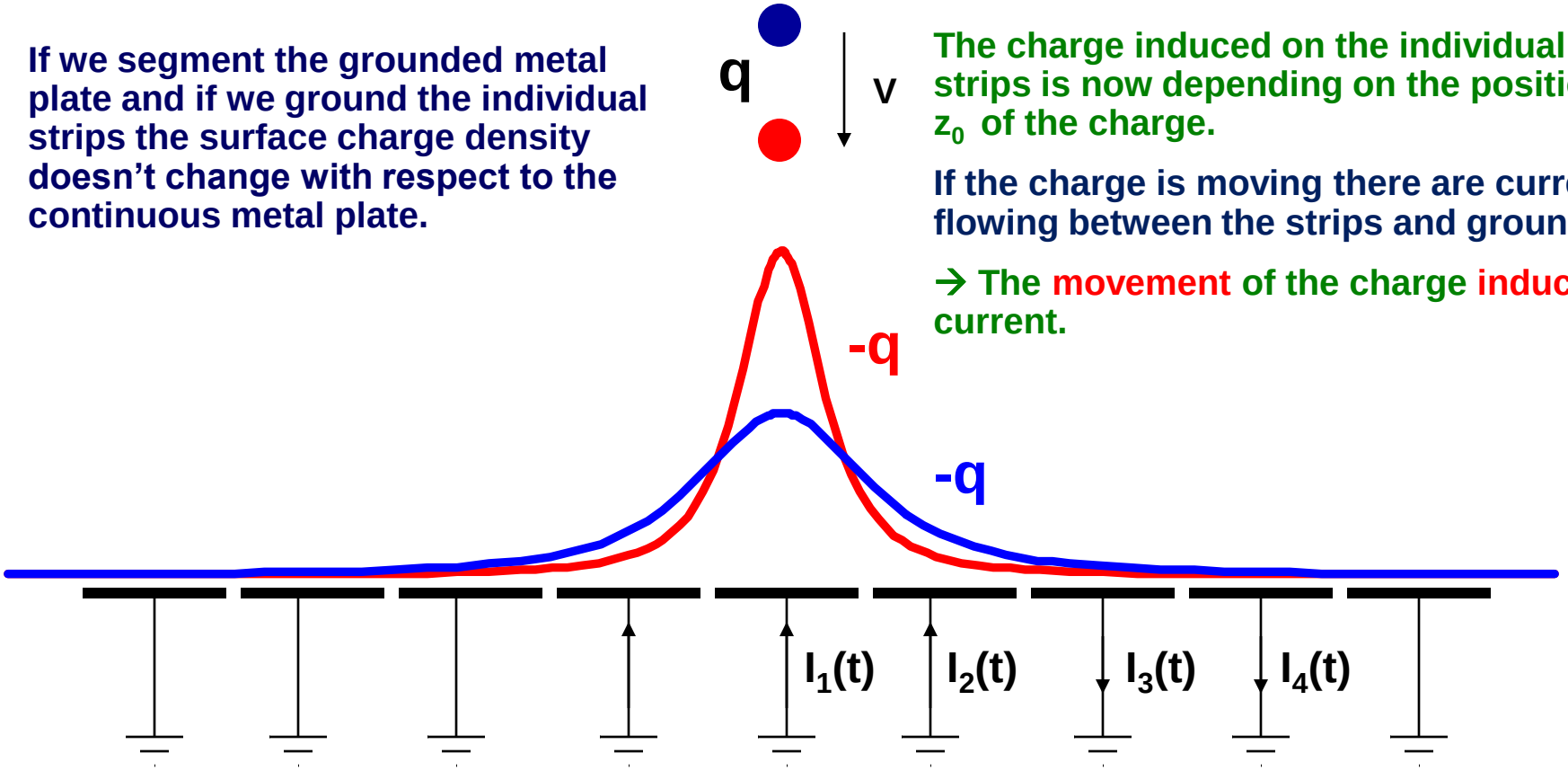

The charge induced on the individual strips is now depending on the position z_0 of the charge.

If the charge is moving there are currents flowing between the strips and ground.

→ The movement of the charge induces a current.

$$Q_1(z_0) = \int_{-\infty}^{\infty}\int_{-w/2}^{w/2} \sigma(x,y)dxdy = -\frac{2q}{\pi}\arctan\left(\frac{w}{2z_0}\right)$$

$$z_0(t) = z_0 - vt$$

$$I_1^{ind}(t) = -\frac{d}{dt}Q_1[z_0(t)] = -\frac{\partial Q_1[z_0(t)]}{\partial z_0}\frac{dz_0(t)}{dt} = \frac{4qw}{\pi[4z_0(t)^2 + w^2]}v$$

Signal Theorems

Placing charges on metal electrodes results in certain potentials of these electrodes. A different set of charges results in a different set of potentials. The reciprocity theorem states that

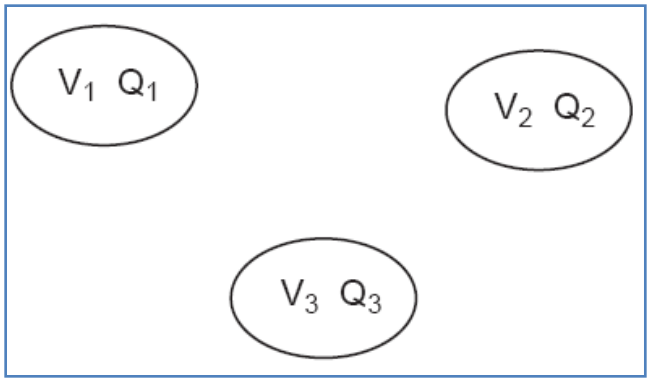

$$\sum_{n=1}^{N} Q_n \overline{V}_n = \sum_{n=1}^{N} \overline{Q}_n V_n$$

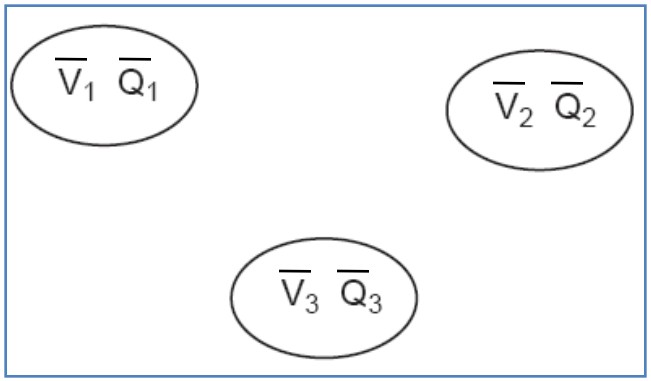

Using this theorem we can answer the following general question: What are the signals created by a moving charge on metal electrodes that are connected with arbitrary discrete (linear) components ?

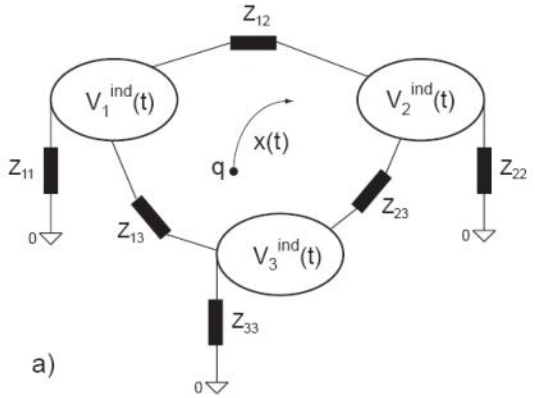

Signal Theorems

What are the charges induced by a moving charge on electrodes that are connected with arbitrary linear impedance elements ?

One first removes all the impedance elements, connects the electrodes to ground and calculates the currents induced by the moving charge on the grounded electrodes.

The current induced on a grounded electrode by a charge q moving along a trajectory x(t) is calculated the following way (Ramo Theorem):

One removes the charge q from the setup, puts the electrode to voltage V_0 while keeping all other electrodes grounded. This results in an electric field $E_n(x)$, the Weighting Field, in the volume between the electrodes, from which the current is calculated by

$$I_n(t) = -\frac{q}{V_0}\vec{E_n}[\vec{x}(t)]\frac{d\vec{x}(t)}{dt} = -\frac{q}{V_0}\vec{E_n}[\vec{x}(t)]\vec{v}(t)$$

These currents are then placed as ideal current sources on a circuit where the electrodes are 'shrunk' to simple nodes and the mutual electrode capacitances are added between the nodes. These capacitances are calculated from the weighting fields by

$$c_{nm} = \frac{\varepsilon_0}{V_w}\oint_{\boldsymbol{A}_n}\boldsymbol{E}_m(\boldsymbol{x})d\boldsymbol{A} \qquad C_{nn} = \sum_m c_{nm} \qquad C_{nm} = -c_{nm} \quad n \neq m$$

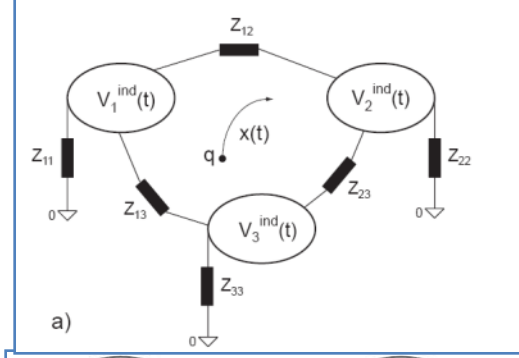

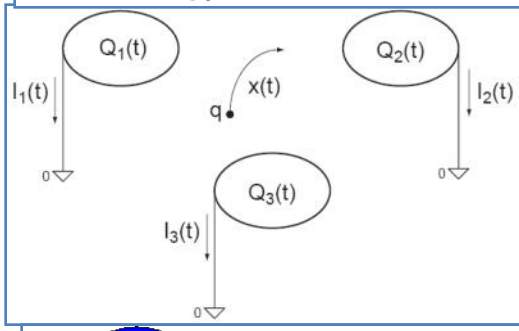

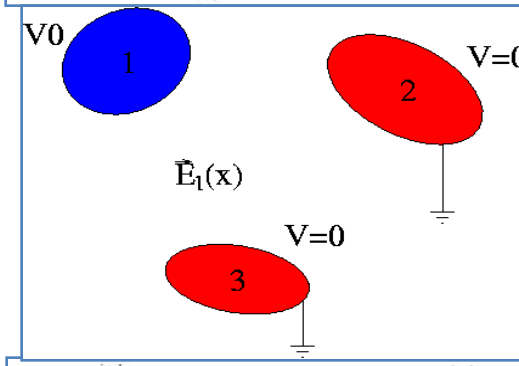

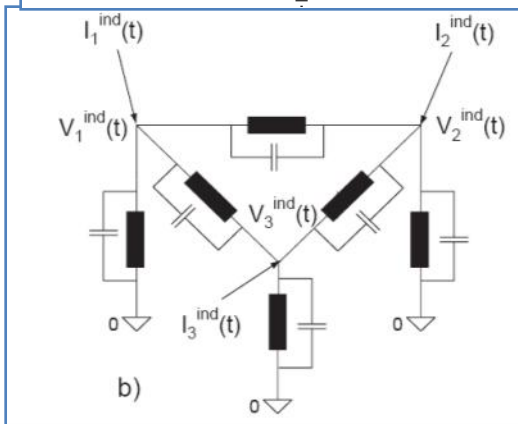

Signal Theorems

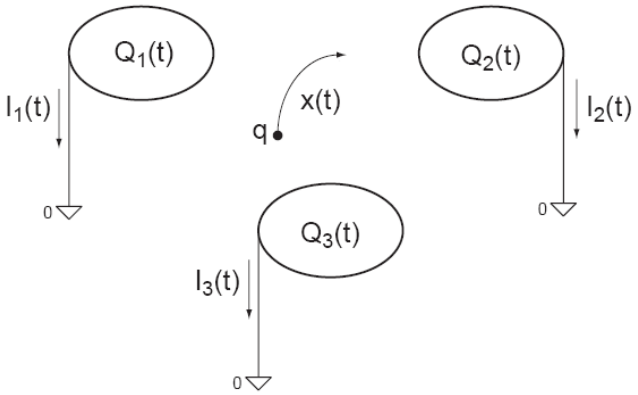

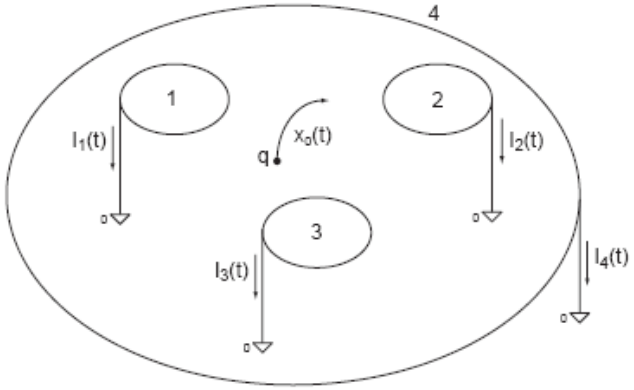

The following relations hold for the induced currents:

1) The charge induced on an electrode in case a charge in between the electrode has moved from a point x_0 to a point x_1 is

$$Q_n^{ind} = \int_{t_0}^{t_1} I_n^{ind}(t)dt = -\frac{q}{V_w}\int_{t_0}^{t_1} \boldsymbol{E}_n[\boldsymbol{x}(t)]\,\dot{\boldsymbol{x}}(t)dt = \frac{q}{V_w}[\psi_n(\boldsymbol{x}_1) - \psi_n(\boldsymbol{x}_0)]$$

and is independent on the actual path.

2) Once ALL charges have arrived at the electrodes, the total induced charge in the electrodes is equal to the charge that has ARRIVED at this electrode.

3) In case there is one electrode enclosing all the others, the sum of all induced currents is zero at any time.

Signals in a Parallel Plate Geometry

E.g.: Elektron-ion pair in gas
or Electron-ion pair in a liquid
or Electron-hole pair in a solid

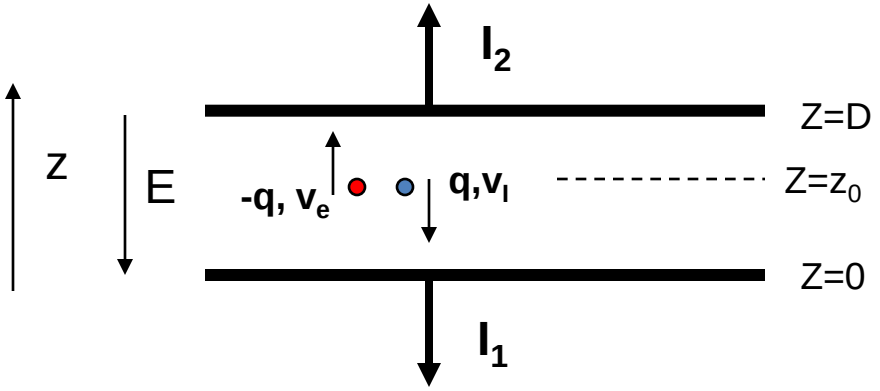

$E_1=V_0/D$
$E_2=-V_0/D$

$I_1= -(-q)/V_0*(V_0/D)*v_e - q/V_0\ (V_0/D)\ (-v_I)$
$= q/D*v_e+q/D*v_I$
$I_2=-I_1$

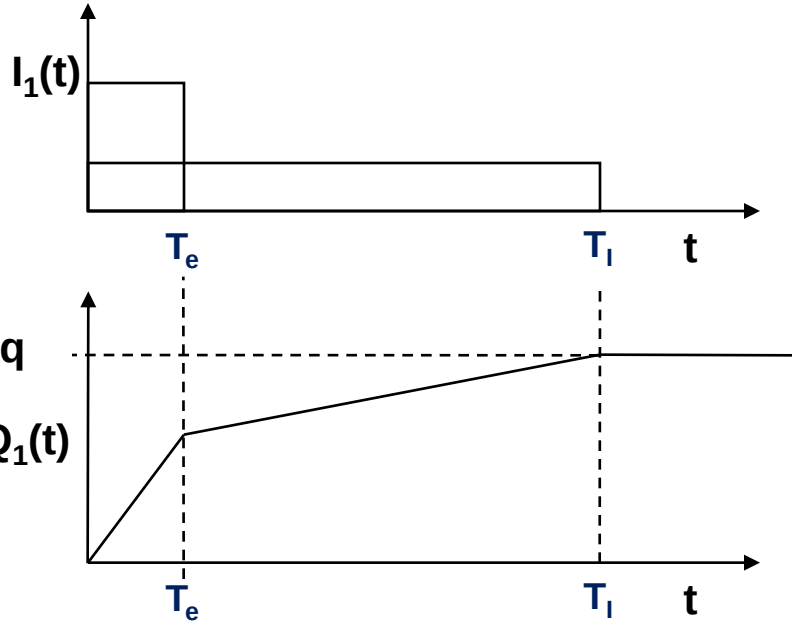

$Q^{tot}_1= \int I_1 dt = q/D*v_e\ T_e + q/D*v_I*T_I$
$= q/D*v_e*(D-z_0)/v_e + q/D*v_I*z_0/v_I$
$= q(D-z_0)/D + qz_0/D =$
$q_e+q_I=q$

The total induced charge on a specific electrode, once all the charges have arrived at the electrodes, is equal to the charge that has arrived at this specific electrode.

Signals in a Parallel Plate Geometry

In case the electrodes are not grounded but connected by arbitrary active or passive elements one first calculates the currents induced on the grounded electrodes and places them as ideal current sources on the equivalent circuit of the electrodes.

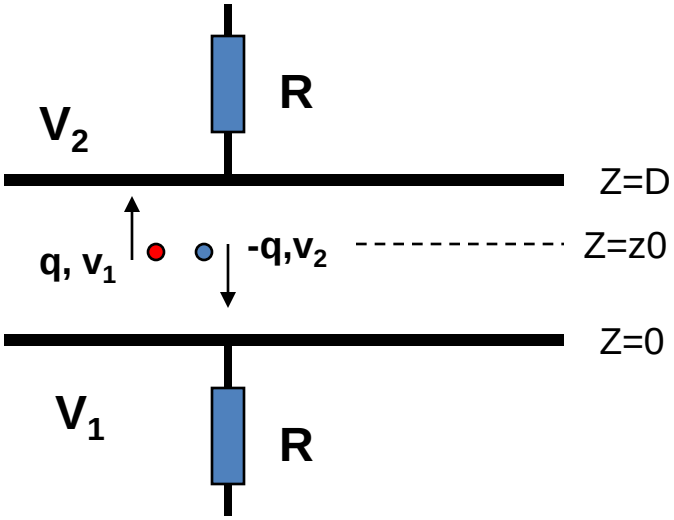

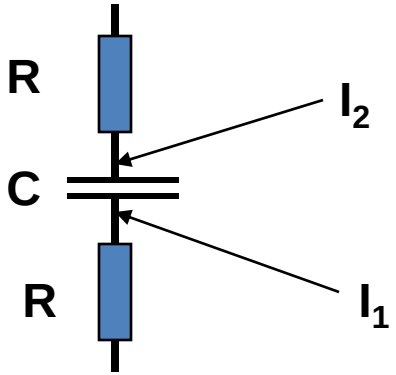

Detectors based on Registration of Ionization: Tracking in Gas and Solid State Detectors

Charged particles leave a trail of ions (and excited atoms) along their path: Electron-Ion pairs in gases and liquids, electron hole pairs in solids.

The produced charges can be registered → Position measurement → Tracking Detectors.

Cloud Chamber: Charges create drops → photography.
Bubble Chamber: Charges create bubbles → photography.
Emulsion: Charges 'blacked' the film.

Gas and Solid State Detectors: Moving Charges (electric fields) induce electronic signals on metallic electrons that can be read by dedicated electronics.

→In solid state detectors the charge created by the incoming particle is sufficient.

→In gas detectors (e.g. wire chamber) the charges are internally multiplied in order to provide a measurable signal.

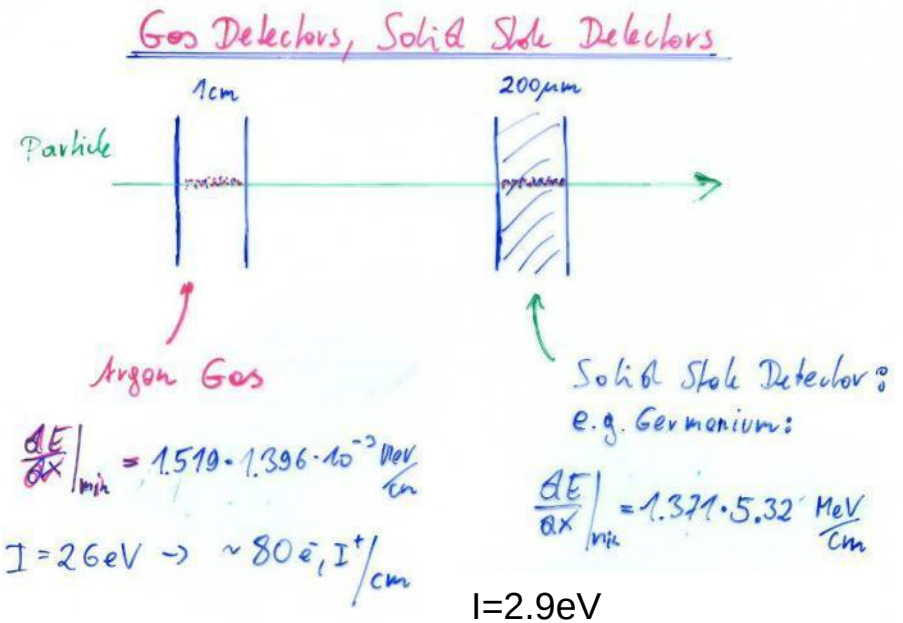

I=2.9eV
2.5 x 10^6 e/h pairs/cm

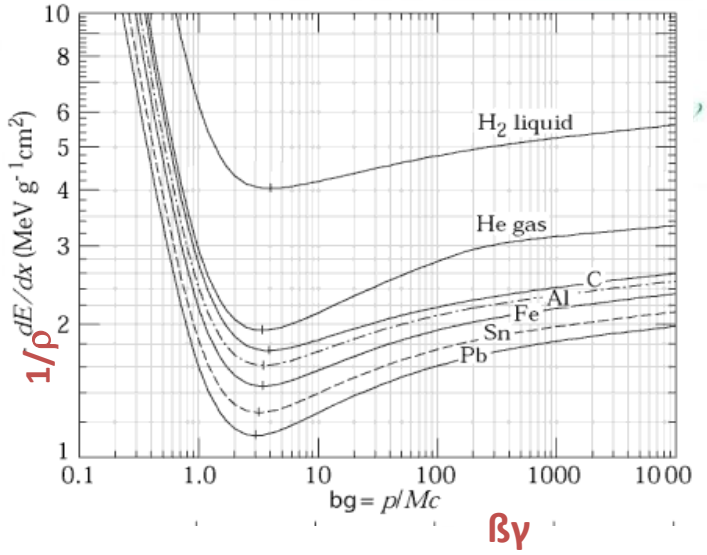

The induced signals are readout out by dedicated electronics.

The noise of an amplifier determines whether the signal can be registered. Signal/Noise >>1

The noise is characterized by the 'Equivalent Noise Charge (ENC)' = Charge signal at the input that produced an output signal equal to the noise.

ENC of very good amplifiers can be as low as 50e-, typical numbers are ~ 1000e-.

In order to register a signal, the registered charge must be q >> ENC i.e. typically q>>1000e-.

Gas Detector: q=80e- /cm → too small.

Solid state detectors have 1000x more density and factor 5-10 less ionization energy.
→Primary charge is 10^4-10^5 times larger than is gases.

Gas detectors need internal amplification in order to be sensitive to single particle tracks.

Without internal amplification they can only be used for a large number of particles that arrive at the same time (ionization chamber).

Gas Detectors with internal Electron Multiplication

Principles of Gas Detectors

Limits of Gas Detectors

Trends in Gas Detector Development

Gas Detectors with internal Electron Multiplication

Principle: At sufficiently high electric fields (100kV/cm) the electrons gain energy in excess of the ionization energy → secondary ionzation etc. etc.

$dN = N \alpha \, dx$ α…Townsend Coefficient

$N(x) = N_0 \exp(\alpha x)$ $N/N_0 = A$ (Amplification, Gas Gain)

Avalanche in a homogeneous field:

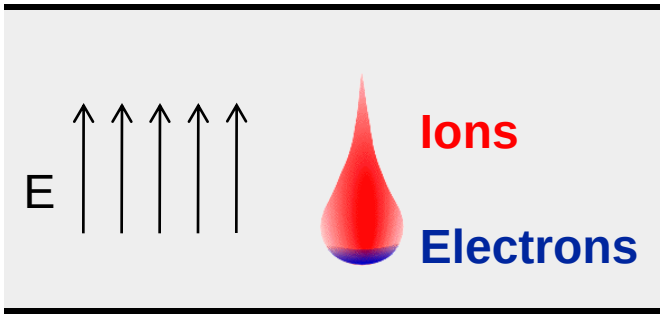

In an inhomogeneous Field: $\alpha(E) \rightarrow N(x) = N_0 \exp[\int \alpha(E(x'))dx']$

Wire Chamber: Electron Avalanche

Wire with radius (10-25μm) in a tube of radius b (1-3cm):

$$E(r) = \frac{\lambda}{2\pi\varepsilon_0}\frac{1}{r} = \frac{V_0}{\ln\frac{b}{a}}\frac{1}{r}, \qquad V(r) = \frac{V_0}{\ln\frac{b}{a}}\ln\frac{r}{a},$$

Electric field close to a thin wire (100-300kV/cm). E.g. V_0=1000V, a=10μm, b=10mm, E(a)=150kV/cm

Electric field is sufficient to accelerate electrons to energies which are sufficient to produce secondary ionization → electron avalanche → signal.

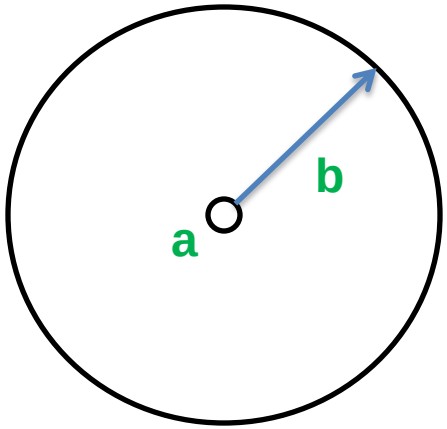

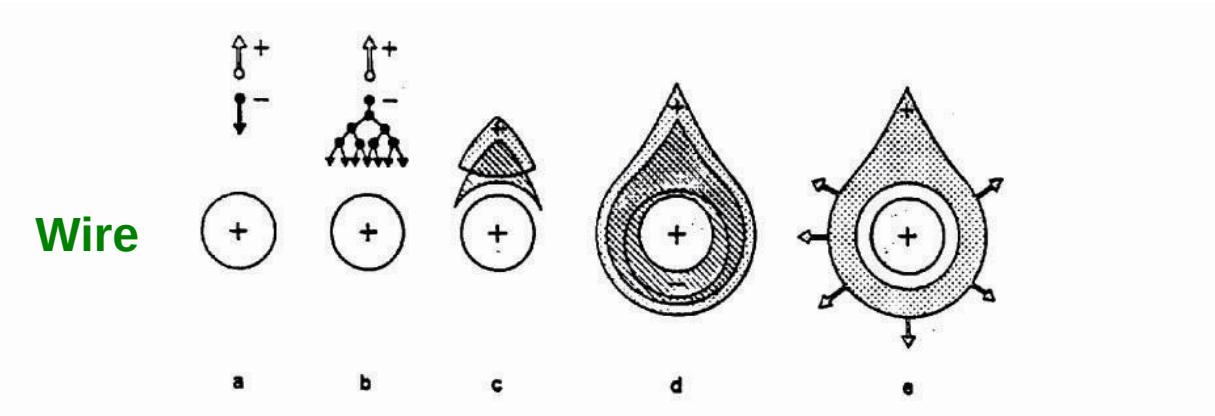

Wire Chamber: Electron Avalanches on the Wire

Proportional region: $A \approx 10^3\text{-}10^4$ — **LHC**

Semi proportional region: $A \approx 10^4\text{-}10^5$
(space charge effect)

Saturation region: $A > 10^6$
Independent the number of primary electrons. — **1970ies**

Streamer region: $A > 10^7$
Avalanche along the particle track.

Limited Geiger region:
Avalanche propagated by UV photons.

Geiger region: $A \approx 10^9$
Avalanche along the entire wire. — **1950ies**

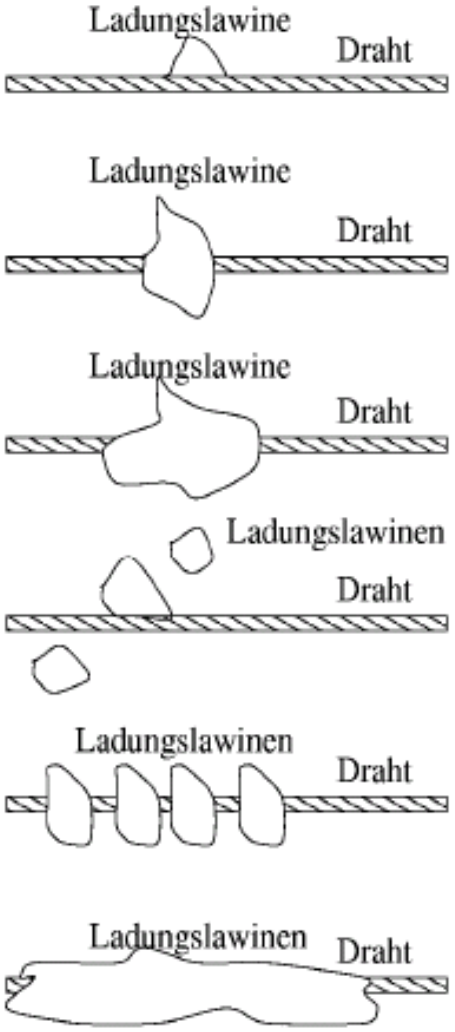

Wire Chamber: Signals from Electron Avalanches

The electron avalanche happens very close to the wire. First multiplication only around R =2x wire radius. Electrons are moving to the wire surface very quickly (<<1ns). Ions are difting towards the tube wall (typically several 100μs.)

The signal is characterized by a very fast 'spike' from the electrons and a long Ion tail.

The total charge induced by the electrons, i.e. the charge of the current spike due to the short electron movement amounts to 1-2% of the total induced charge.

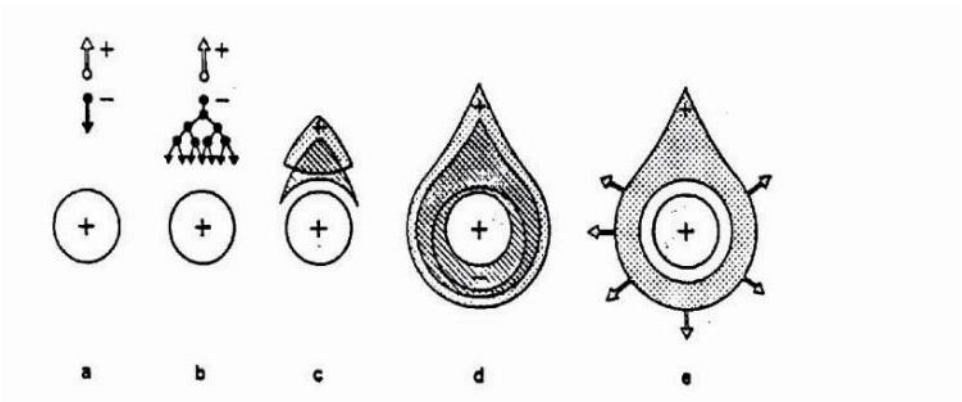

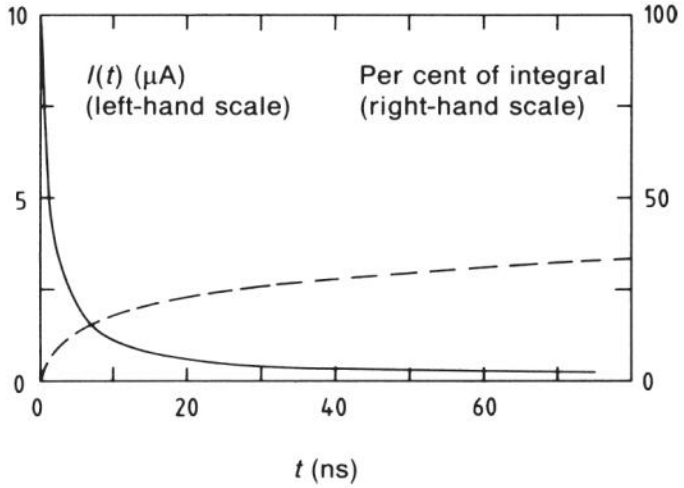

Detectors with Electron Multiplication

Rossi 1930: Coincidence circuit for n tubes

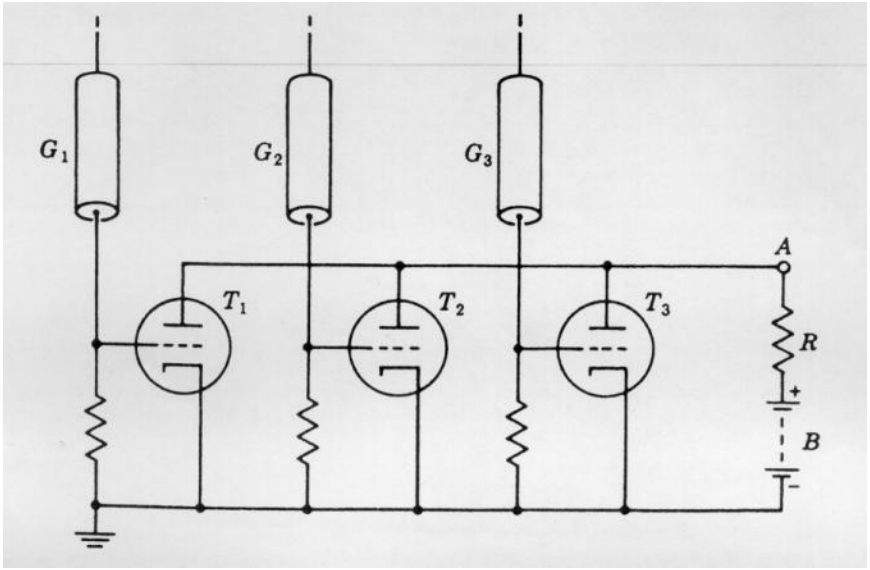

Cosmic ray telescope 1934

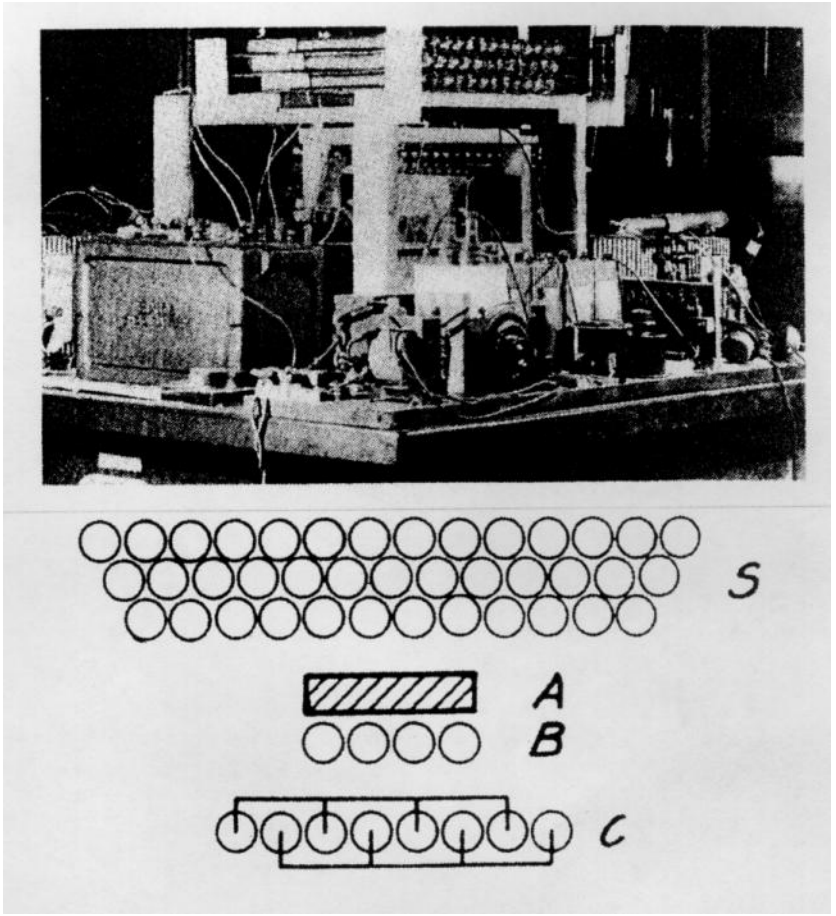

Geiger mode, large deadtime

Position resolution is determined by the size of the tubes.

Signal was directly fed into an electronic tube.

Multi Wire Proportional Chamber

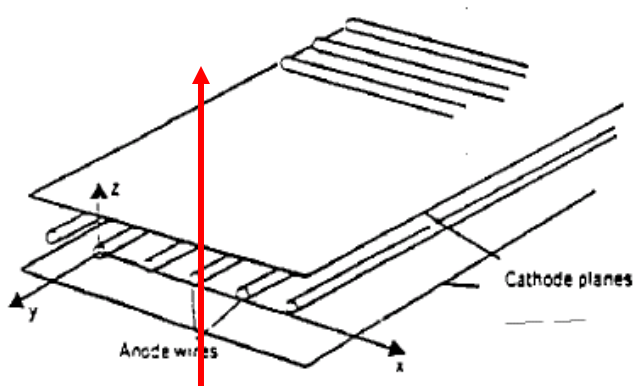

Abbildung 2.27: *Vieldrahtproportionalkammer.*

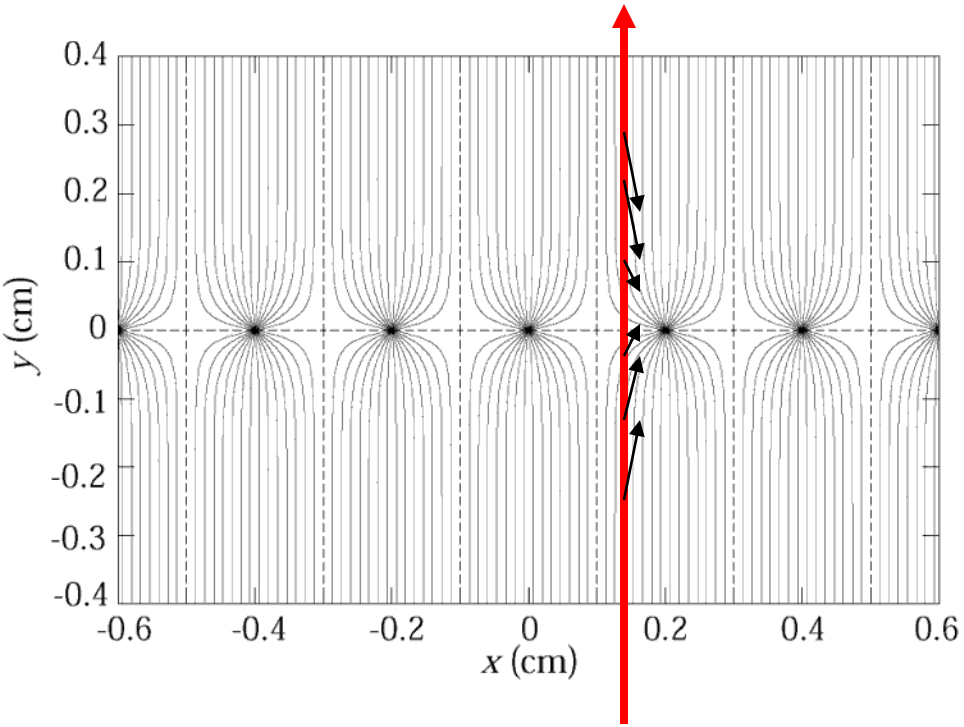

Classic geometry (Crossection), Charpak 1968 :

One plane of thin sense wires is placed between two parallel plates.

Typical dimensions:

Wire distance 2-5mm, distance between cathode planes ~10mm.

Electrons (v≈5cm/μs) are collected within ≈ 100ns. The ion tail can be eliminated by electronics filters → pulses of <100ns length.

For 10% occupancy → every μs one pulse

→ 1MHz/wire rate capabiliy !

→ Compare to Bubble Chamber with 10 Hz !

ELECTRONIC IMAGING OF IONIZING RADIATION WITH LIMITED AVALANCHES IN GASES

Nobel Lecture, December 8, 1992

GEORGES CHARPAK

CERN, Geneva, Switzerland

There still remained one challenging problem, that of the capacitive coupling between the wires. The closer they were, the more likely it was that a pulse induced in one wire would be propagated on its neighbours. This was true for pulses produced by an external electric generator but untrue for the internal generator formed by the positive and negative ions separating under the effect of the electric field. There had, in the past, been examples of wire counters, especially in cosmic-ray experiments, where this fear of coupling led to the insulation of each of the positive amplifying wires by partitions or thick intermediate wires. We merely have to examine the pulse-generation mechanism in a proportional counter to see that, whatever the distance between the wires, the one which is the seat of an avalanche will develop a negative signal, whereas the neighbouring wires and, in general, all the neighbouring electrodes, develop a positive signal which is therefore easy to distinguish from the other.

Multi Wire Proportional Chamber

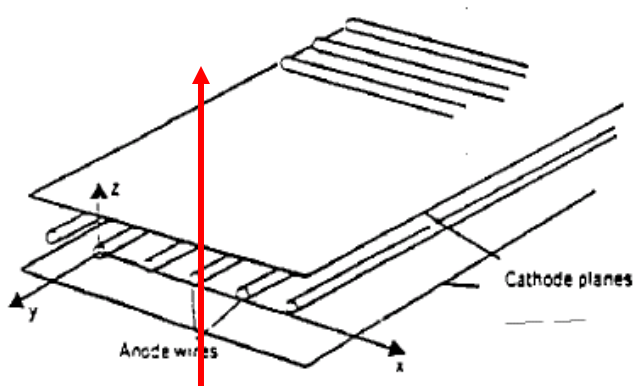

Abbildung 2.27: *Vieldrahtproportionalkammer.*

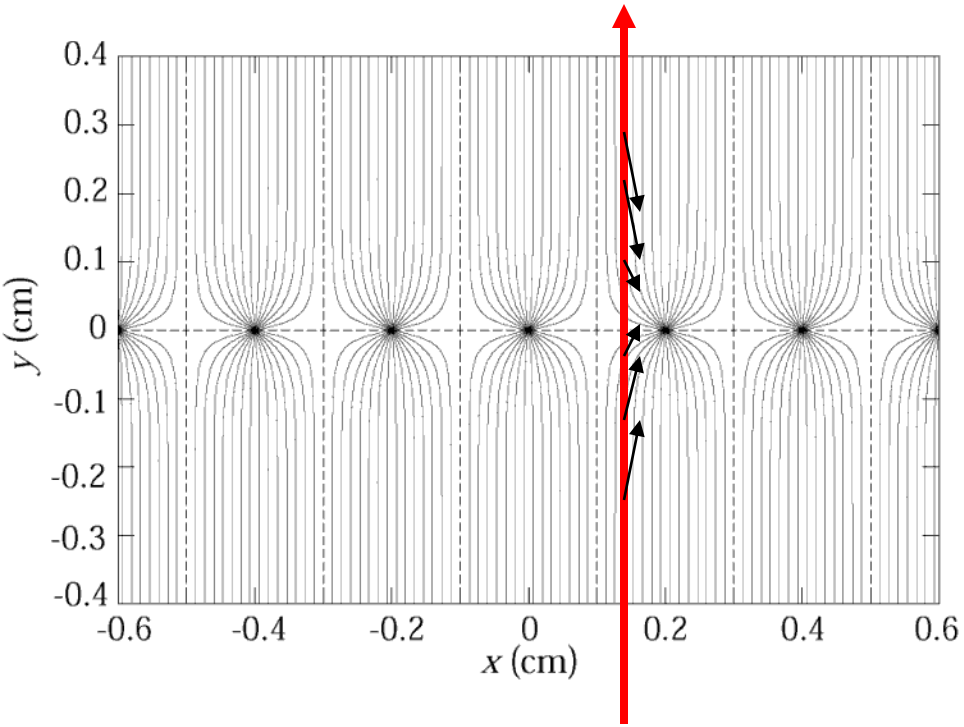

In order to eliminate the left/right ambiguities: Shift two wire chambers by half the wire pitch.

For second coordinate:

→Another chamber at 90^0 relative rotation

→Signal propagation to the two ends of the wire.

→Pulse height measurement on both ends of the wire. Because of resisitvity of the wire, both ends see different charge.

Segmenting of the cathode into strips or pads:

The movement of the charges induces a signal on the wire AND on the cathode. By segmentation of the cathode plane and charge interpolation, resolutions of 50μm can be achieved.

Multi Wire Proportional Chamber

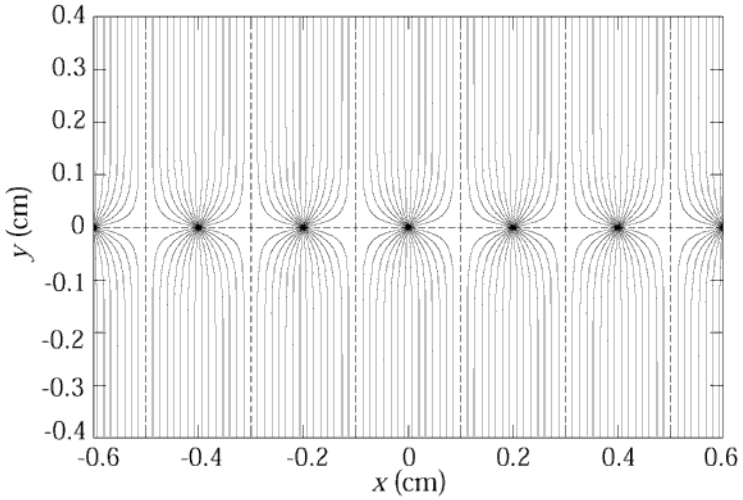

Cathode strip:

Width (1σ) of the charge distribution ≈ distance between Wires and cathode plane.

'Center of gravity' defines the particle trajectory.

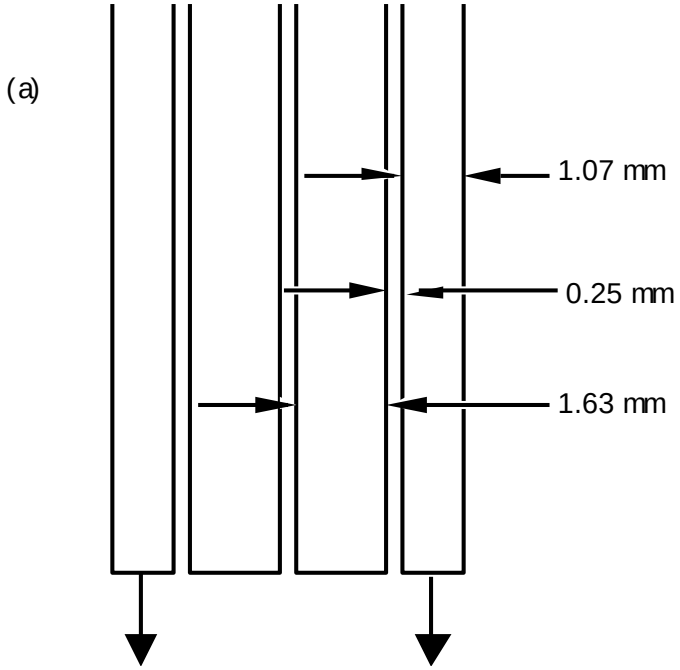

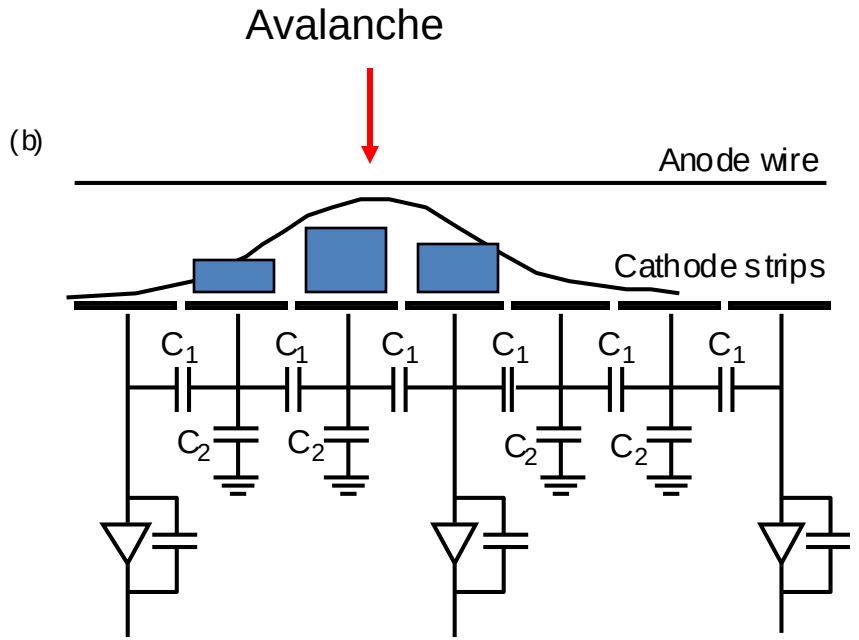

Signals in Particle Detectors

Many people from the audience were interested in the creation of signals in particle detectors.

To my knowledge there aren't any good writeups of this topic. General signal theorems and signals in wire chambers are discussed in detail in the new edition of 'particle detection with drift chambers', which will appear in summer 2008.

There will be a 1 or 2 hour detector seminar this year (probably summer 2008) that discusses signal theorems and signals in all particle detectors

Ionization Chambers

Wire Chamber

Micro Pattern Gas Detectors

Resistive Plate Chambers

Solid State Detectors

Noble Liquid Calorimeters

together with basics of frontend electronics to read these signals. The lecture notes should then serve as a complete write-up of signals in particle detectors.

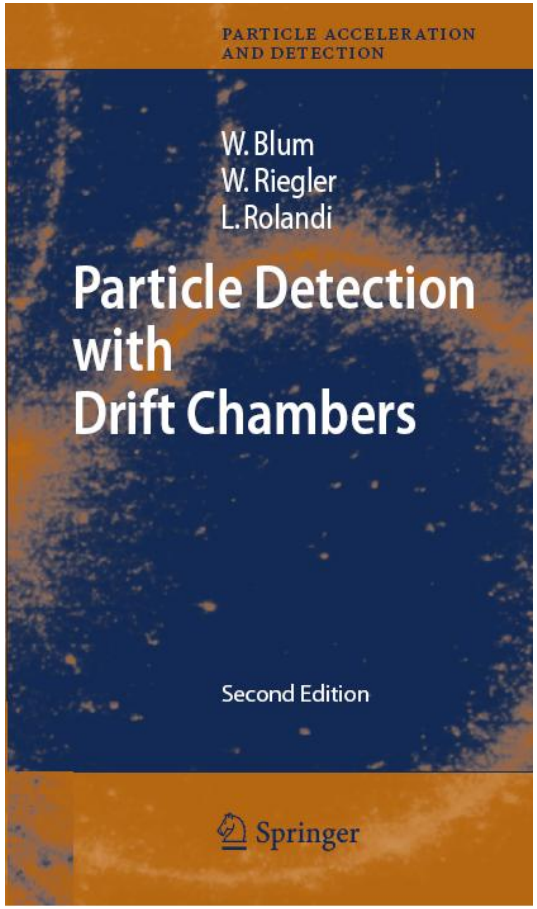

Drift Chambers

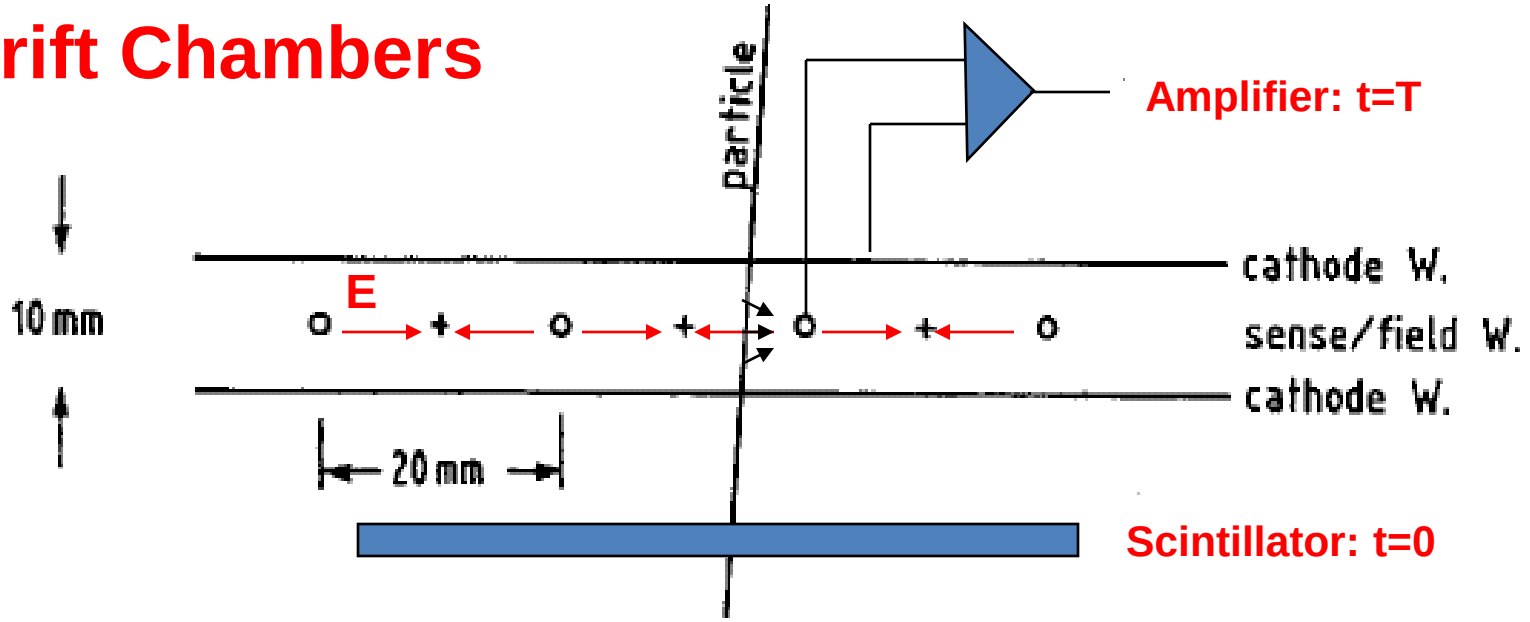

In an alternating sequence of wires with different potentials one finds an electric field between the 'sense wires' and 'field wires'.

The electrons are moving to the sense wires and produce an avalanche which induces a signal that is read out by electronics.

The time between the passage of the particle and the arrival of the electrons at the wire is measured.

The drift time T is a measure of the position of the particle !

By measuring the drift time, the wire distance can be increased (compared to the Multi Wire Proportional Chamber) → save electronics channels !

Drift Chambers, typical Geometries

Electric Field ≈ 1kV/cm

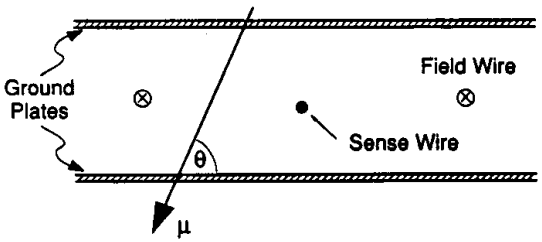

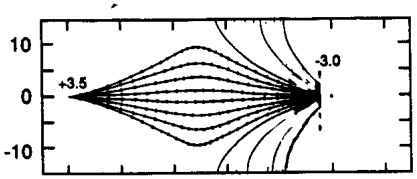

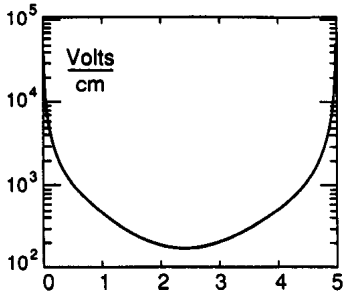

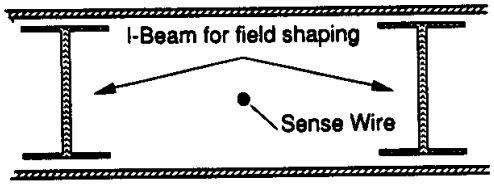

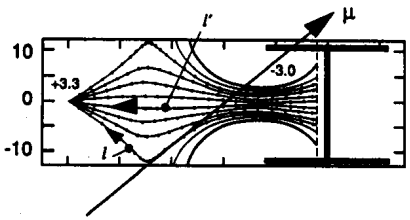

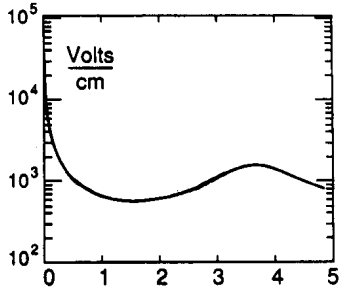

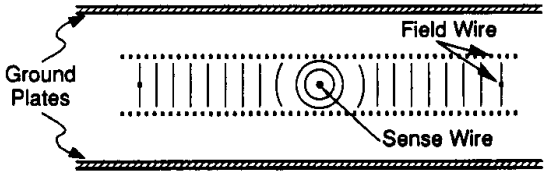

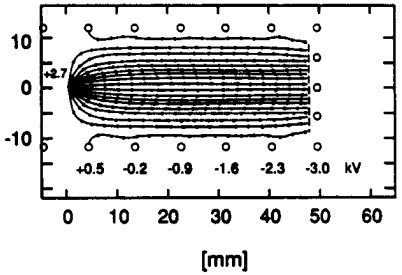

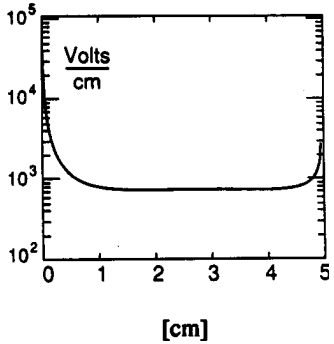

W. Klempt, Detection of Particles with Wire Chambers, Bari 04

The Geiger Counter reloaded: Drift Tube

ATLAS MDT R(tube) =15mm

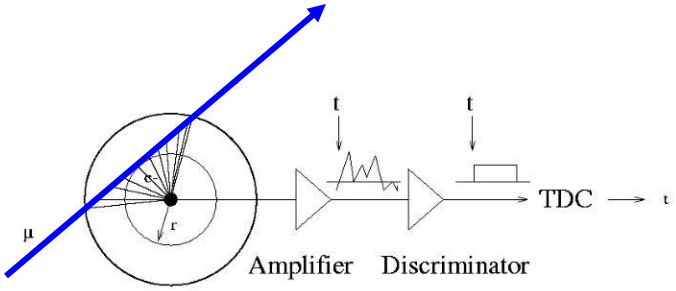

Calibrated Radius-Time correlation

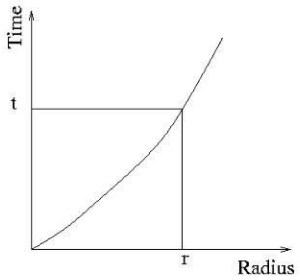

Primary electrons are drifting to the wire.

Electron avalanche at the wire.

The measured drift time is converted to a radius by a (calibrated) radius-time correlation.

Many of these circles define the particle track.

ATLAS Muon Chambers

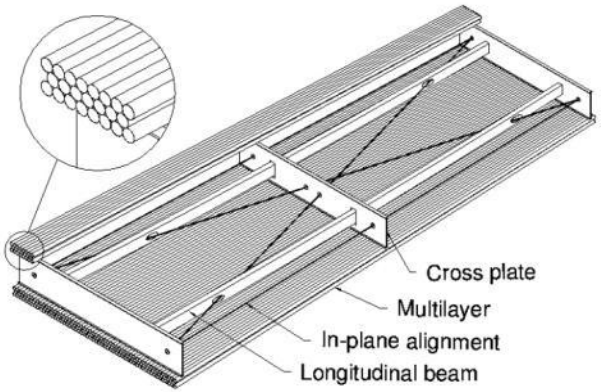

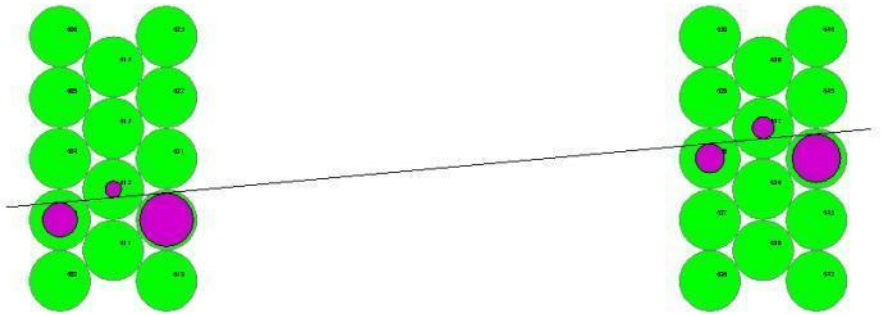

ATLAS MDTs, 80μm per tube

The Geiger counter reloaded: Drift Tube

Atlas Muon Spectrometer, 44m long, from r=5 to11m.

1200 Chambers

6 layers of 3cm tubes per chamber.

Length of the chambers 1-6m !

Position resolution: 80μm/tube, <50μm/chamber (3 bar)

Maximum drift time ≈700ns

Gas Ar/CO_2 93/7

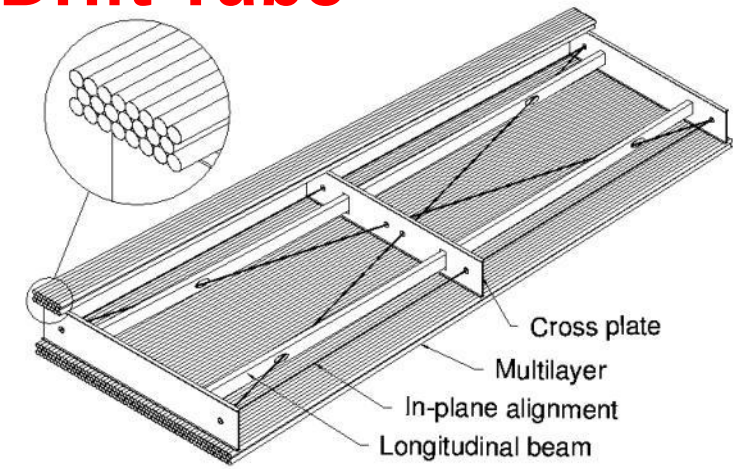

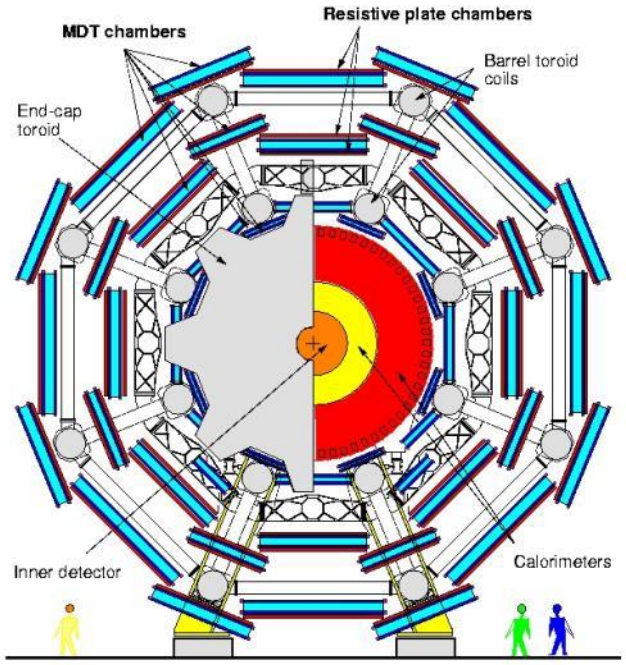

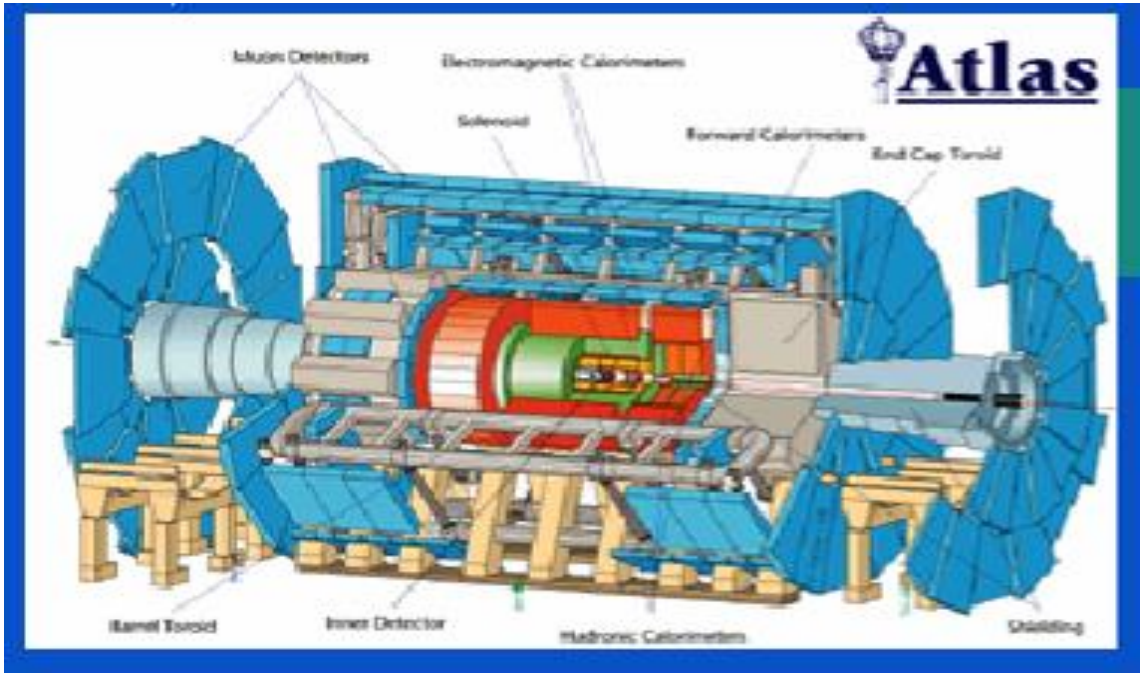

Large Drift Chambers

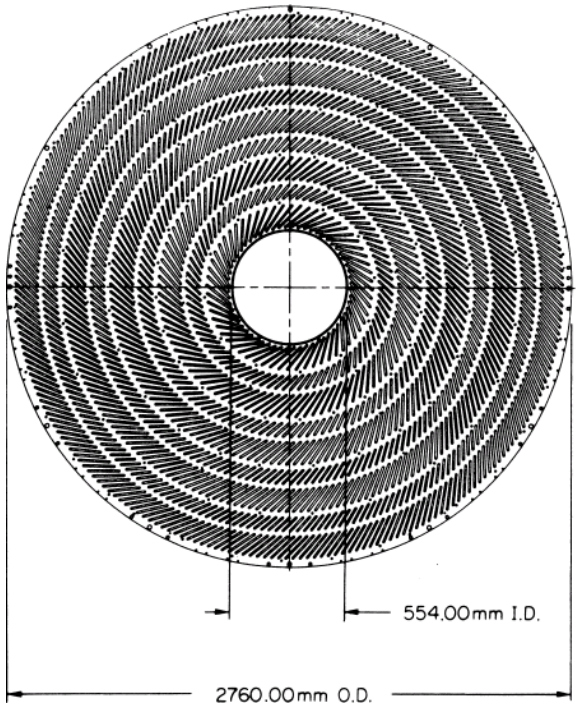

Central Tracking Chamber CDF Experiment.

660 drift cells tilted 45^0 with respect to the particle track.

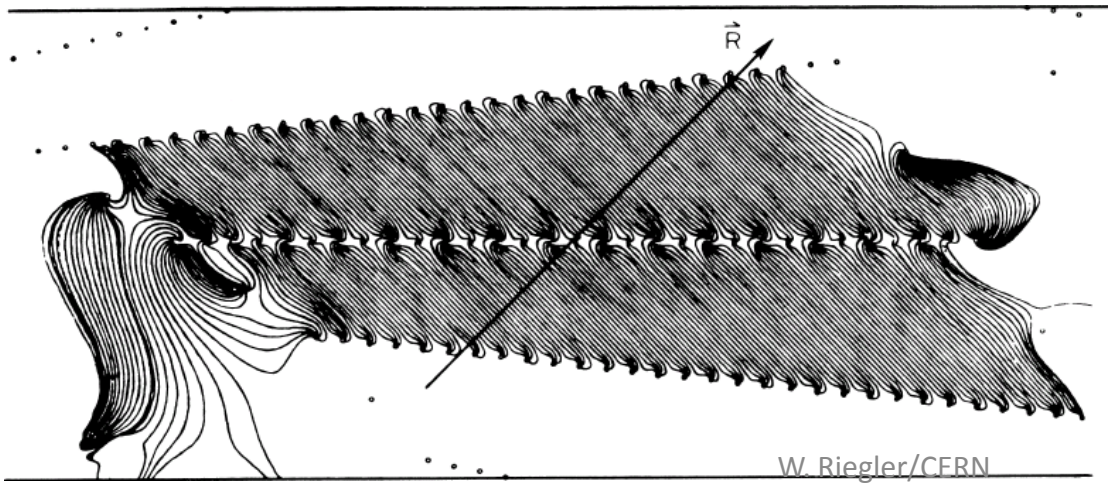

Drift cell

Time Projection Chamber (TPC):

Gas volume with parallel E and B Field.
B for momentum measurement. Positive effect:
Diffusion is strongly reduced by E//B (up to a factor 5).

Drift Fields 100-400V/cm. Drift times 10-100 μs.
Distance up to 2.5m !

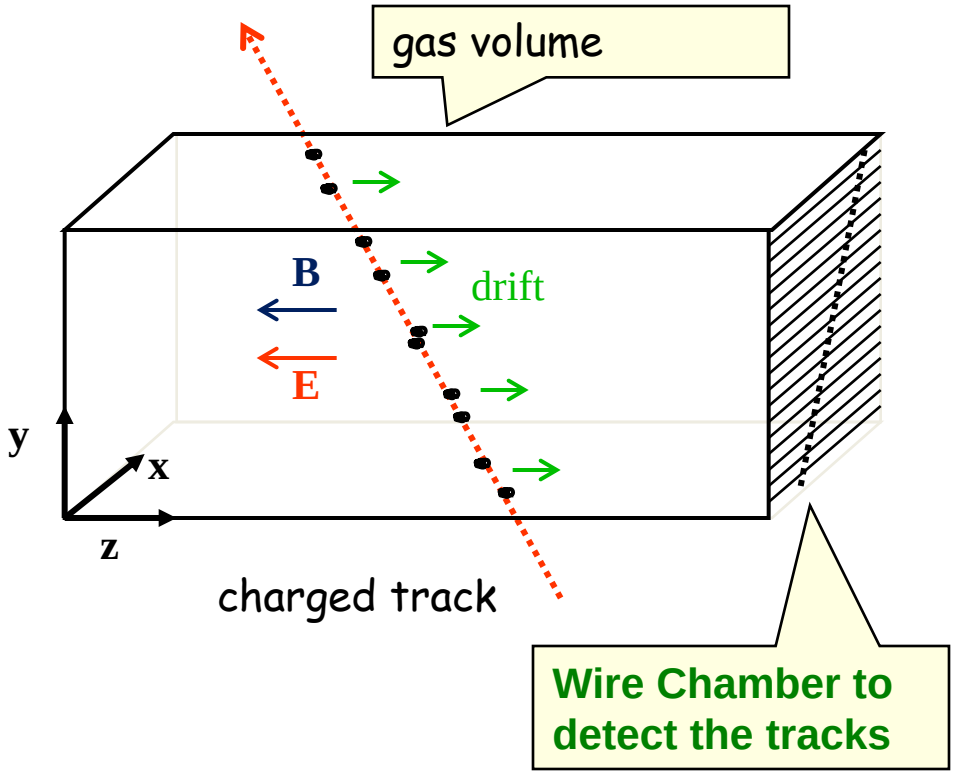

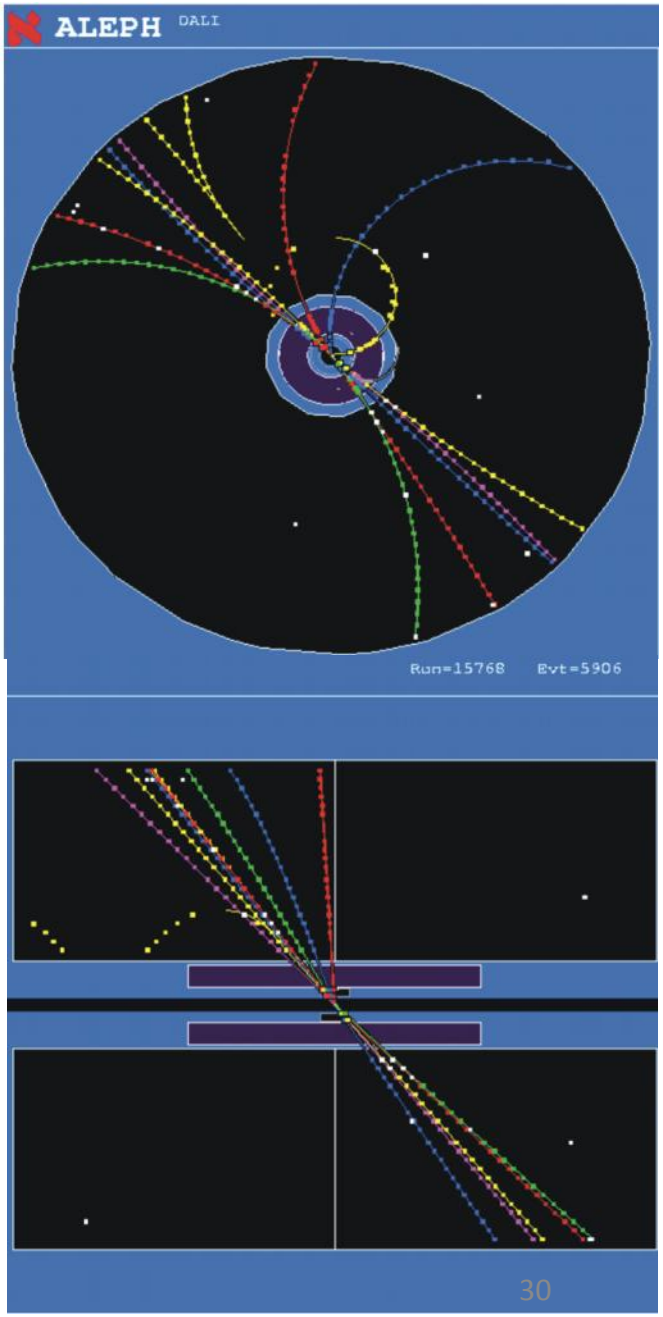

STAR TPC (BNL)

Event display of a Au Au collision at CM energy of 130 GeV/n.

Typically around 200 tracks per event.

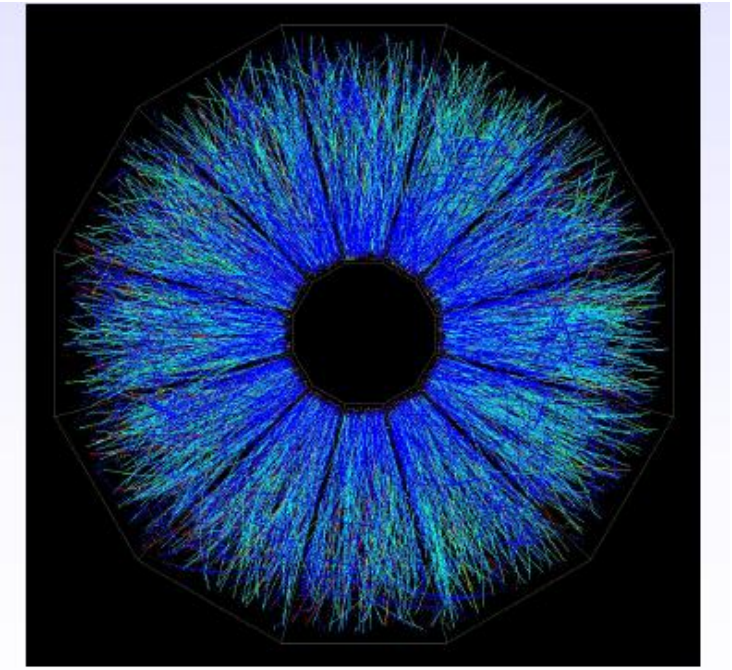

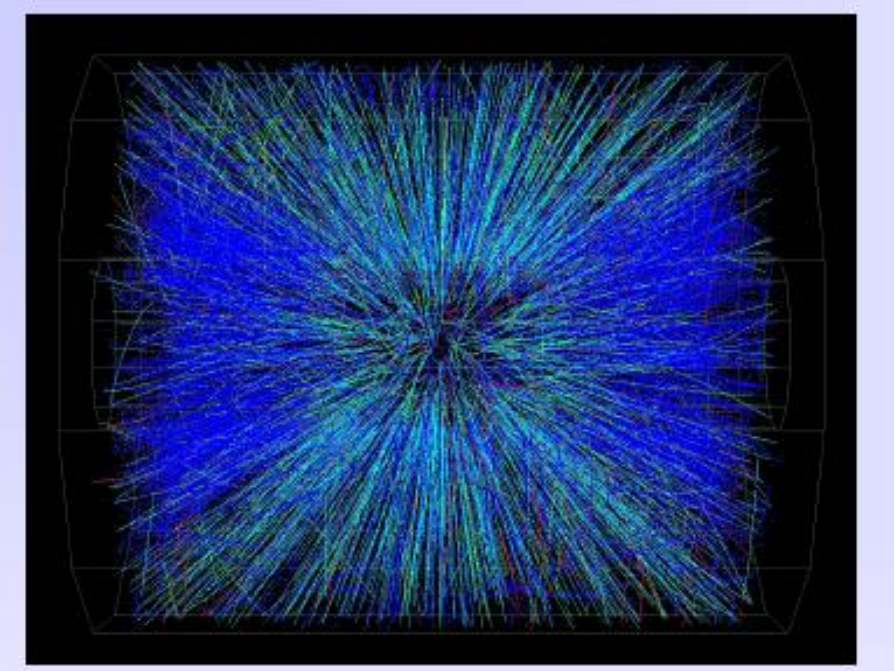

ALICE TPC: Detector Parameters

- Gas Ne/ CO_2 90/10%
- Field 400V/cm
- Gas gain >10^4
- Position resolution σ= 0.25mm
- Diffusion: σ_t= 250μm $\sqrt{cm}$
- Pads inside: 4x7.5mm
- Pads outside: 6x15mm
- B-field: 0.5T

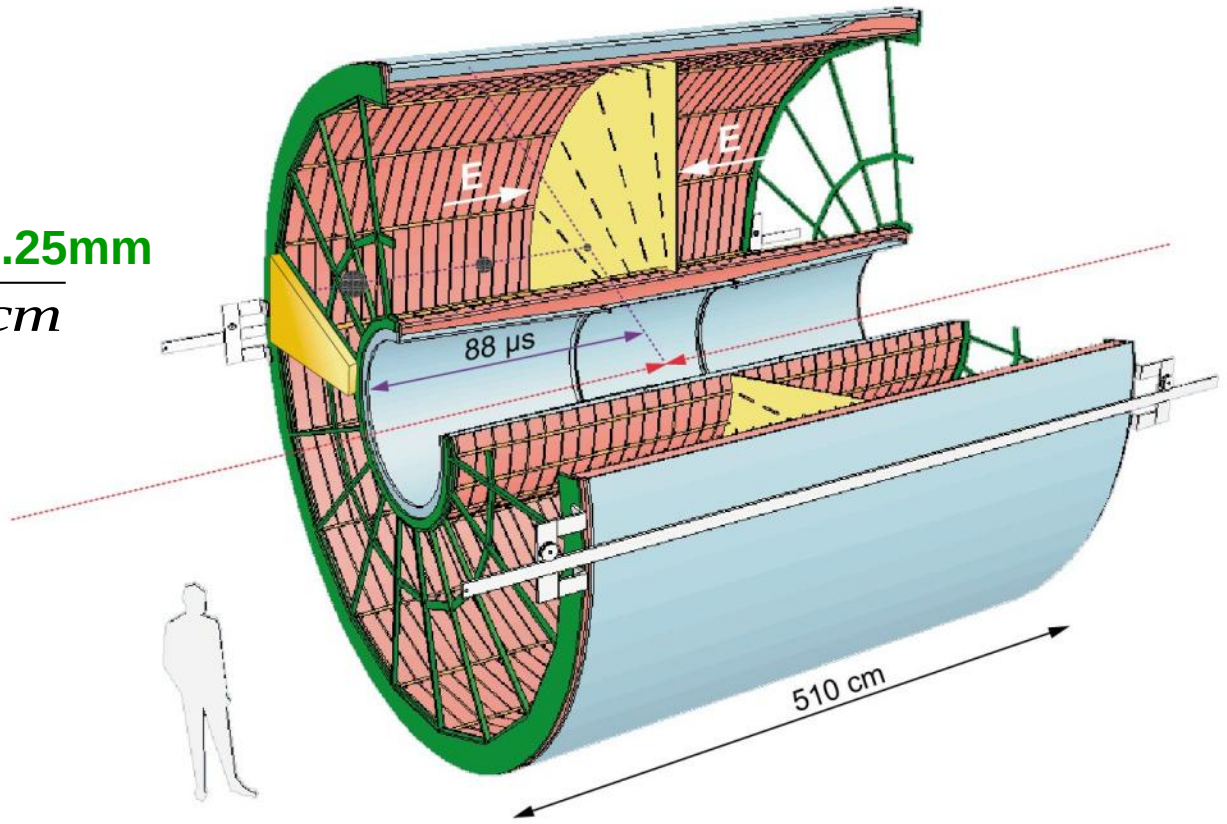

ALICE TPC: Construction Parameters

- **Largest TPC:**
  - **Length 5m**
  - **Diameter 5m**
  - **Volume 88m^3**
  - **Detector area 32m^2**
  - **Channels ~570 000**
- **High Voltage:**
  - **Cathode -100kV**
- **Material X_0**
  - **Cylinder from composite materials from airplane industry (X_0= ~3%)**

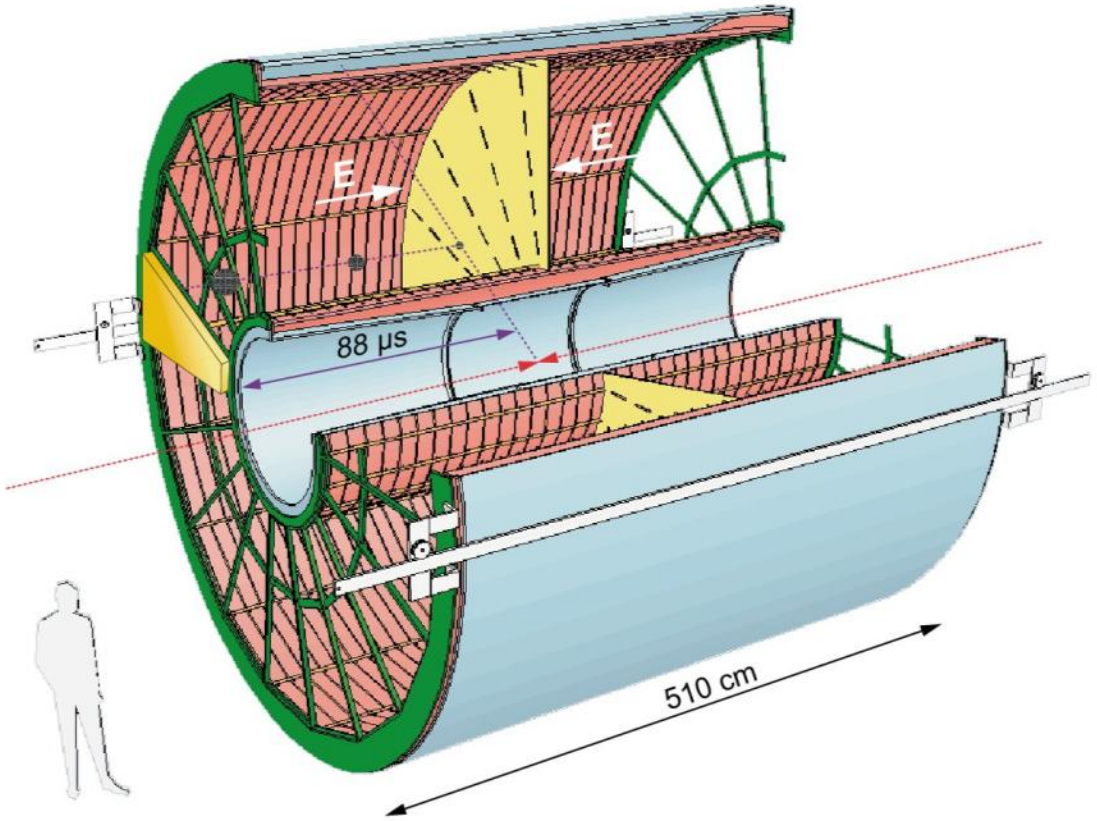

ALICE TPC: Pictures of the Construction

Precision in z: 250μm

End plates 250μm

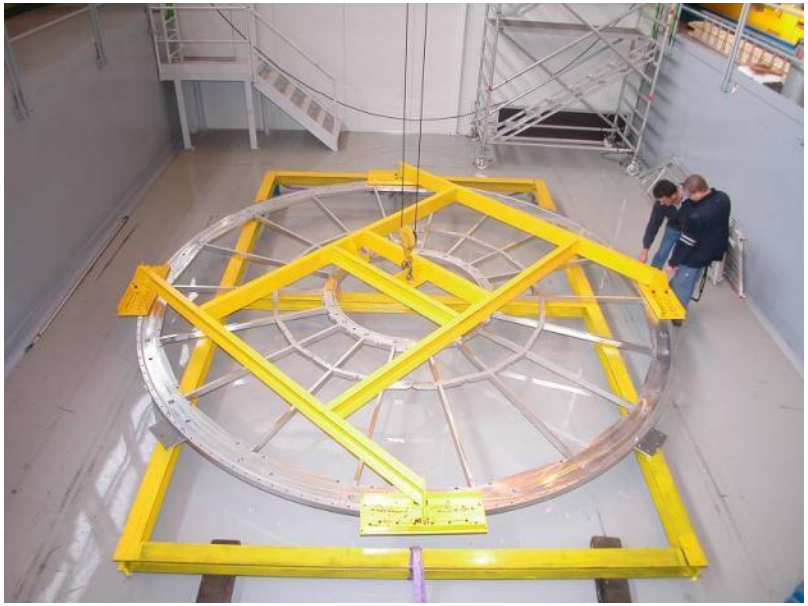

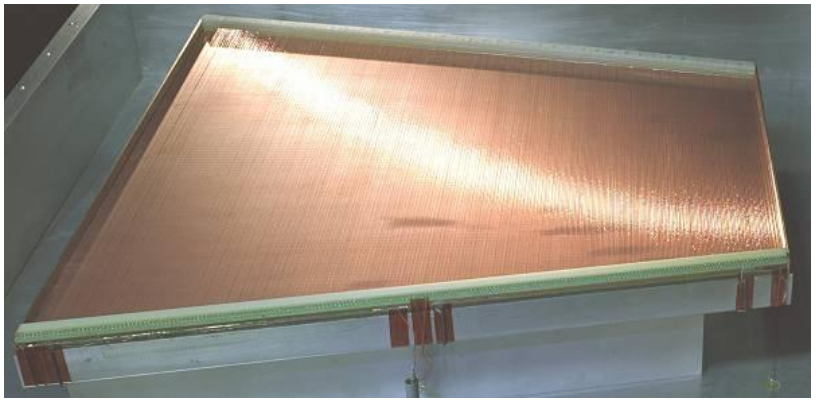

Wire chamber: 40μm

ALICE : Simulation of Particle Tracks

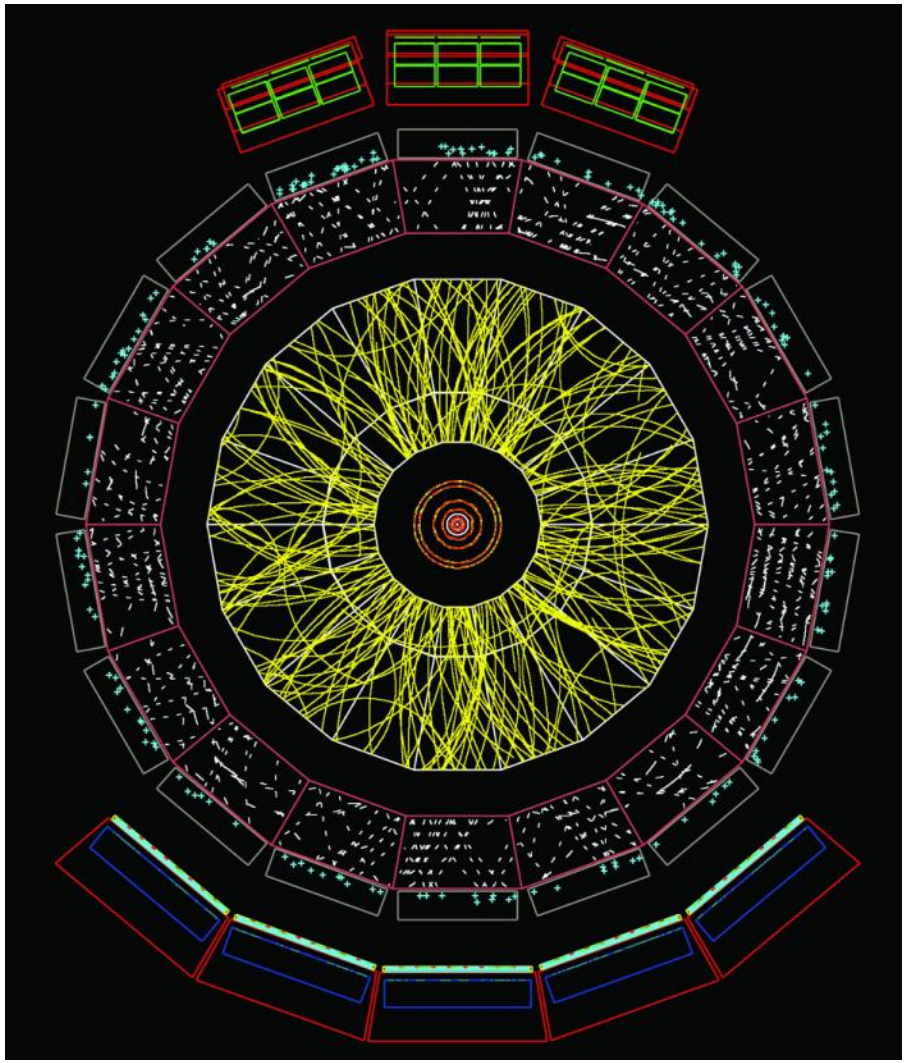

- Simulation of particle tracks for a Pb Pb collision (dN/dy ~8000)
- Angle: Θ=60 to 62º
- If all tracks would be shown the picture would be entirely yellow !
- Up to 40 000 tracks per event !
- TPC is currently under commissioning

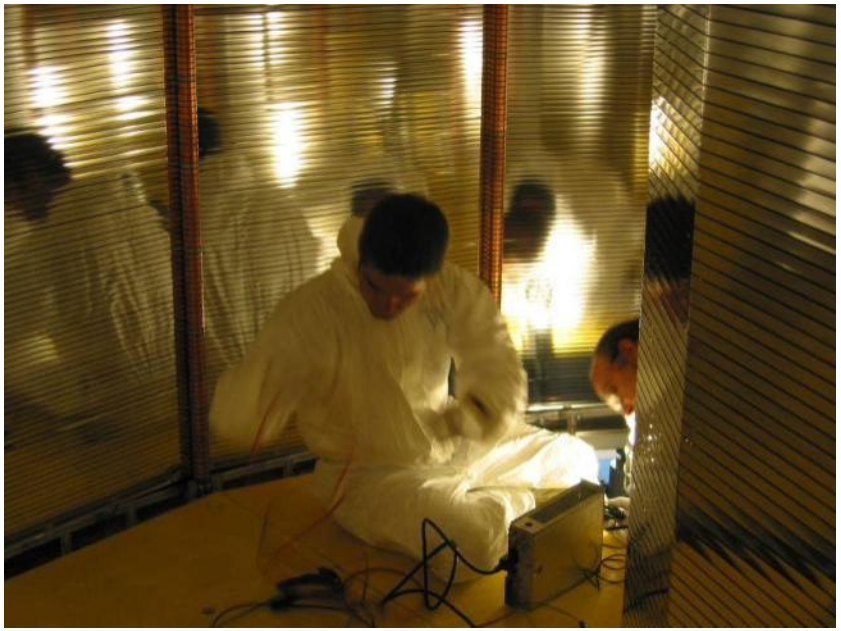

ALICE TPC Construction

My personal contribution:

A visit inside the TPC.

Transport of Electrons in Gases: Drift-velocity

Electrons are completely 'randomized' in each collision. The actual drift velocity along the electric field is quite different from the average velocity of the electrons i.e. →about 100 times smaller.

The driftvelocity v is determined by the atomic crossection σ(ε) and the fractional energy loss Δ(ε) per collision (N is the gas density i.e. number of gas atoms/m³, m is the electron mass.):

$$v = \sqrt{\frac{eE}{mN\sigma}}\sqrt{\frac{\Delta}{2}} \qquad u = \sqrt{\frac{eE}{mN\sigma}}\sqrt{\frac{2}{\Delta}}$$

Because σ(ε)und Δ(ε) show a strong dependence on the electron energy in the typical electric fields, the electron drift velocity v shows a strong and complex variation with the applied electric field.

v is depending on E/N: doubling the electric field and doubling the gas pressure at the same time results in the same electric field.

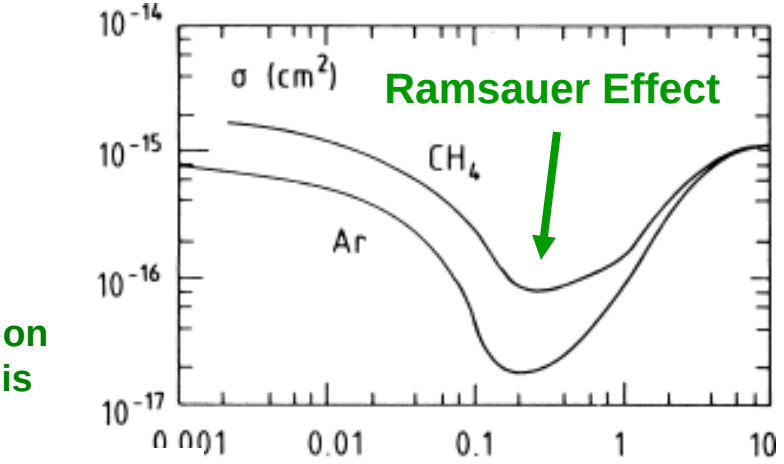

$$\frac{u}{v} = \sqrt{\frac{2}{\Delta}}$$

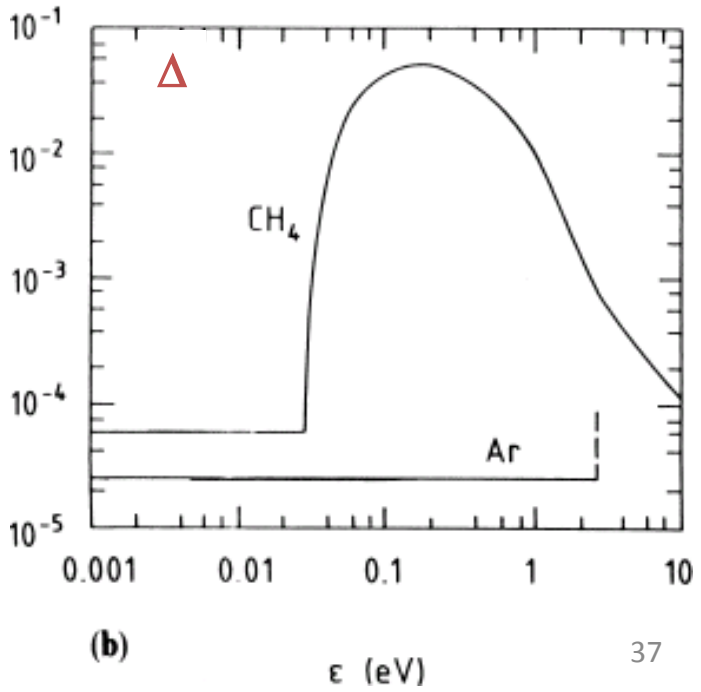

Transport of Electrons in Gases: Drift-velocity

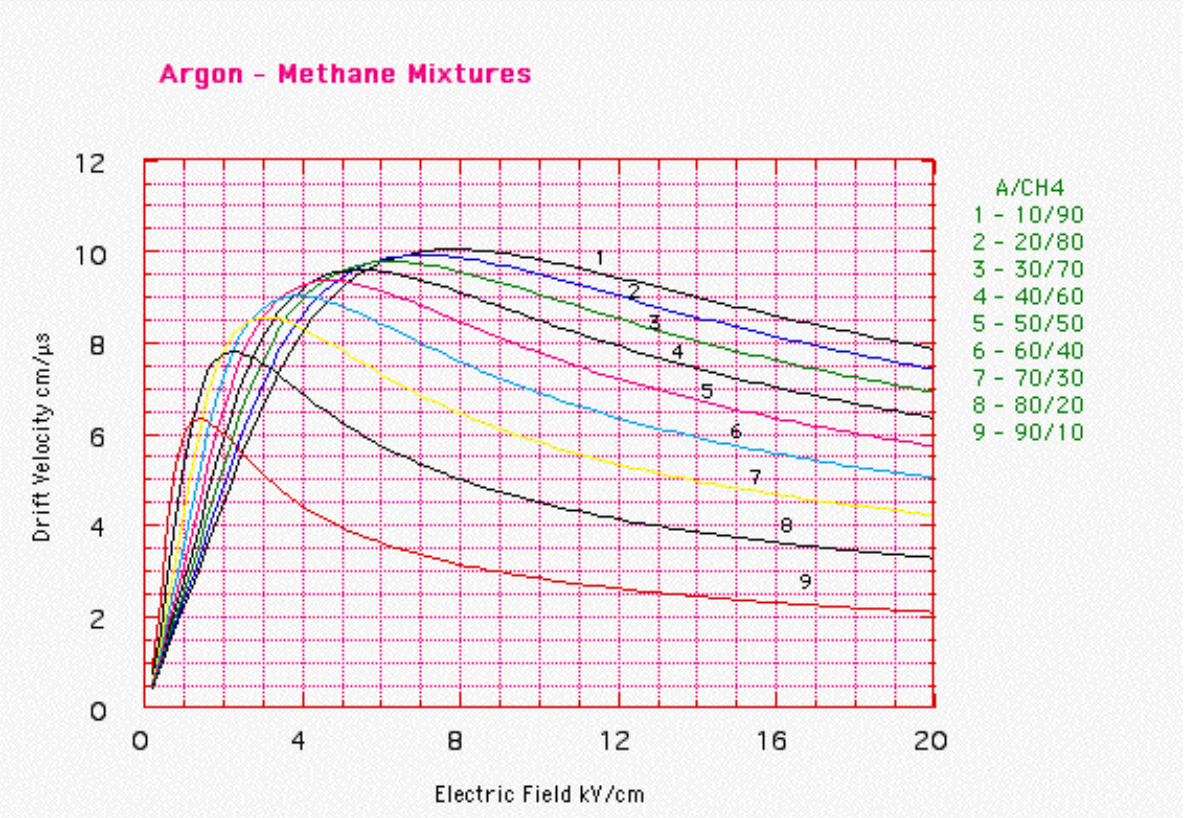

Typical Drift velocities are v=5-10cm/μs (50 000-100 000m/s).
The microscopic velocity u is about ca. 100mal larger.

Only gases with very small electro negativity are useful (electron attachment)
→Noble Gases (Ar/Ne) are most of the time the main component of the gas.
→Admixture of CO_2, CH_4, Isobutane etc. for 'quenching' is necessary (avalanche multiplication – see later).

Transport of Electrons in Gases: Diffusion

An initially point like cloud of electrons will 'diffuse' because of multiple collisions and assume a Gaussian shape. The diffusion depends on the average energy of the electrons. The variance σ^2 of the distribution grows linearly with time. In case of an applied electric field it grows linearly with the distance.

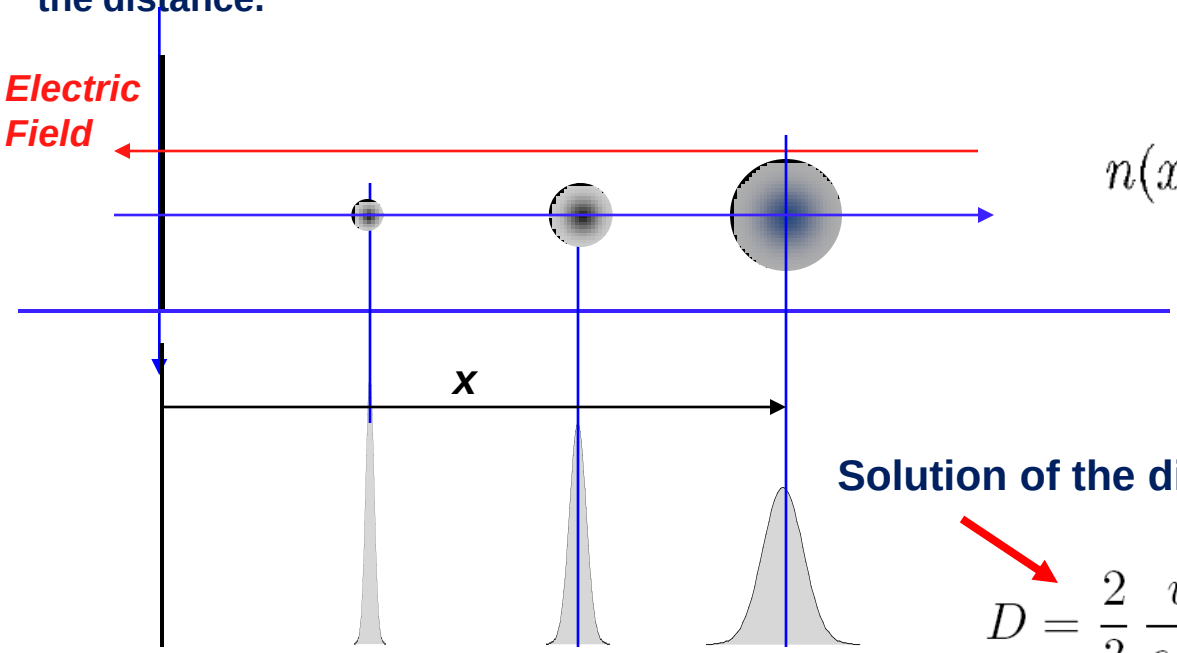

$$n(x) = \left(\frac{1}{\sqrt{4\pi Dt}}\right)^3 e^{\frac{-(x-v_D t)^2}{4Dt}}$$

$$\sigma_x = \sqrt{2Dt}$$

Solution of the diffusion equation (l=drift distance)

$$D = \frac{2}{3}\frac{v}{eE}\epsilon \quad \rightarrow \quad \sigma_x = \sqrt{\frac{4}{3}\frac{l}{eE}\epsilon}$$

Thermodynamic limit:

$$\epsilon = \frac{3}{2}kT \quad \rightarrow \quad \sigma_x = \sqrt{\frac{2kTl}{eE}}$$

Because ε= ε(E/P) $\sigma = \frac{1}{\sqrt{P}} F\left(\frac{E}{P}\right)$

Transport of Electrons in Gases: Diffusion

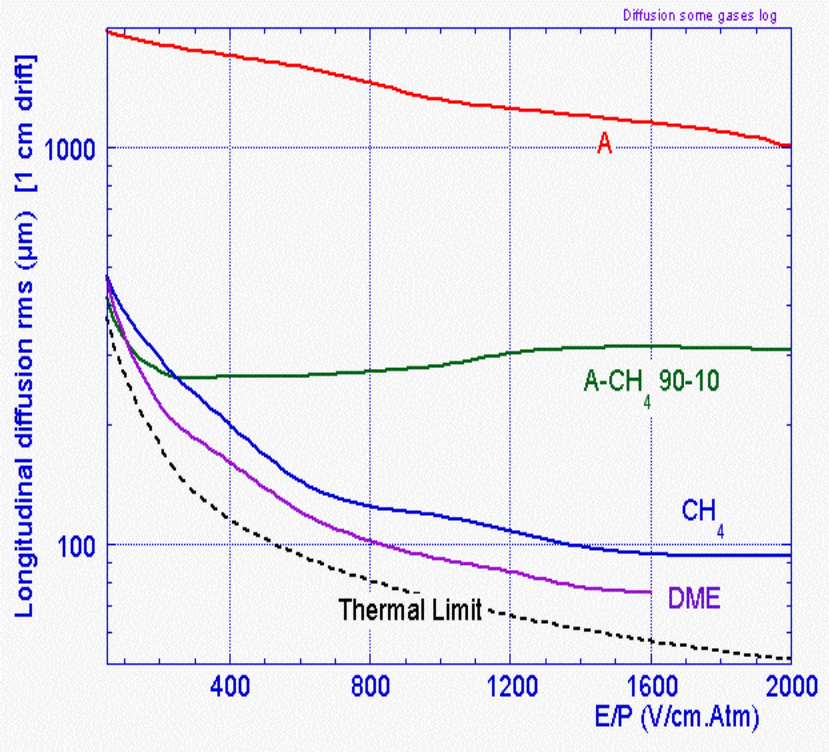

The electron diffusion depends on E/P and scales in addition with $1/\sqrt{P}$.

At 1kV/cm and 1 Atm Pressure the thermodynamic limit is σ=70μm for 1cm Drift.

'Cold' gases are close to the thermodynamic limit i.e. gases where the average microscopic energy $\varepsilon = 1/2mu^2$ is close to the thermal energy 3/2kT.

CH_4 has very large fractional energy loss → low ε → low diffusion.

Argon has small fractional energy loss/collision → large ε → large diffusion.

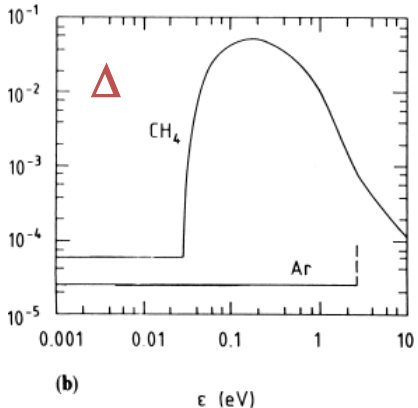

Drift of Ions in Gases

Because of the larger mass of the Ions compared to electrons they are not randomized in each collision.

The crossections are ≈ constant in the energy range of interest.

Below the thermal energy the velocity is proportional to the electric field
$v = \mu E$ (typical). Ion mobility $\mu \approx$ 1-10 cm^2/Vs.

Above the thermal energy the velocity increases with $\sqrt{E}$.

$V = \mu E$, $\mu(Ar) = 1.5 cm^2/Vs$ → 1000V/cm → v=1500cm/s=15m/s → 3000-6000 times slower than electrons !

Position Resolution/Time resolution

Up to now we discussed gas detectors for tracking applications. Wire chambers can reach tracking precisions down to 50 micrometers at rates up to <1MHz/cm^2.

What about time resolution of wire chambers ?

It takes the electrons some time to move from thir point of creation to the wire. The fluctuation in this primary charge deposit together with diffusion limits the time resolution of wire chambers to about 5ns (3ns for the LHCb trigger chambers).

By using a parallel plate geometry with high field, where the avalanche is starting immediately after the charge deposit, the timing fluctuation of the arriving electrons can be eliminated and time resolutions down to 50ps can be achieved !

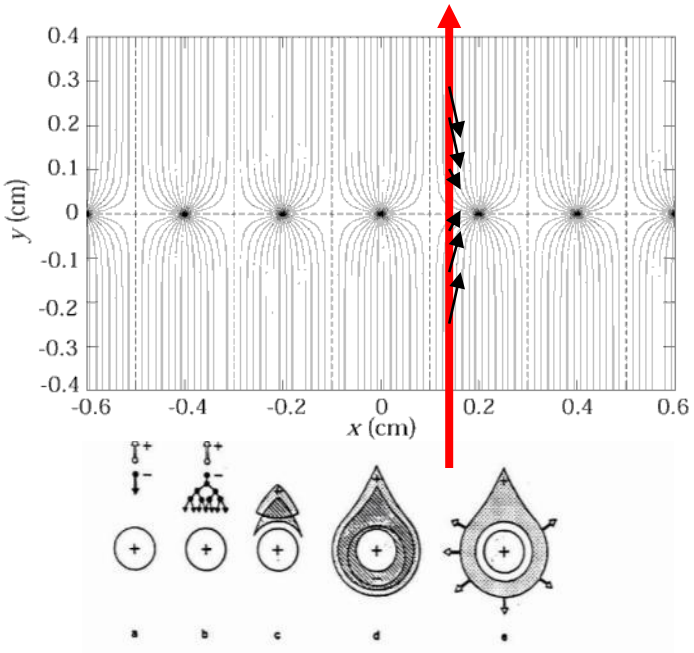

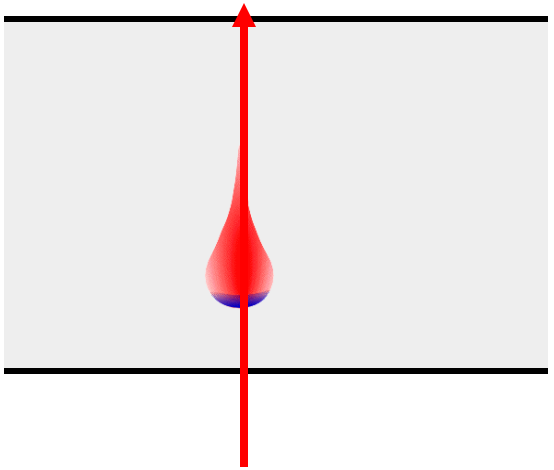

Resistive Plate Chambers (RPCs)

Keuffel 'Spark' Counter:

High voltage between two metal plates. Charged particle leaves a trail of electrons and ions in the gap and causes a discharge (Spark).

→Excellent Time Resolution(<100ps).

Discharged electrodes must be recharged → Dead time of several ms.

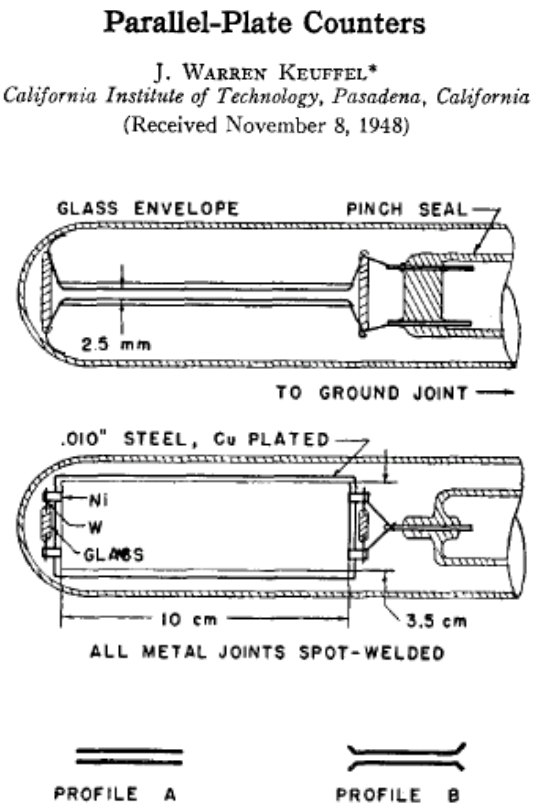

Parallel Plate Avalanche Chambers (PPAC):

At more moderate electric fields the primary charges produce avalanches without forming a conducting channel between the electrodes. No Spark → induced signal on the electrodes. Higher rate capability.

However, the smallest imperfections on the metal surface cause sparks and breakdown.
→ Very small (few cm^2) and unstable devices.

In a wire chamber, the high electric field (100-300kV/cm) that produces the avalanche exists only close to the wire. The fields on the cathode planes area rather small 1-5kV/cm.

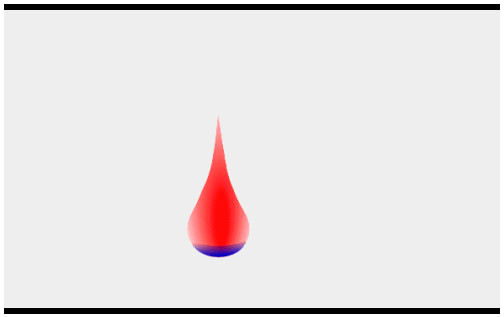

Resistive Plate Chambers (RPCs)

→ **Place resistive plates in front of the metal electrodes.**

No spark can develop because the resistivity together with the capacitance (tau ~ $\varepsilon * \rho$) will only allow a very localized 'discharge'. The rest of the entire surface stays completely unaffected.

→ **Large area detectors are possible !**

Resistive plates from Bakelite ($\rho = 10^{10}$-10^{12} Ωcm) or window glass ($\rho = 10^{12}$-10^{13} Ωcm).

Gas gap: 0.25-2mm.
Electric Fields 50-100kV/cm.
Time resolutions: 50ps (100kV/cm), 1ns(50kV/cm)

Application: Trigger Detectors, Time of Flight (TOF)

Resistivity limits the rate capability: Time to remove avalanche charge from the surface of the resistive plate is (tau ~ $\varepsilon * \rho$) = ms to s.

Rate limit of kHz/cm^2 for 10^{10} Ωcm.

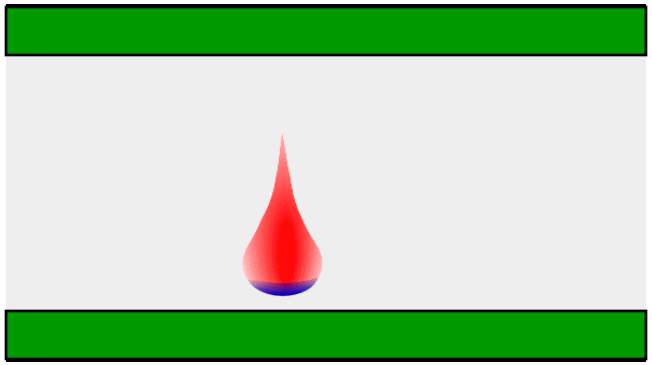

ALICE TOF RPCs

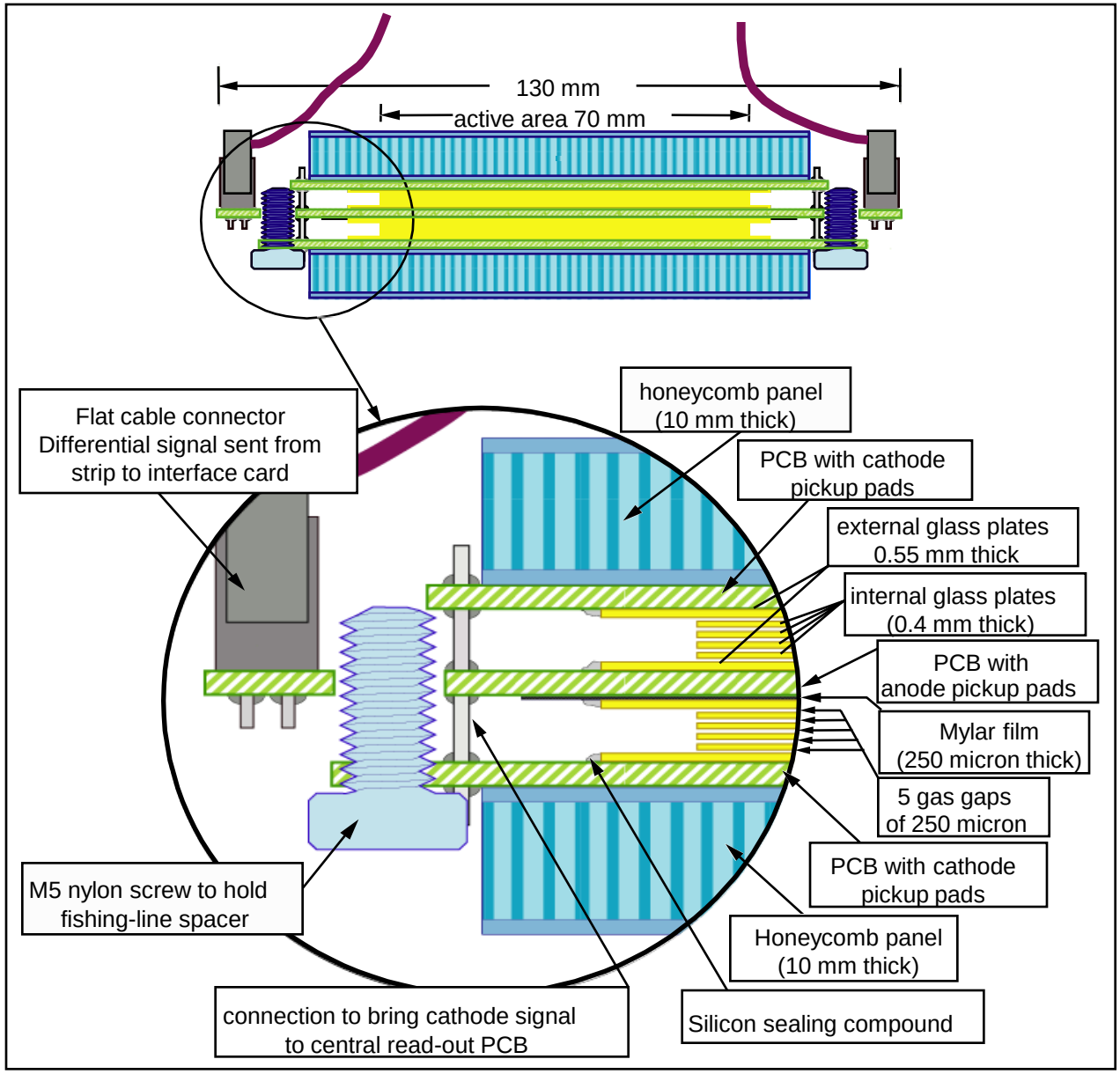

Several gaps to increase efficiency. Stack of glass plates.

Small gap for good time resolution: 0.25mm.

Fishing lines as high precision spacers !

Large TOF systems with 50ps time resolution made from window glass and fishing lines !

Before RPCs → Scintillators with very special photomultipliers – very expensive. Very large systems are unaffordable.

LHC Gas Detector Inventory

Despite the development of the fine grained silicon detectors which now outperform the wire chambers near the interaction point, the large detector volumes surrounding modern experiments have to rely on drift chambers because of their simplicity and also because their measurement accuracy in relation to their size is better than it is in any other instrument. Time Projection Chambers with electron drift lengths up to 2.5 m are the most important tools for studying heavy ion collisions, because of their very low material budget, channel number economy and particle identification capabilities. TPCs are also studied as principle detectors for future electron colliders. 36 years after the first working drift chamber, these instruments are still going strong.

Preface to the second Edition of 'Particle Detection with Drift Chambers', 2008.

After giving an overview of gas detectors at LHC we look at the limits of gaseous detectors.

ATLAS

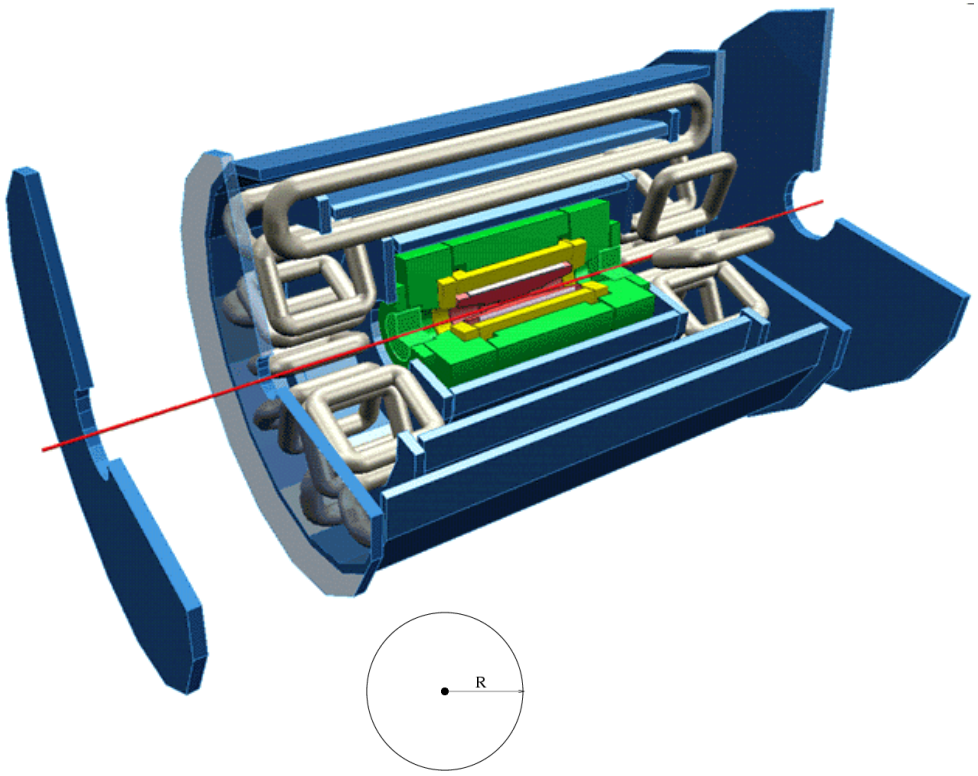

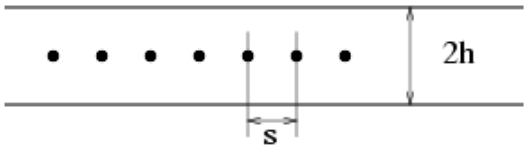

- **Cathode Strip Chambers (Tracking):**
  - h=2.54mm, s=2.54mm
  - 67k cathode channels
  - $Ar/CO_2/CF_4$
  - < 60 μm
- **Thin Gap Chambers (Trigger)**
  - h=1.4mm, s=1.8mm
  - 440k cathode and anode channels
  - n-Pentane /CO_2 45/55
  - < 99% in 25ns with single plane

- **Monitored Drift Tubes (Tracking)**
  - R=15mm
  - 370k anode channels
  - Ar/CO_2 93/7 (3 bars)
  - < 80μm
- **Transition Radiation Tracker (Tracking)**
  - R=2mm
  - 372k anode channels
  - $Xe/CO_2/CF_4$ 70/10/20
  - $Xe/CO_2/O_2$ 70/27/3
  - < 150 μm

- **RPCs (Trigger):**
  - g=2mm, 2mm Bakelite
  - 355k channels
  - $C_2F_4H_2$/Isobutane/SF_6 96.7/3/0.3
  - < 98% with a single plane in 25ns

CMS

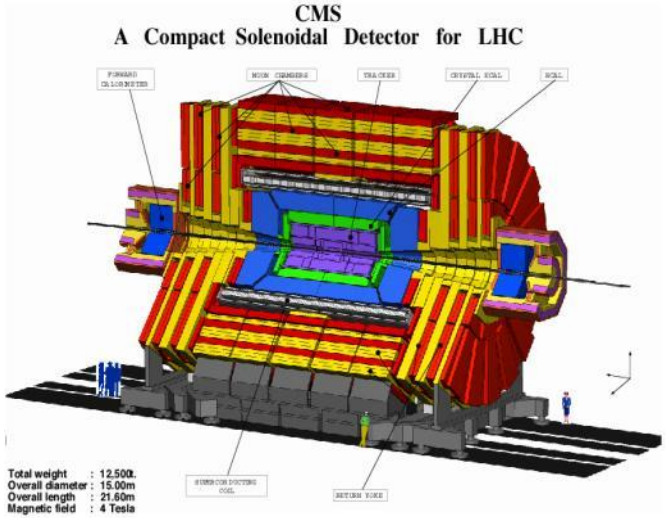

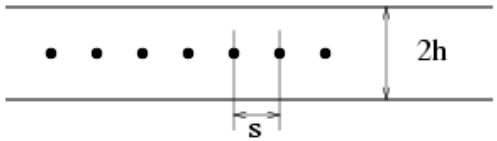

- **Cathode Strip Chambers (Trigger, Tracking):**
  - h=4.25mm, s=3.12mm
  - 211k anode channels for timing
  - 273k cathode channels for position
  - $Ar/CO_2/CF_4$ 30/50/20
  - < 75-150 μm

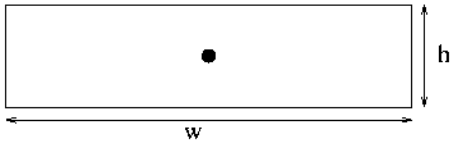

- **Rectangular 'Drift Tubes' (Trigger, Tracking)**
  - w=42mm, h=10.5mm
  - 195k anode channels
  - Ar/CO_2 85/15
  - < 250 μm

- **RPCs (Trigger):**
  - g=2mm, 2mm Bakelite
  - Many k channels
  - $C_2F_4H_2$/Isobutane/SF_6 96.5/3.5/0.5
  - < 98% with a single plane in 25ns

LHCb

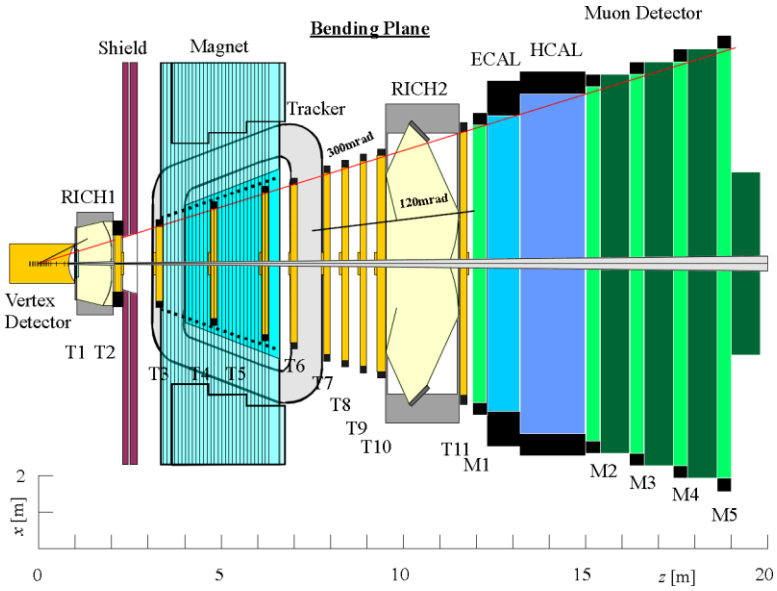

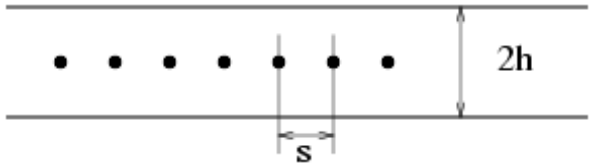

- **Muon Chambers (Trigger):**
  - h=2.5mm, s=2mm
  - 125k cathode and anode pads
  - Ar/CO_2/CF_4 40/55/5
  - < 3ns for two layers
- **GEM (Trigger):**
  - 5k channels
  - Ar/CO_2/CF_4 75/10/15
  - <4.5 ns for one triple GEM

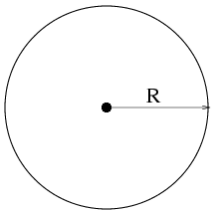

- **Outer Tracker (Tracking):**
  - R=2.5mm
  - 51k anode channels
  - Ar/CO_2/CF_4 75/10/15
  - < 200 μm

ALICE

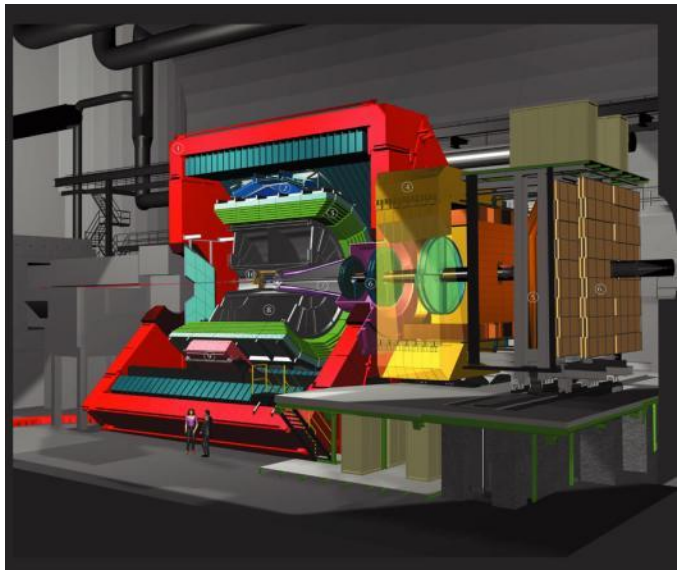

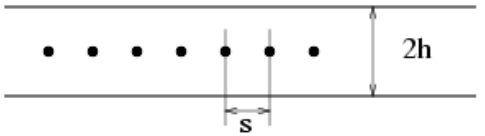

- TPC with wire chamber cathode pad readout
  - 1.25-2.5mm wire pitch
  - 2 - 3 mm plane separation
  - 570k Readout Pads
  - Ne/CO_2 90/10
- TRD
  - 1160 k channels
  - Xe/CO_2 85/15
  - s=5mm, h=3.5mm
- HMPID
  - s=2mm, h=2mm
  - Methane
  - 160k channels
- Muon Chambers
  - 1000k channels
  - <100um
  - S=2.5mm, h=2.5mm
  - Ar/CO_2 80/20

- TOF RPCs
  - G=0.25mm, 0.4mm glass, 10gaps
  - 160k channels
  - <50ps/10gaps
  - $C_2F_4H_2$/Isobutane/SF_6 96.5/3.5/0.5
- Trigger RPCs
  - G=2mm, 2mm bakelite
  - Ar/Isobutane/$C_2F_4H_2$/SF_6 49/7/40/4
  - 21k channels

TOTEM

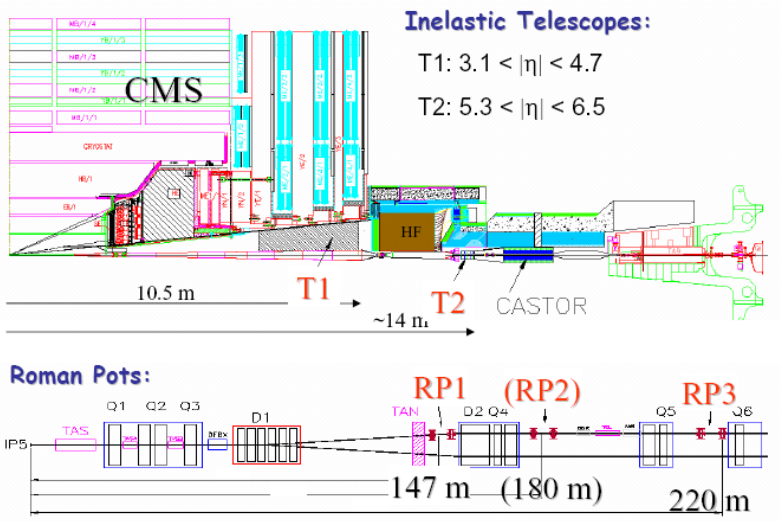

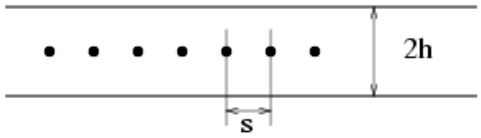

- **T1: CSCs**
  - 13k anode channels
  - 21k cathode channels
  - s=3mm, h=5mm
  - Ar/CO_2 50/50
- **T2: GEMs**
  - Ar/CO_2 50/50
  - 24.5k channels

Limits of LHC Gas Detectors

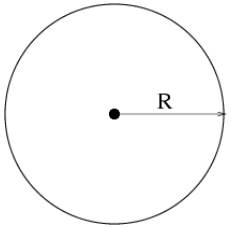

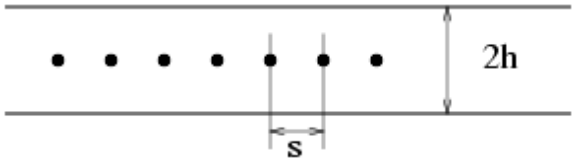

Occupancy

Space Charge Effects (Wire Chambers), Voltage Drop (RPCs)

Aging

Occupancy

The occupancy is the fraction of time a readout channel is occupied by a signal. With a pulse-width of T and a rate of ν the occupancy is equal to T x ν. Occupancy scales with the particle rate.

ATLAS TRT: ν=10MHz, T=20ns, occupancy = 0.2 → 20%.

Large occupancy results in inefficiency and fake tracks.

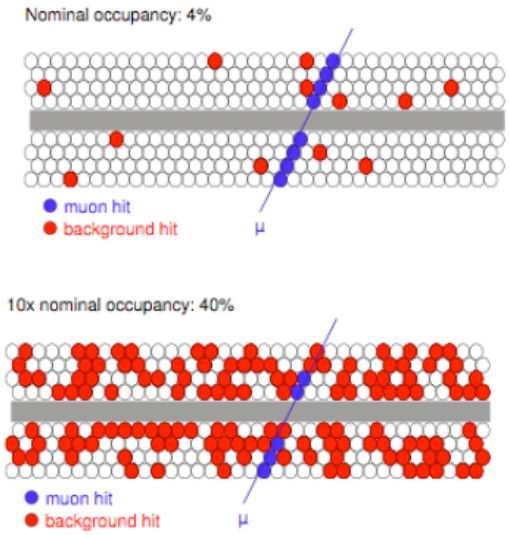

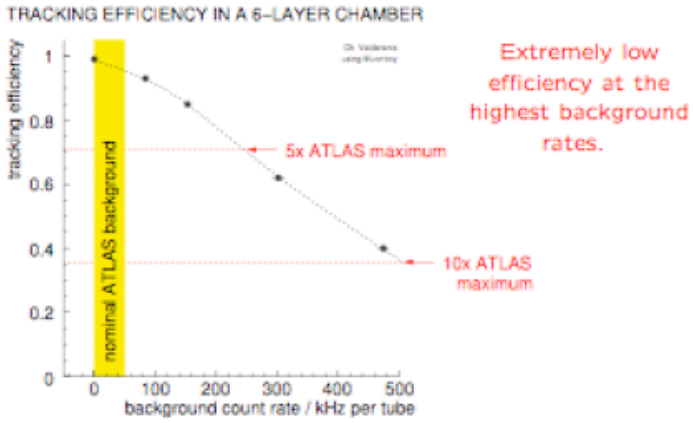

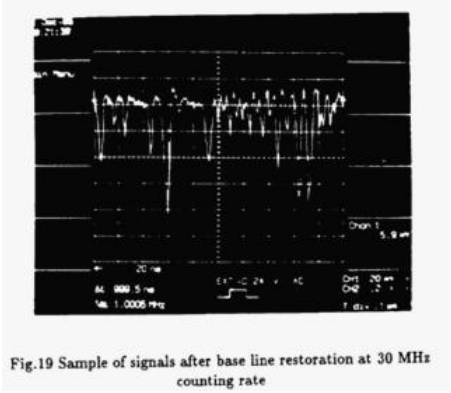

Fig.19 Sample of signals after base line restoration at 30 MHz counting rate

Occupancy, Pulsewidth T

Wire Chambers:

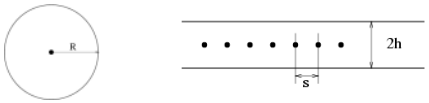

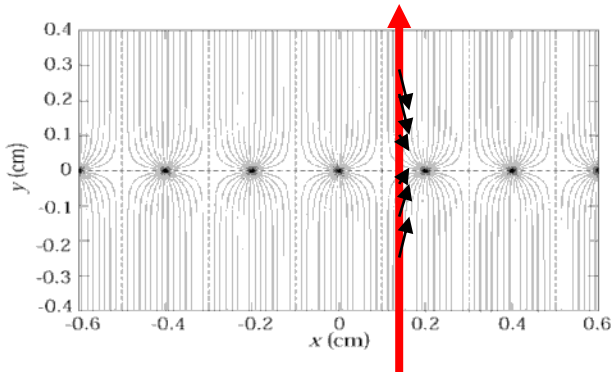

Irreducible pulse-width:
Avalanche signal stops when all electrons have reached the wire.

Electronics:
Shape of the individual avalanche signals is determined by the electronics. Wire chamber signals have a short electron component and a long ion tail $i(t)=Q_e\delta(t)+I_0/(t+t_0)$. t_0=1.5ns for ATLAS TRT, t_0=10ns for ATLAS MDT.

In order to accumulate a certain amount of ion signal charge the electronics peaking time tp should be >= t_0.
ATLAS MDT tp=15ns. ATLAS TRT, tp=5ns. Design such that 'irreducible' pulse-width dominates.

For charge measurement on cathode strips (position resolution) one has to integrate significantly longer (100-200ns) to arrive at a good S/N ratio.

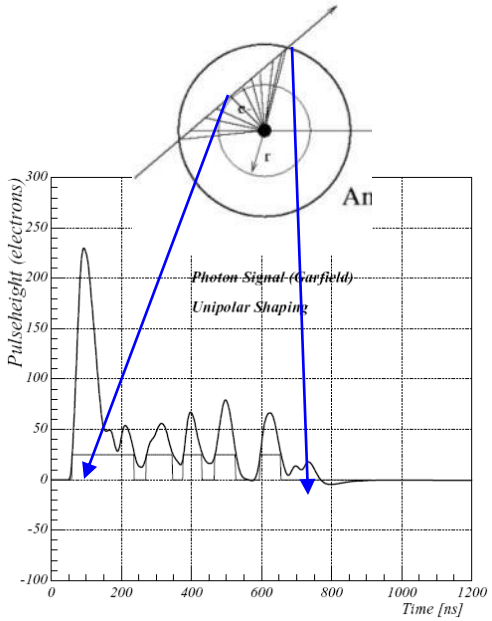

ATLAS MDT T_{av}≈520ns
ATLAS TRT T_{av}≈20ns

Occupancy: Pulsewidth T

Occupancy is a limiting factor for LHC wire chambers. This is obvious by design – for economical reasons the channel granularity was designed such that the occupancy is 'just' O.K. – typically few %.

ATLAS TRT has already 20% occupancy at nominal LHC rates. Will be fully occupied at SHLC.

ATLAS muon system wire chambers (MDTs, TGCs, CSCs) were designed to work at 5x the nominal background rate with a few % occupancy. Large safety factor (complex background processes) and large variation of occupancy in η. Possibly additional shielding foreseen. From point of view of frontend channel occupancy the idea is that the current system will (just) work at SHLC. Some higher level electronics and trigger algorithms will have to be modified.

CMS wire chambers (Barrel Drift Tubes, Forward CSCs) follow the same line of thought.

Space Charge Effects in Wire Chambers

The Ions, drifting from the wires to the cathode are representing a space charge in the chamber volume.

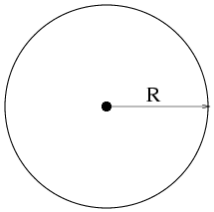

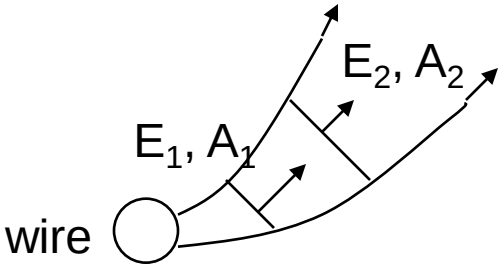

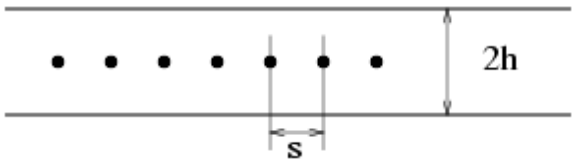

$v_{Ion} = \mu E$

$E_1 A_1 = E_2 A_2$ (Gauss' Law)

Volume= A*v*dt = μEAdt

Since EA = constant along the 'flux tube', the ion charge density is constant along the entire flux tube.

In case the electric field is uniform around the wire and the wire is uniformly irradiated (which is the case for the standard LHC geometries), the volume entered by the fields lines from the wire is filled with a constant space charge density.

For both geometries this means that the entire chamber volume is filled with a constant space charge density.

This charge density causes a drop of the electric field near the wire and therefore a reduced gas gain.

Space Charge Effects in Wire Chambers

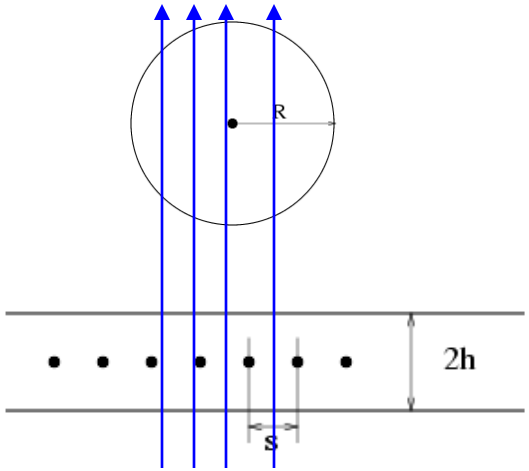

$$\Delta V = \frac{R^3 q \ln \frac{R}{R_a}}{4\pi\varepsilon_0 \mu V_0} \times Flux$$

$$\Delta V = \frac{s h^2 q \ln \frac{R_c}{R_a}}{4\pi\varepsilon_0 \mu V_0} \times Flux \qquad R_c = \frac{s}{2\pi} e^{\frac{\pi h}{s}}$$

Flux = tracks/cm^{2}s
R_a = wire radius
μ= ion mobility
V_0=applied wire voltage
q=average total avalanche charge per track

dV = effective voltage drop, i.e. gas gain reduction due to the spacecharge is equal to the a voltage reduction of dV without spacecharge.

Strongest dependence on chamber geometry.
MDT, TRT: (15mm/2mm)^3=422
In addition: MDT 3 bars, TRT 1 bar → ion mobility of TRT is factor 3 higher → factor 422*3=1265 higher rate capability !

0.5 kHz/cm^2 → 10% gain loss.

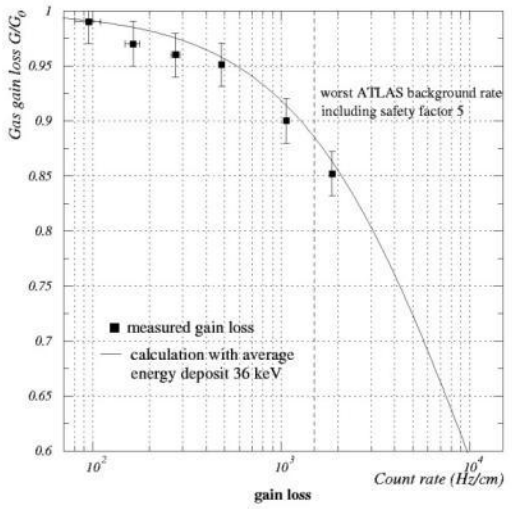

NIMA 446(2000) 435-43

Space Charge Effects in Wire Chambers

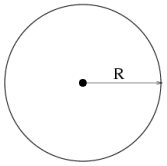

R^3/μ

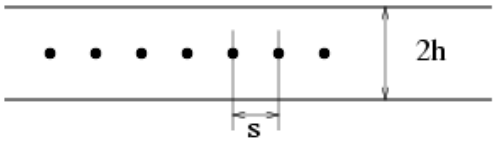

sh^2/μ μ(ARGON,1bar) ≈ 1.5cm²/Vs

			10%loss @	real rate
ATLAS MDT:	**R^3/μ =6.75 (Vcm s)**	→	**0.5 kHz/cm²**	**0.5 kHz/cm²**

Assuming naïve scaling only due to geometry (same gain, HV, Ionization …)

ATLAS TRT:	**sh^2/μ= 0.0053**	**fact 1274**	**637 kHz/cm²**	**1200kHz/cm²**
LHCb OT:	**R^3/μ =0.0104**	**fact 650**	**324 kHz/cm²**	**500kHz/cm²**
CMS CSCs:	**sh^2/μ=0.03757**	**fact 180**	**90 kHz/cm²**	**0.5kHz/cm²**
ATLAS CSCs:	**sh^2/μ=0.011**	**fact 614**	**307 kHz/cm²**	**0.5kHz/cm²**
LHCb MWPC:	**sh^2/μ=0.00833**	**fact 810**	**405 kHz/cm²**	**50kHz/cm²**
TOTEM CSCs:	**sh2/μ=0.05**	**fact 135**	**67kHz/cm²**	
(ATLAS TGCs:	**sh^2/μ=0.0023**	**fact 2934**	**1450 kHz/cm²**	**0.2kHz/cm²**

(Resistivity Limit 0.5kHz/cm², gain 10^6)

→LHC drift chambers are operated at particle rates where gain drop due to spacecharge effects becomes significant.

→LHC MWPCs (CSCs) have a large margin.

Space Charge Effects in Wire Chambers

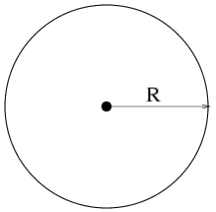

In addition to the gain loss, the space charge changes the relation between radius and drift time. This would in principle not change the resolution (if the space charge is constant).

At a given stationary particle rate there is still a fluctuation due to Poisson statistics, so the space charge is fluctuating. This fluctuation of the space charge results in a fluctuating field and therefore a deterioration of the resolution.

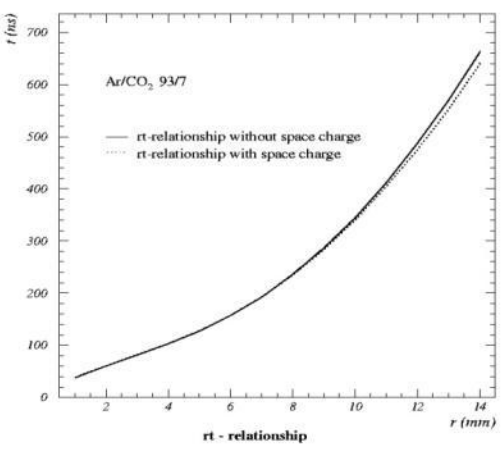

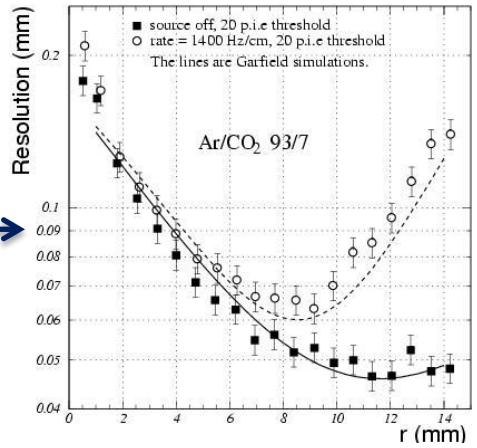

M. Aleksa et al. NIMA 446(2000) 435-43

Note that the solid lines represent a first principle GARFIELD simulation with inclusion of fluctuating space charge !!

ATLAS MDTs and CMS DT will have reduced resolution due to this effect.

Rate Effects in RPCs

The rate limitation of an RPC is due to the resistive plates. The current due to the incident particles flows through the plates and causes a voltage drop in the as gap reducing the gas gain.

A typical operating voltage is 10kV. The voltage drop is given by $dV=R*I = 2\rho\nu gQ$
Example ATLAS, CMS RPCs: Q=total charge/track=25pC, ν=rate Hz/cm^2, g=2mm, ρ=volume resistivity =$10^{10}\Omega$cm.

100Hz/cm^2 → 10V. Operation up to 1kHz/cm^2 has been proven in testbeams.
The typcal nominal rates for the RPCs in ATLAS and CMS (eta<1.6) are <10Hz/cm^2, so from this point of view the chambers might operate at SLHC in most regions (if ageing effects can be brought under control and the resistivity stays constant over time).

CMS forward region has already >100Hz/cm^2 at nominal LHC rates, so there one will push the limit at SLHC rates.

Wire Chamber Aging

The typical gas gain of LHC wire chambers is 2×10^4

Magic number for charge deposit in 10 years of LHC operation is 1C/cm of wire (LHCb OT 2.5C/cm, ATLAS TRT 8C/cm) and $1C/cm^2$ of cathode.
Fortunately gas mixtures have been found which seem to withstand this accumulated charge.

Aging effects are in general the main decisive factor for the gas choice.

'Traditional Gases' containing hydrocarbons as quenchers showed severe aging effects at deposited charges much much lower than the ones needed for LHC. The effect is mainly due to polimerization resulting in deposits on wires and cathodes (painful learning process).

Wire chambers prototypes have been proven to work for the entire LHC period without performance degradation. Since the testing conditions shouldn't be far from reality these tests took several years.

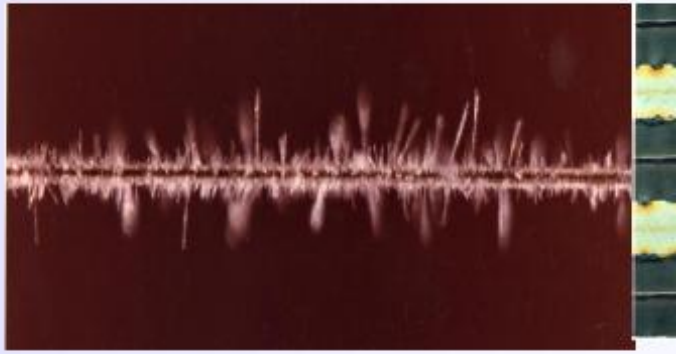

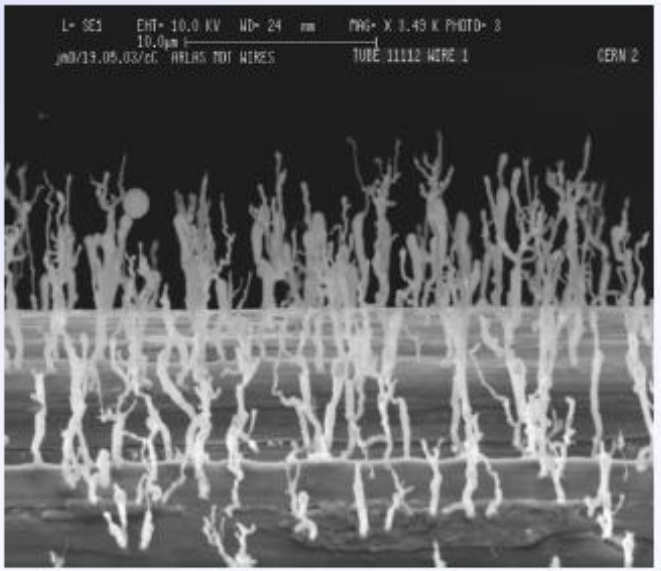

Wire Chamber Aging

All LHC wire chambers are based on noble gases (Ar, Xe, Ne) together with $C0_2$ for quenching.

Some of them add CF_4 for 'cleaning'. CF_4 --- Medicine or Poison ?

Attractive because of fast electron drift velocity, it can prevent polymer formation and even remove them from electrodes if already present.

CF_4 is however also etching detector materials, especially in connection with water. ATLAS TRT had to abandon CF_4 because glass wire joints inside the modules were etched to the point of breakage. CF_4 mixture will only be used for dedicated cleaning runs. LHCb wire chambers had to reduce CF_4 because of etching of the FR_4 boards.

Wire Chamber Aging

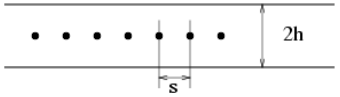

LHCb MWPCs:

Wire after 0.5C/cm

Ar/CO_2/CF_4 40/40/20

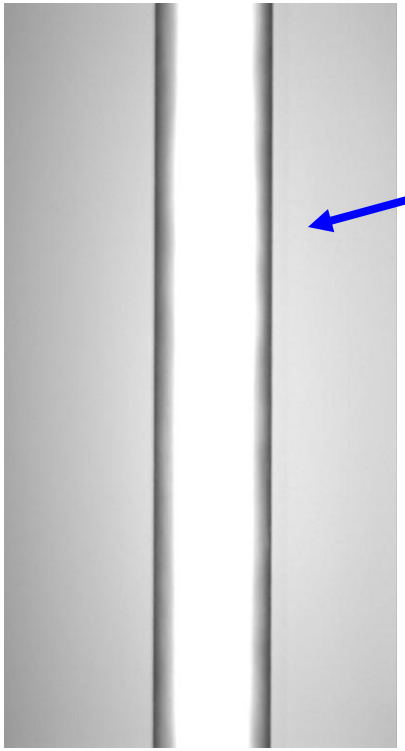

CF_4 is a fantastic gas !

Cathode after 1.7C/cm^2

CF_4 is a terrible gas !

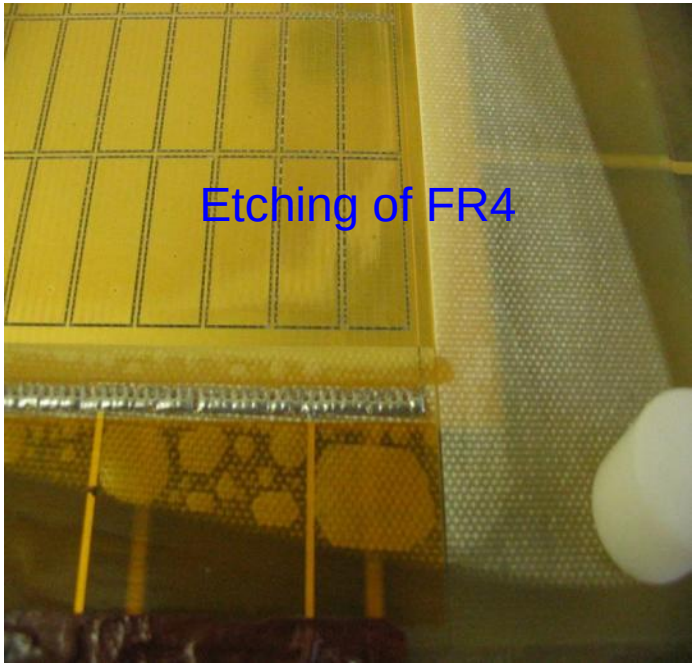

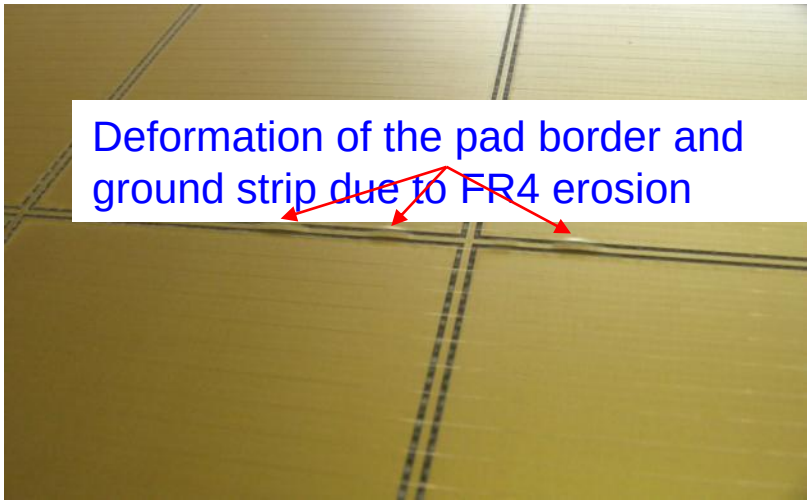

Wire Chamber Aging

LHCb MWPCs:
Cathode after 1.7C/cm^2 Ar/CO2/CF4 40/40/20 → Decision to go back to 5% CF_4
→ Delicate Balance

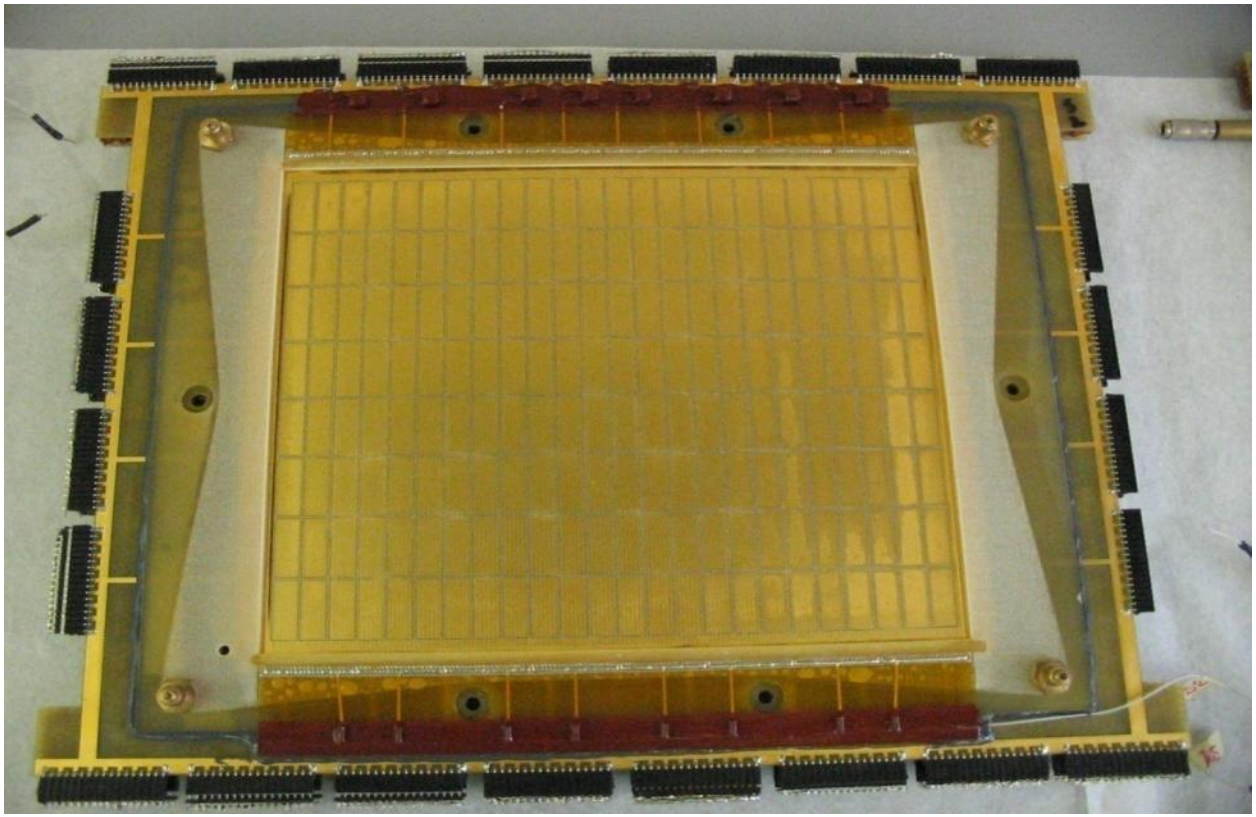

RPC Aging

All LHC RPCs use Freon/Isobutane/SF_6 gas mixtures. Non flammable heavy gas (large primary ionization, efficiency) with strong electronegativity (streamer suppression).

Long term operation of resistive plate chambers is known to produce two main ageing effects:

1) **Gradual increase of the electrode resistivity (i.e. reduced rate capability) under very high working currents. The reason is the drying out of the bakelite plates. Humidification of the gas and also the external environment is necessary to limit the problem.**

2) **Degradation of the inner surface of the plates due to operation with fluorine-rich gas mixtures, leading to an increase of the noise in the detector. Gas flow must be properly adjusted.**

Up to 0.25C/cm^2 have been accumulated at GIF tests over the last years.
10(Hz/cm^2)*10^7(s/year)*10(years)*50pC(per hit)=0.05C/cm^2
Certified for ATLAS and CMS barrel regions. Not yet for forward CMS regions.

Gas Detector Aging

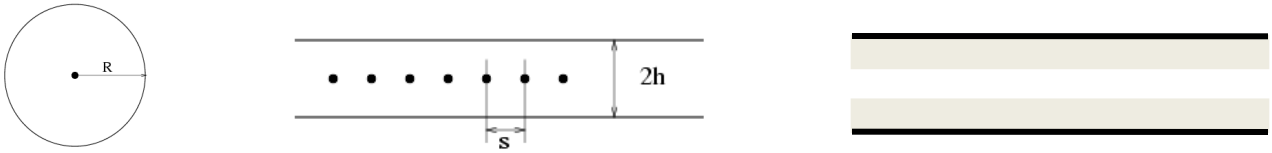

Aging tests have (hopefully) shown that LHC gas detectors can survive 10 years of LHC operation. Clearly, several C/cm wire or cm^2 of cathode are not 'a piece of cake'.

The success will strongly depend on the proper operation of gas systems and gas quality controls.

In principle one has reason to hope that LHC gas detectors will survive even SLHC rates, although this clearly has to be proven.

Aging test are clearly a central point for SHLC Gas detector R&D.

Limits of Wire Chambers

The rate limit of wire chambers (with reasonable geometry) is around 1MHz/cm^2 . At this rate, gas gain drop due to ions, accumulating in the chamber volume, poses a fundamental limit on the operation.

In terms of aging, the limit on the total deposited charge is about 1C/cm of wire and 2.5C per cm^2 of cathode surface. Such a high dose is only achievable for very specialized gases e.g. Ar/Ne/Xe + CO_2 and extreme care in the choice of detector material and cleanness must be taken.

There are of course many practical aspects that limit the use of wire chambers.

Trends for gaseous detectors: Micro Pattern Gas Detectors

MICRO-GROOVE CHAMBER

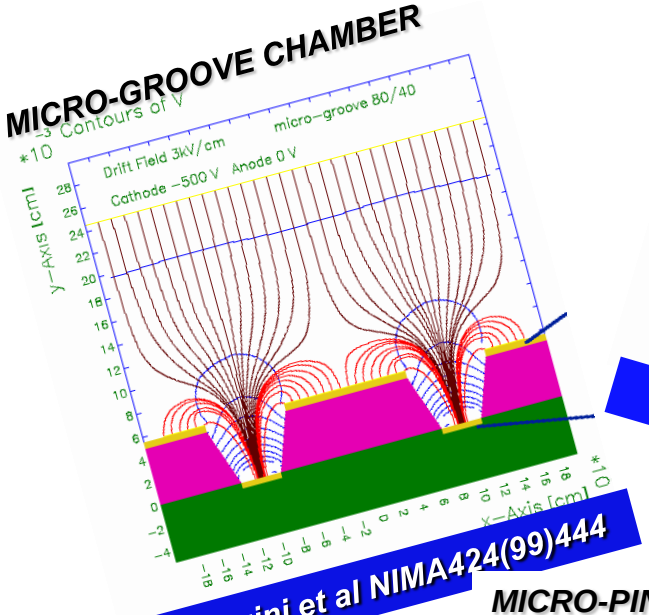

Bellazzini et al NIMA424(99)444

MICROWIRE CHAMBER

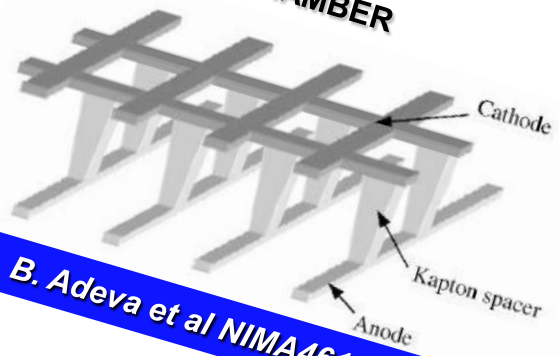

B. Adeva et al NIMA461(2001)33

MICRO-PIXEL CHAMBER

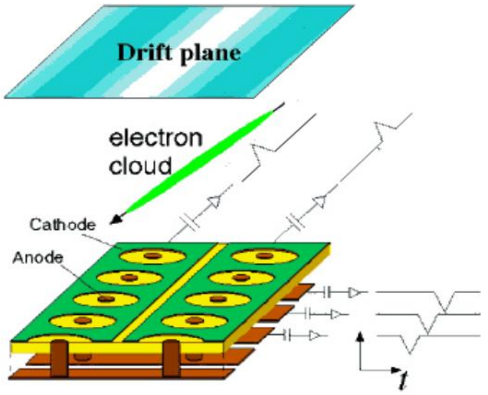

Ochi et al NIMA471(2001)264

MICRO-PIN ARRAY (MIPA)

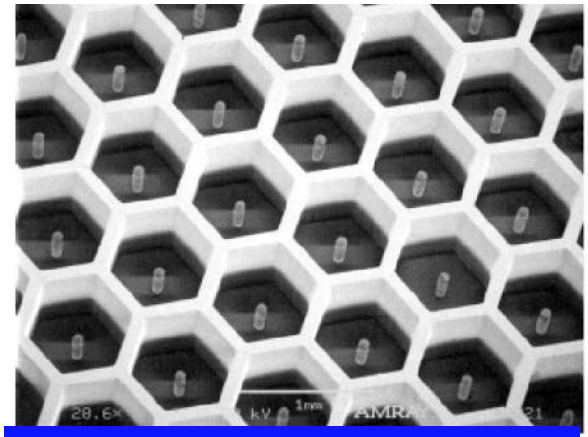

P. Rehak et al TNS NS47(2000)1426

FIELD GRADIENT LATTICE DETECTOR (FGLD)

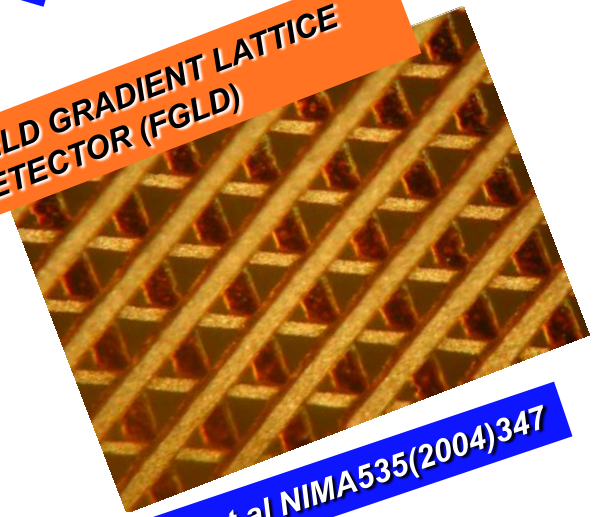

L.Dick et al NIMA535(2004)347

Trends for gaseous detectors: Micro Pattern Gas Detectors

MICROMEGA | **MSGC** | **GEM**

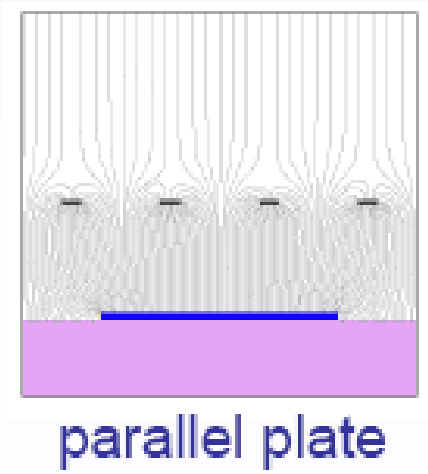

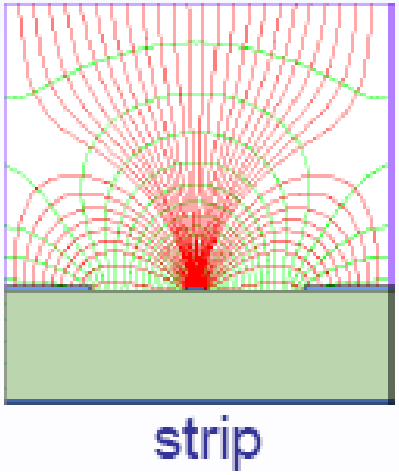

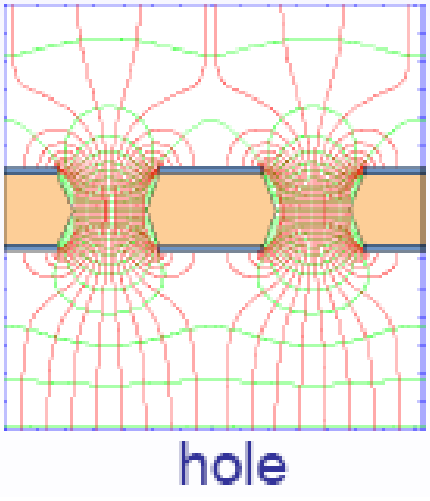

MicroMeshGasdetector | **MicroStripGasChamber** | **GasElectronMultiplier**

Trends for gaseous detectors: Micro Pattern Gas Detectors

The death of gas detectors within the next few years has been predicted during the last 25 years. However, Gas Detectors are further from 'death' than ever.

Although Silicon Detectors of gigantic size have replaced gas detectors around the interaction points, the experiments are growing in size to dimensions that make gas detectors the only possible candidate for the 'outer layers' of the experiments.

TPCs are unbeatable in terms of low radiation length (only gas), channel economy and track multiplicity capability.

During the 1990s, Micro Strip Gas Chambers (MSGCs) were developed with the idea of producing affordable large area tracking systems. They were prominent in the inner tracking system of the ATLAS and CMS experiments.

The falling cost of Silicon Detectors and increasing difficulties with MSGCs 'forced' the LHC community to abandon these detectors.

Out of the MSGC efforts there emerged however several new so called Micro Pattern Gas Detectors (MPGDs) which are starting to find their way into many experiments.

Micro Strip Gas Chambers (MSGCs)

Gas gain is provided not by wires but by metal strips on resistive electrodes.

Due to small pitch and fast ion collection MSGCs have very high rate capability.

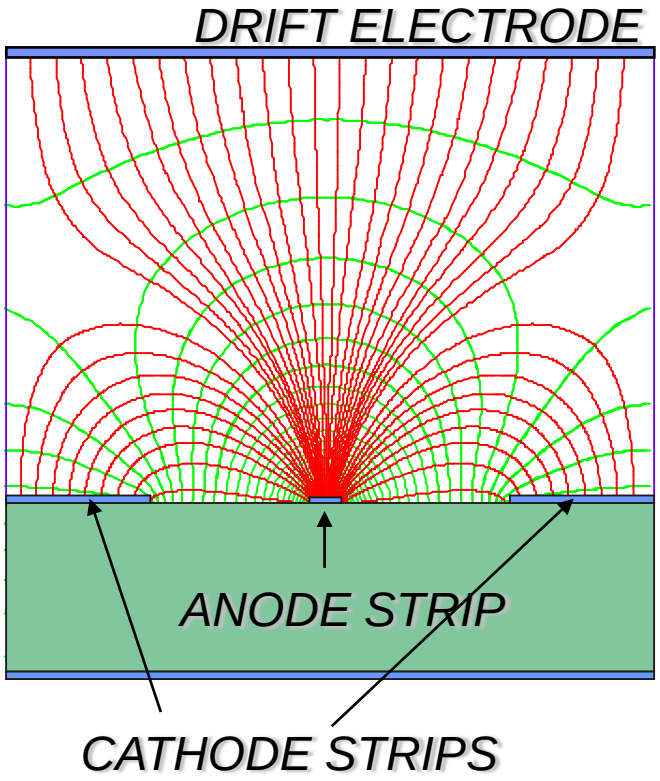

A.Oed, Nucl. Instr. and Meth. A263(1988)351

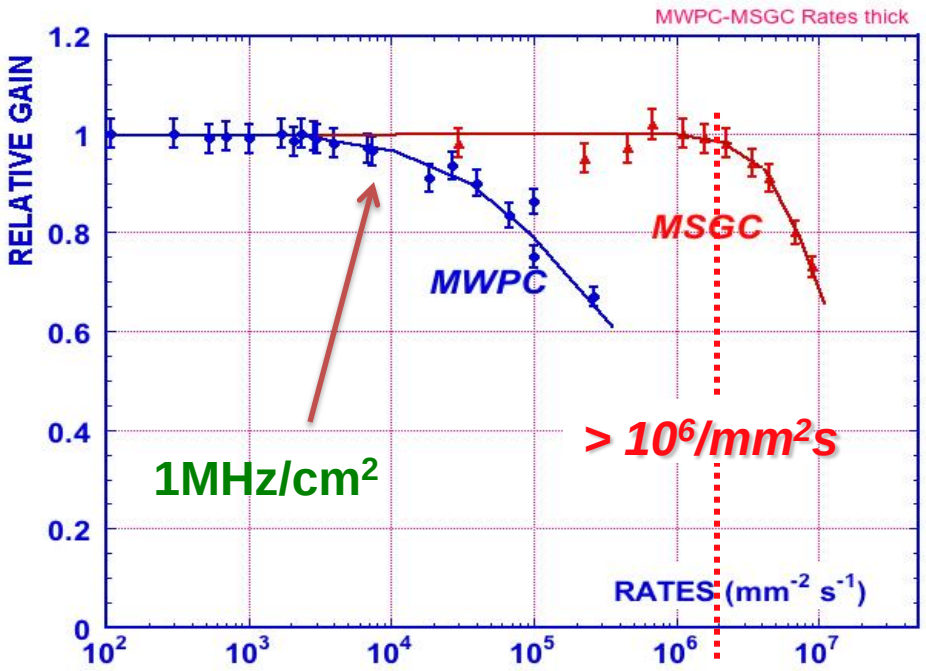

R. Bouclier et al, Nucl. Instr. and Meth. A323(1992)240

Micro Strip Gas Chambers (MSGCs)

Unfortunately MSGCs are rather prone to discharge, particularly in hostile environments.

Discharges measured in the CMD MSGC prototypes at PSI:

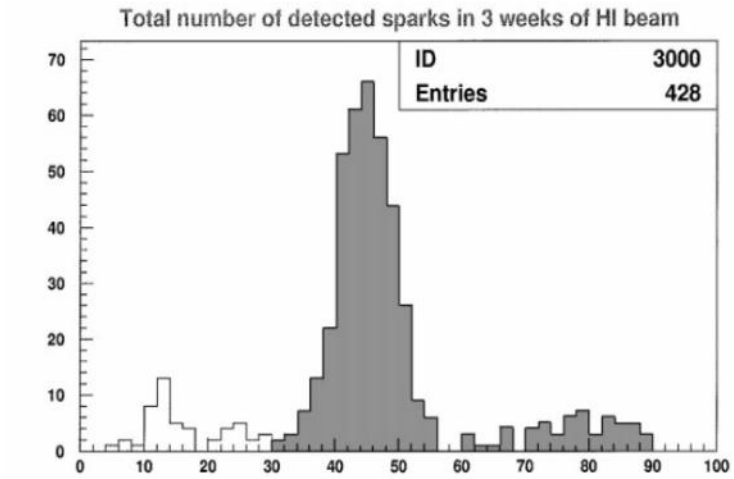

Strip damages due to Micro Discharges and heavy sparks:

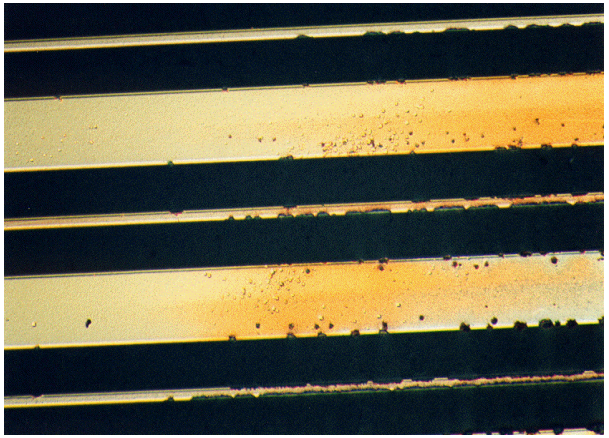

CERN-GDD

R. Bellazzini et al, Nucl. Instr. and Meth. A457(2001)22

GEMs & MICROMEGAS

MICROMEGAS

Narrow gap (50-100 μm) PPC with thin cathode mesh
Insulating gap-restoring wires or pillars

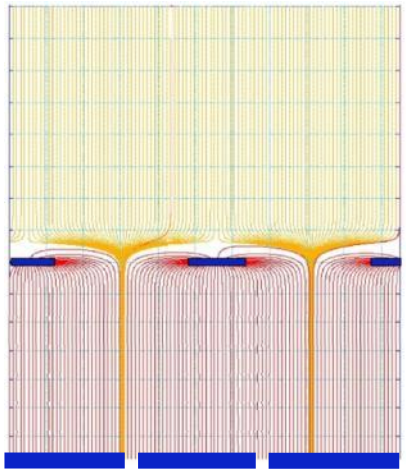

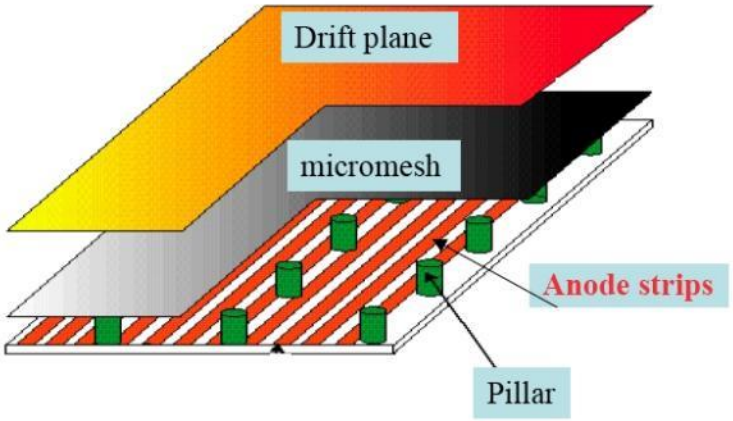

Y. Giomataris et al, Nucl. Instr. and Meth. A376(1996)239

GEM

Thin metal-coated polymer foils
70 μm holes at 140 mm pitch

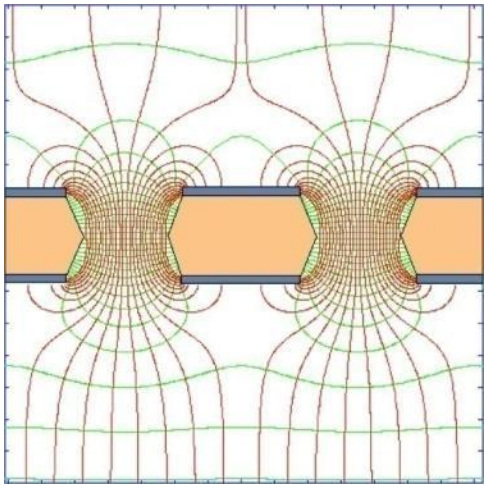

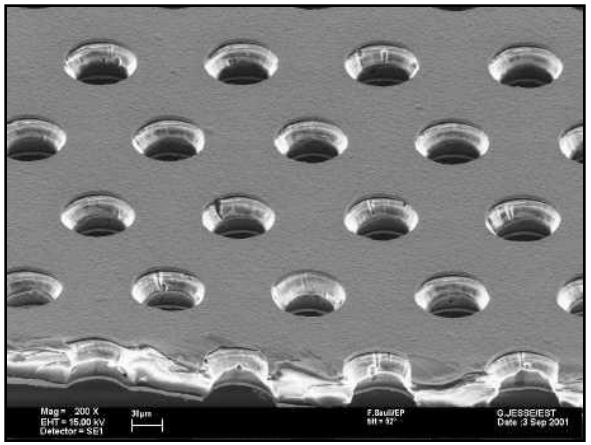

F. Sauli, Nucl. Instr. and Methods A386(1997)531

GEMs & MICROMEGAS

MICROMEGA

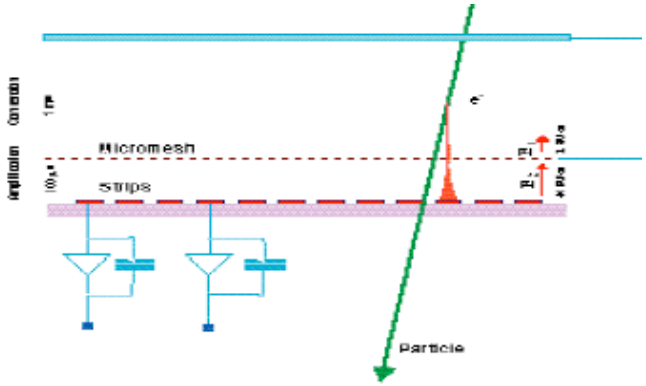

GEM

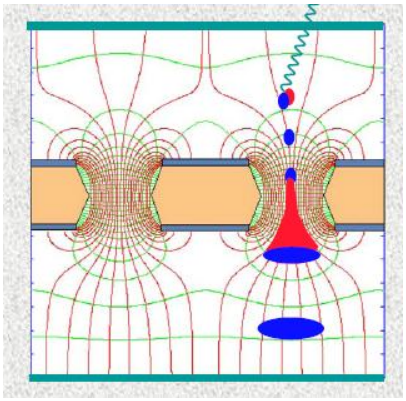

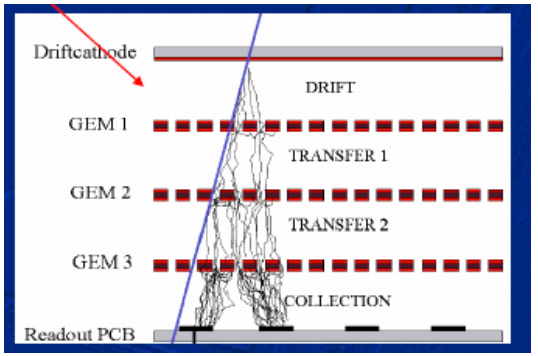

Micromegas use typical drift gaps of 1-3mm and avalanche multiplication gaps of 50-100um.

GEMs are typically cascaded in order to reduced the gain/stage and therefore the sparking probability.

GEM and MICROMEGAs show intrinsic rate capabilities of up to 200MHz/cm^2

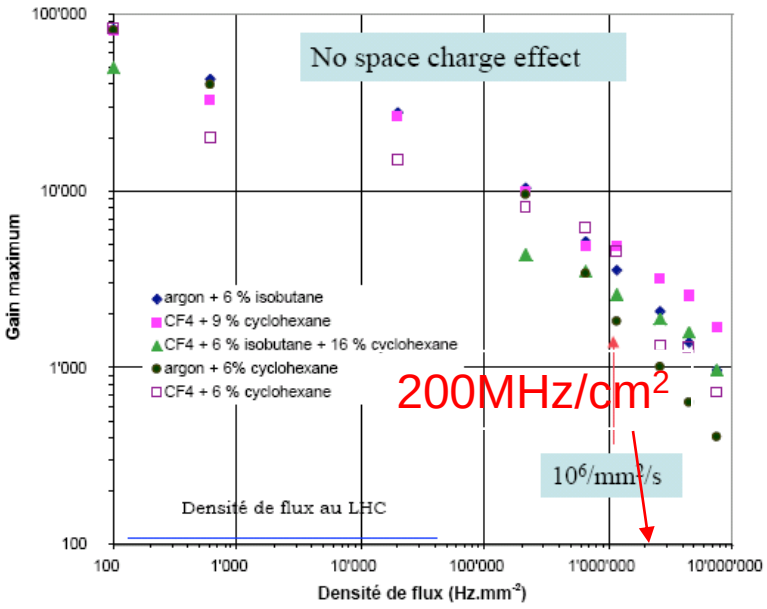

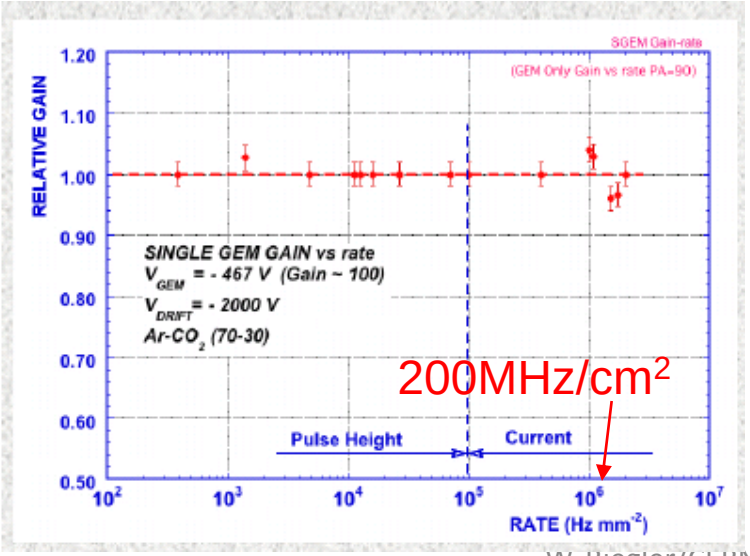

Micropattern Gas Detectors, Sparks

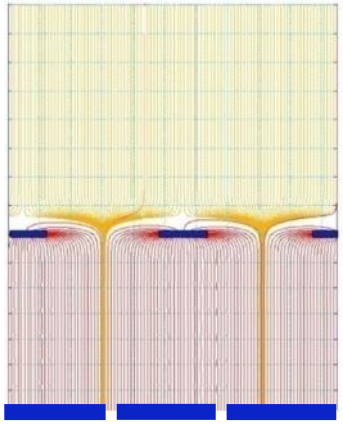

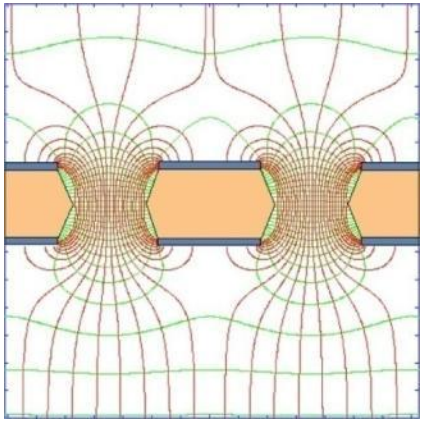

Due to the presence of insulators and 'undefined' edges with high electric fields, MPGDs are suffering from spark discharges that can either damage the detector, damage the electronics and cause dead time due to the recharging time of the electrodes.

In this respect the wire chamber is a very nice device. The high electric field on the thin wire is well defined. There are no 'undefined' edges with high fields in a wire chamber.

Although a major effort on the MSGC technology reduced the spark rates to acceptable limits, they were finally abandoned …

GEMs and MICROMEGAS are 'not' damaged by sparks. The problem of dead-time is addressed by segmentation of the GEM foils of MICROMEGA meshes.

GEMs have strongly reduced the sparking problems due to cascading of GEM stages (Triple GEM).

MICROMEGAs have reduced spark rates by technological improvements and are trying to use resistive layers on the readout plane for protection of the electronics.

First Large Scale Use of GEMs and MICROMEGAs

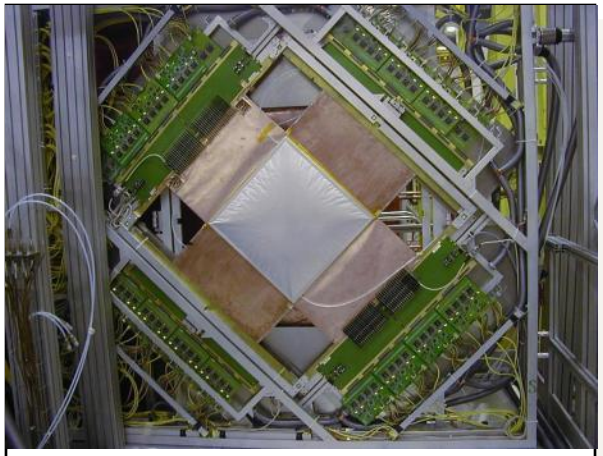

Micromegas: σ_x~90μm

Tracking in the COMPASS Experiment

GEM: σ_x~70μm

First Large Scale Use of GEMs and MICROMEGAs

- Two orthogonal sets of 768 parallel Cu strips, insulated by $50\,\mu m$ Kapton, both open to charge collection
- Top: $80\,\mu m$, bottom: $350\,\mu m$ width, pitch: $400\,\mu m$
- Charge sharing adjusted $\sim 1:1$

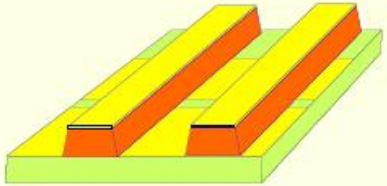

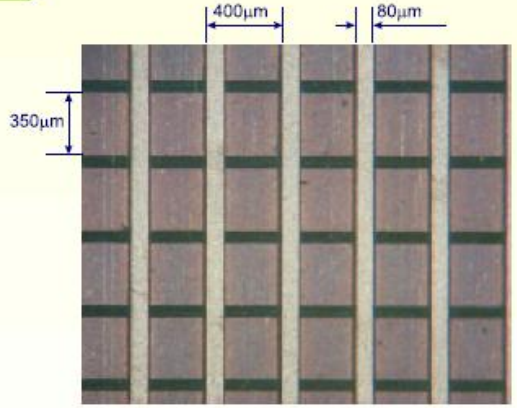

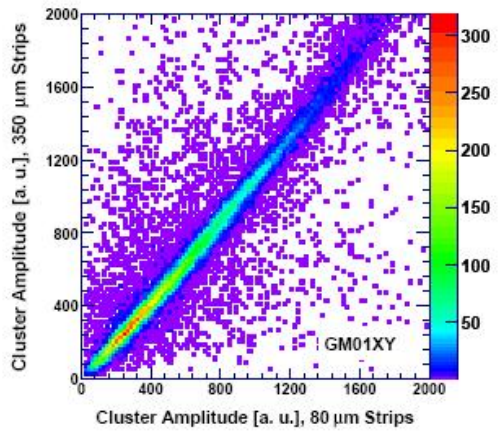

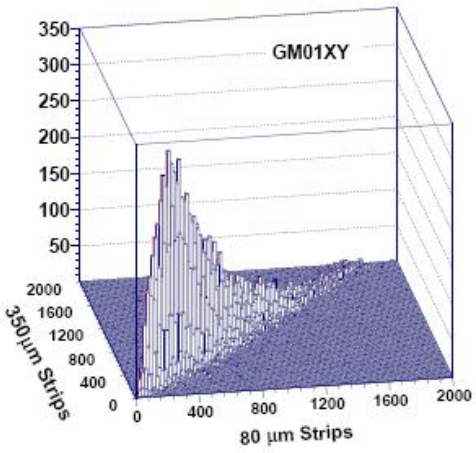

First Large Scale Use of GEMs and MICROMEGAs

GEM detectors: mature technique as tracking devices in HEP

- Bridge gap between silicon detectors and drift chambers
- High rate capability
- Large active areas
- Little material

COMPASS:

- First large-scale experiment to rely on GEM (+Micromegas!) tracking detectors
- Full setup (22 detectors, 44 planes, 33800 channels) operational since 2002
- Triple GEM amplification ensures stable operation: no single channel lost!

Position Resolution of 70um at rates up to 2.5MHz/cm^2 was achieved for the GEMs in COMPASS.

Several Large Scale GEM Trackers are currently being built or designed TOTEM, CLOE, PANDA …

Conclusions Micromegas for COMPASS and KABES

Two high precision, high rate and low mass detectors

COMPASS:

- 12 planes 40x40 cm^2 in 30 MHz total flux , 12000 channels
- operated reliably from 2002 to 2004, no aging
- resolutions : 70/90 μm , 9 ns
- future: hadron beams

MPGDs for Future TPCs

Detectors for ILC foresee Large TPCs as central tracking devices, (ILC rates are much lower than LHC rates !)

Advantage of TPC versus full-silicon tracker à la CMS :

- small material budget in front of precision calorimeter
- little multiple scattering improves momentum resolution
- measurement of dE/dx
- efficient pattern recongnition

drift chamber (TPC)

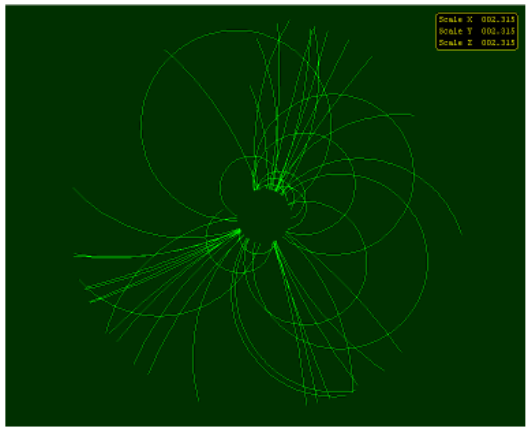

silicon detector

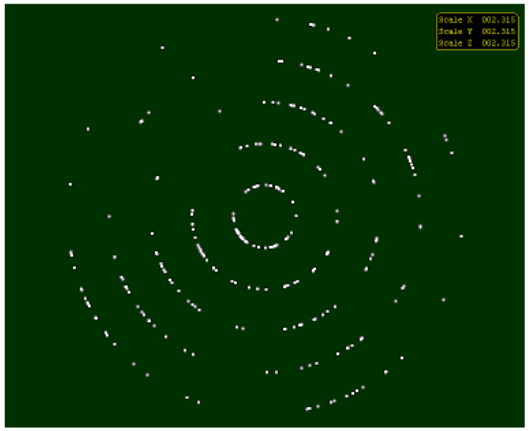

much smaller particle rates than at the LHC !

S. Roth

MPGDs for Future TPCs

TPCs with wire chamber readout must be 'gated' in order to prevent ions created in the avalanches to propagate back into the TPC drift volume (Track distortions …) ALEPH, Delphi, STAR, ALICE … The TPC must therefore be synchronized with the Bunch crossing.

The plan is to make a continuously sensitive TPC by reading using MPGDs for readout. Multistage GEMs and MICROMEGAs have intrinsically 'low' ion feedback and therefore automatically prevent the ions from drifting back into the TPC volume.

The only ions present in the TPC volume should be the ones from the promary ionization. The ion backflow should therefore be larger than 1/GasGain which around $1/10^3$

Ion Back-Drift

LEP: Gating between bunches
$\Delta t = 22\ \mu s$

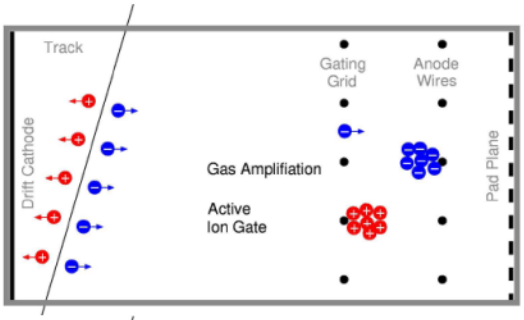

ILC: Length of bunch train
$2820 \times 337\ ns = 950\ \mu s$

Drift time is about 50 µs, no Gating between individual events possible

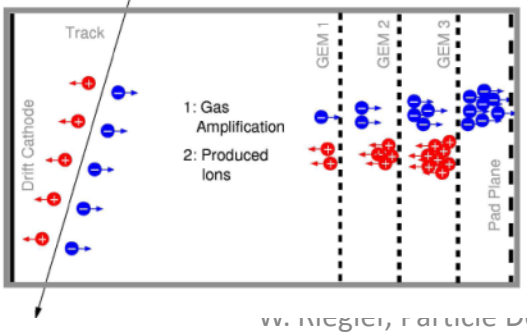

MICROMEGA ION backflow $2\text{-}3 \times 10^{-3}$

Almost there !

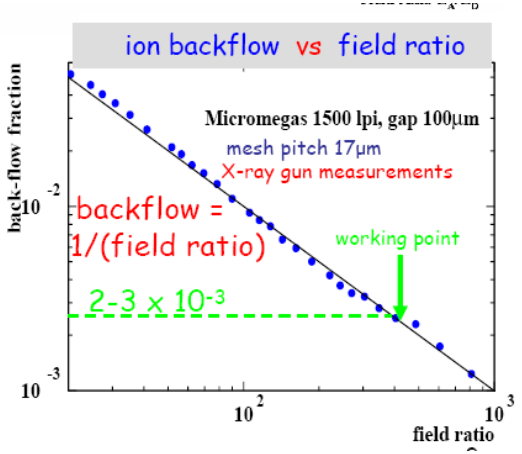

GEM ION backflow $2\text{-}3 \times 10^{-3}$

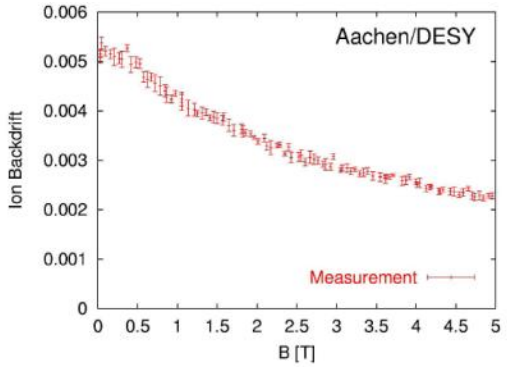

MPGDs for Future TPCs

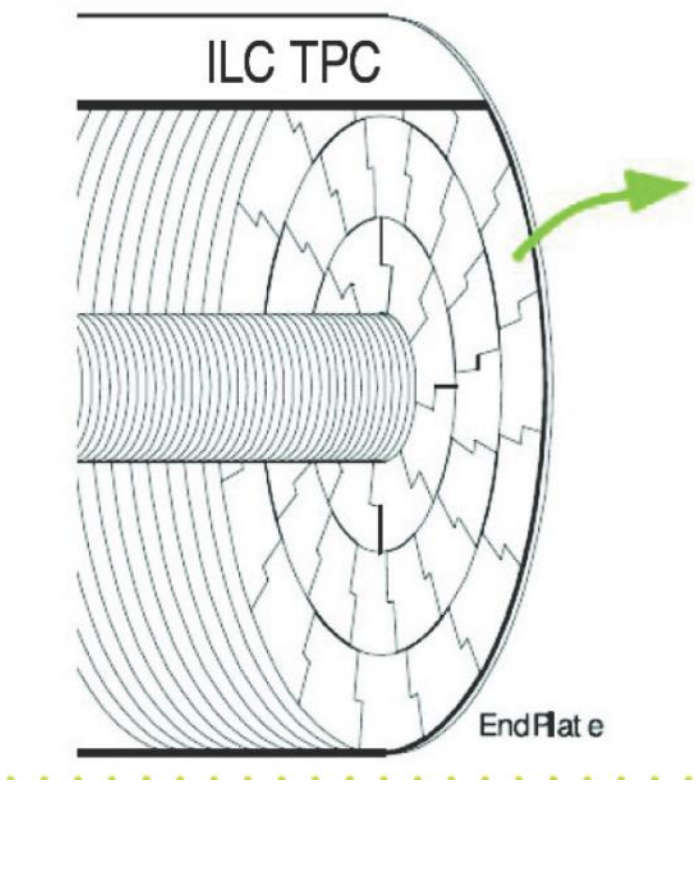

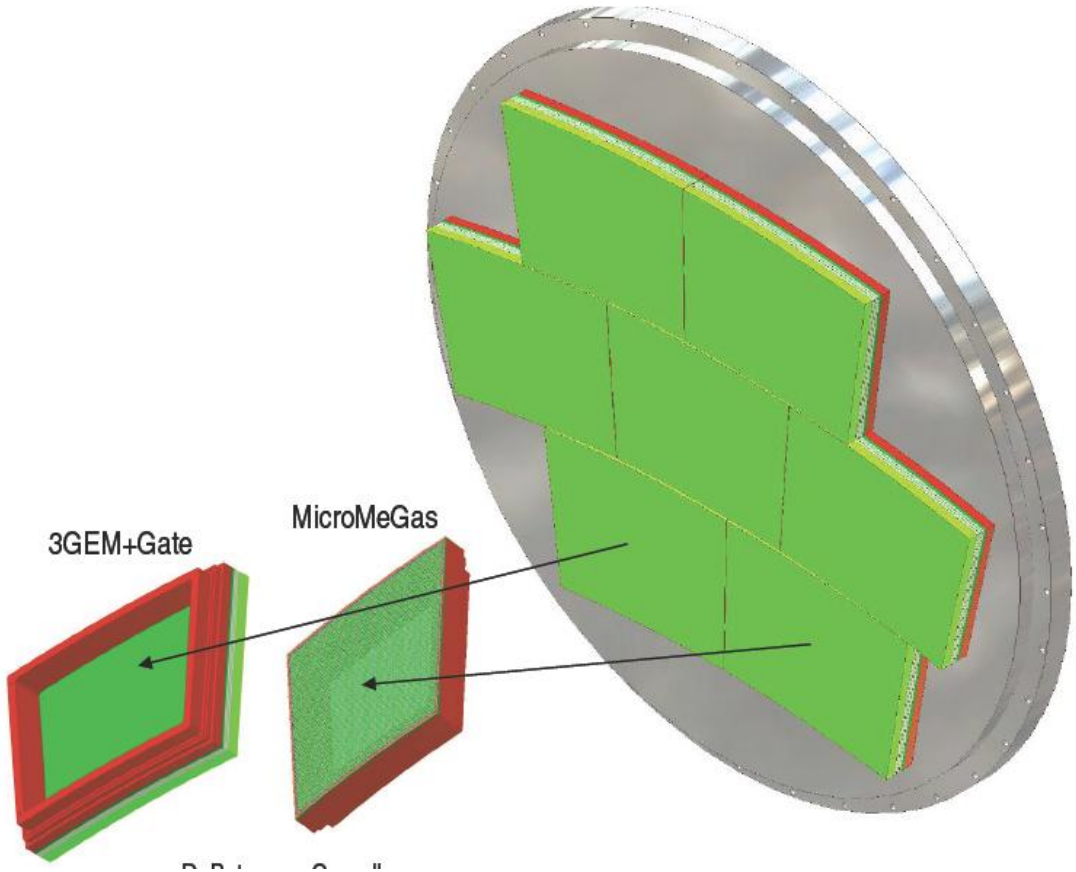

A Future Experiment, PANDA at FAIR

Facility for Antiproton and Ion Research, Darmstadt, Germany

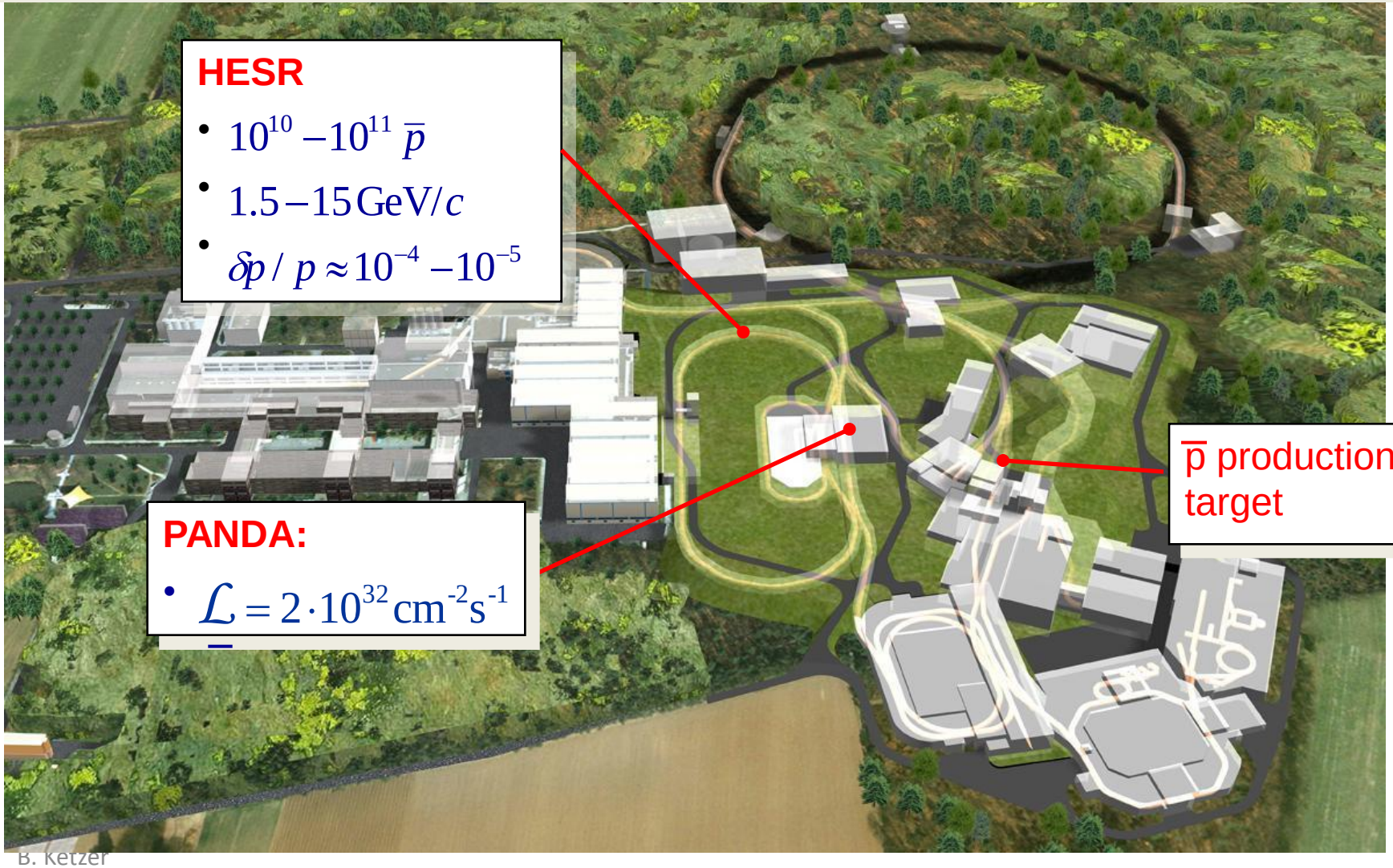

A Future Experiment, PANDA at FAIR

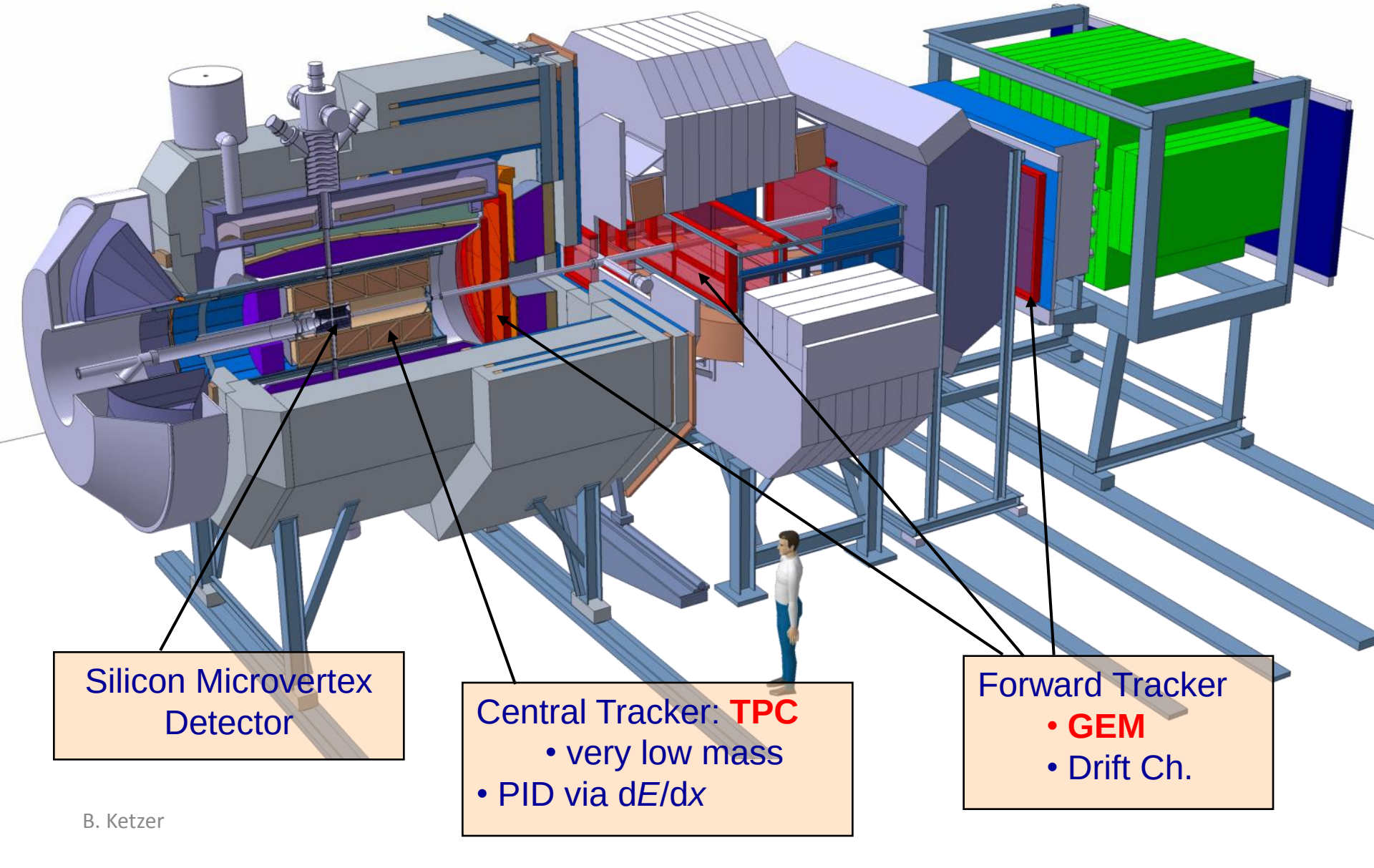

MPGDs for Photon Detection

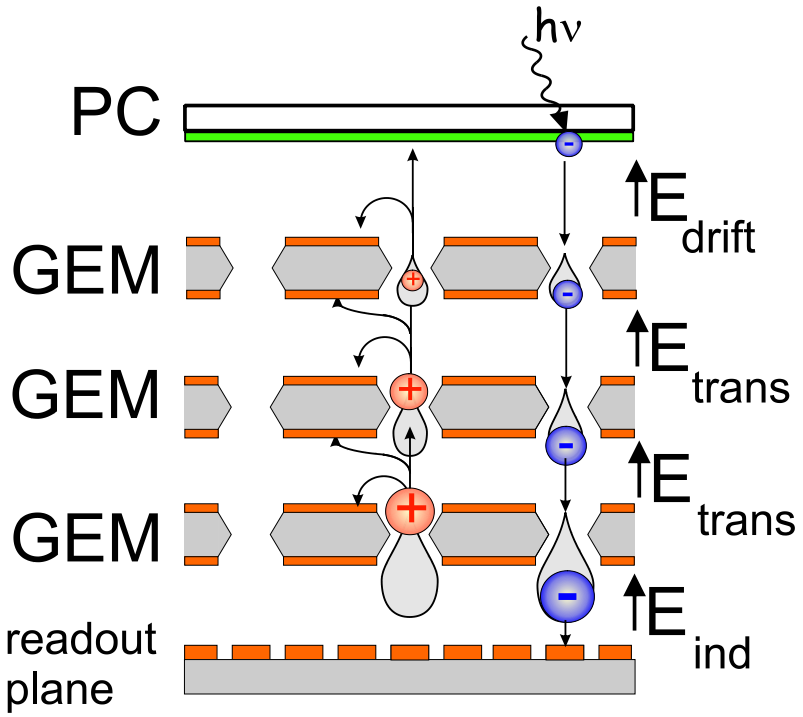

Single Electron (photon) Sensitivity was proven with 3-4 cascaded GEMs. Ion and photon feedback must be eliminated in order to avoid secondary photon emission (photon feedback) and damage of the PhotoCathode from Ion bombardement (Ion Feedback).

O.K. for UV photon detection with CsI Photo Cathode, but not yet O.K. for visible light detection Photo Cathodes.

Bachman et al. NIMA438(1999)376 5% @ 0.5kV/cm, Gain ~10^5
Breskin et al. NIM A478(2002)225 2-5%@ 0.5kV/cm, Gain ~10^5
Bondar et al. NIM A496(2003)325 3% @ 0.5kV/cm, Gain ~ 10^5

MPGDs for Photon Detection

Bresking et al.

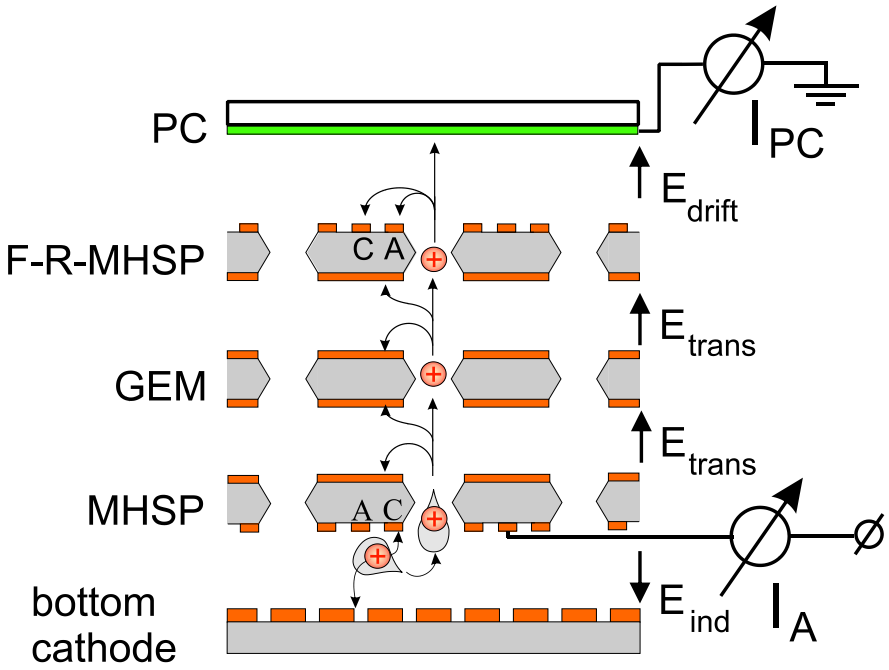

Using GEMs with special potential arrangements on the foils (Micro Hole Strip Plate) the ion feedback is again suppressed by a factor of 100 and visible light detection with single photon detection capabilities seems possible !

MPGDs with on Chip Readout Electrodes

Traditionally, the GEM and MICROMEGA signals are readoud out by PCBs with strips or Pads that are then connected to the readout electronics.

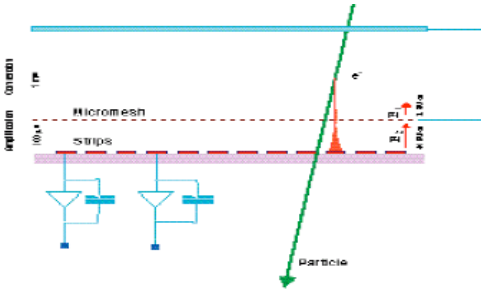

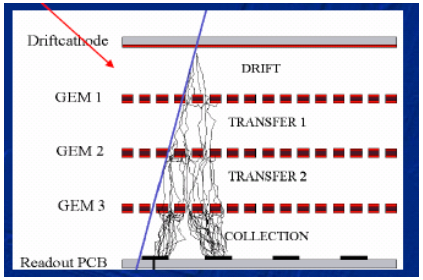

Another line of development uses metal pads on the silicon chip itself as readout electrodes i.e. the pixelized readout electrode and readout electronics are a monolithic unit !

GEM+Medipix Chip,

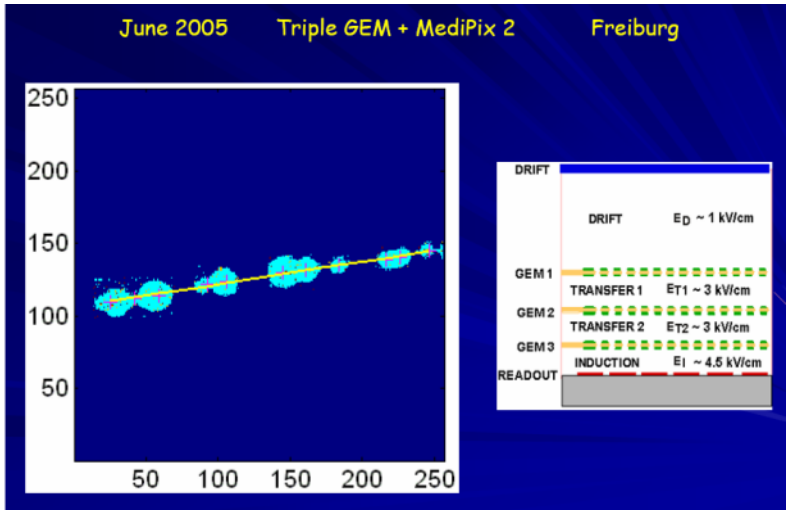

MICROMEGA + Medipix Chip

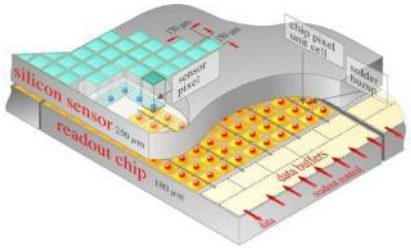

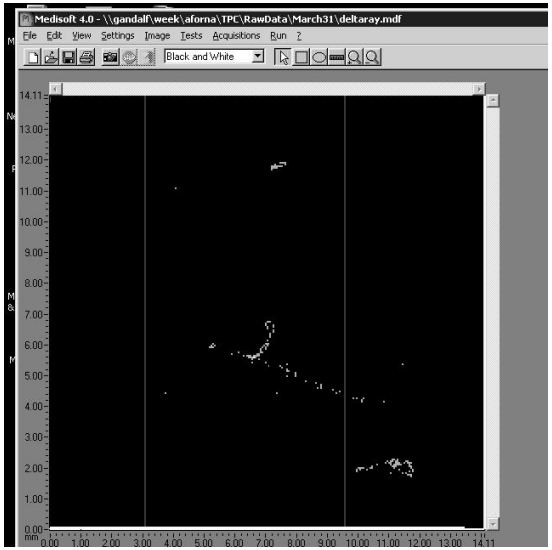

MPGDs with Integrate Micromesh, INGRID

Going even another step further, by wafer post-processing techniques, MPGD structure scan be put on top of a pixelized readout chip, making the entire detector a monolithic unit !
→ IntegratedGrid (INGRID) . In addition a TDC was put on each pixel measuring drift times →

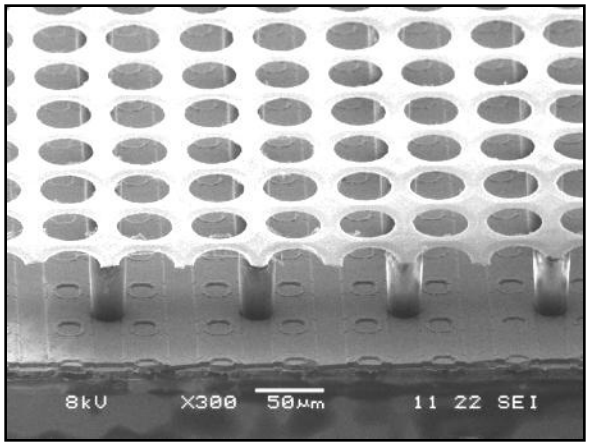

Micromesh on a pixelized readout chip produced by Opto-Chemical Wafer Post-Processing Techniques.

With 3cm Drift gap: 5 cm³ Mini TPC !
Tracks from Sr90 source in 0.2T Magnetic Field !

Single ionization electrons are seen.

Fantastic position resolution …

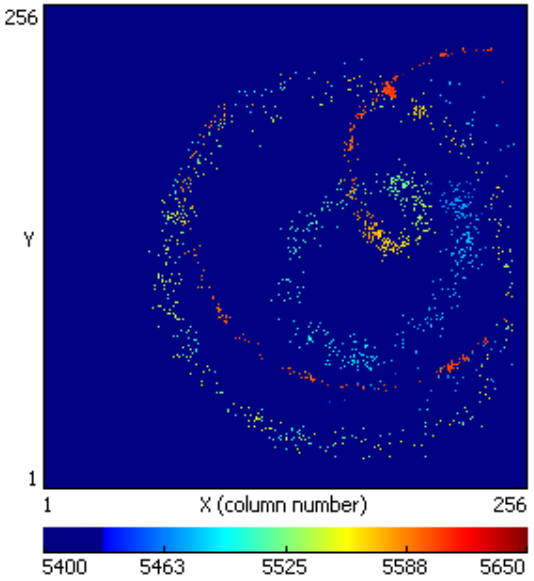

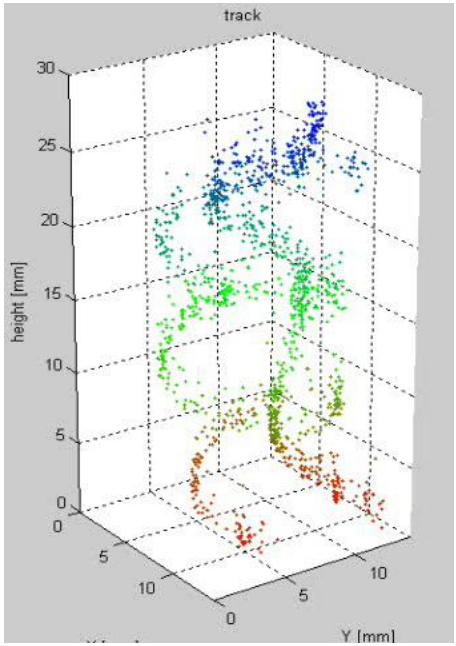

MPGDs with on Chip Readout Electrodes, INGRID

Proponents of this technology claim that these kind of monolithic gas detectors could even be superior to Silicon detectors and claim back the inner tracking regions in particle experiments for Gas Detectors ! Some ideas for ALL GAS ILC detectors were put forward …

General principle of new gaseous detector:

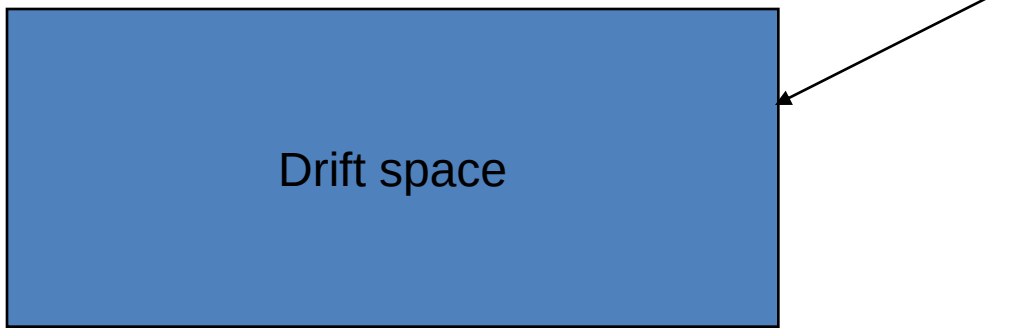

readout plane:
MPGD +
- pixel anode chips
or
- hybrid pad pcb +
feedthrough + FE chips

With drift length of

2000 mm: TPC
200 mm: (μ)TPC
20 mm: drift chamber
2 mm: Gossip

MPGDs with on Chip Readout Electrodes, INGRID

Gas On Slimmed Silicon Pixel (GOSSIP):
a detector combining a thin gas layer as signal generator with a CMOS readout pixel array.

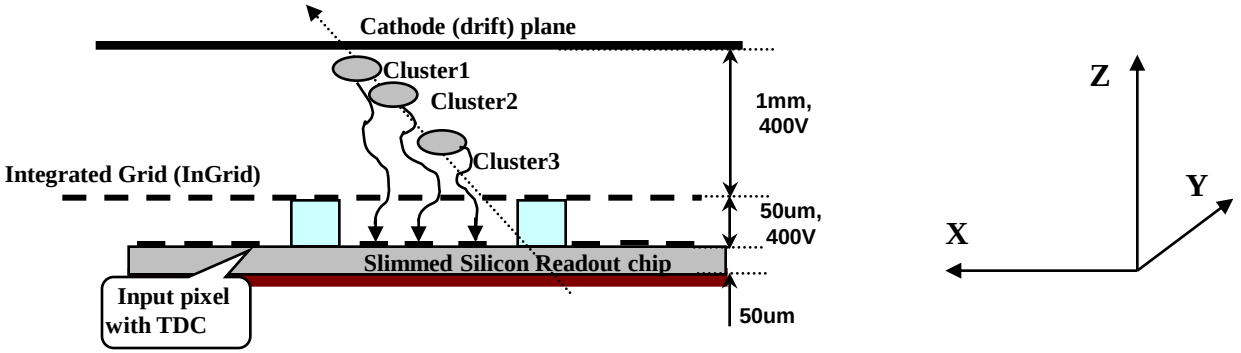

3-D track reconstruction ➡ Cluster drift time measurements

low capacitance on the pixel (down to 10 fF).
narrow drift gap (1 mm).
fast charge collection time (20 ns).
low diffusion of the primary electrons (70 um/1.6 ns)

→ 'Proposed' as an alternative to SHLC trackers …

Summary on Gas Detectors

Wire chambers feature prominently at LHC. A decade of very extensive studies on gases and construction materials has lead to wire chambers that can track up to several MHz/cm^2 of particles, accumulate up to 1-2C/cm of wire and 1-2 C/cm^2 of cathode area.

While silicon trackers *currently* outperform wire chambers close to the interaction regions, wire chambers are perfectly suited for the large detector areas at outer radii.

Large scale next generation experiments foresee wire chambers as large area tracking devices.

The Time Projection Chamber – if the rate allows it's use – is unbeatable in terms of low material budget and channel economy. There is no reason for replacing a TPC with a silicon tracker.

Novel gas detectors, the Micro Pattern Gas Detectors, have proven to work efficiently as high rate, low material budget trackers in the 'regime' between silicon trackers and large wire chambers.

One of the key gas detector development efforts is the construction of a continuously sensitive TPC with MPGD readout (Panda, ILC).

Very recent developments on Monolithic MPGDs are extremely interesting and open an entirely new domain of applications.